

'X-Ray Studies of the Structures of Some  
Biologically Significant Molecules'

A Thesis Presented for the Degree  
of Doctor of Philosophy of the  
University of London

by

David John Hunt, B.Sc., A.R.C.S.

Department of Chemistry,

Imperial College,

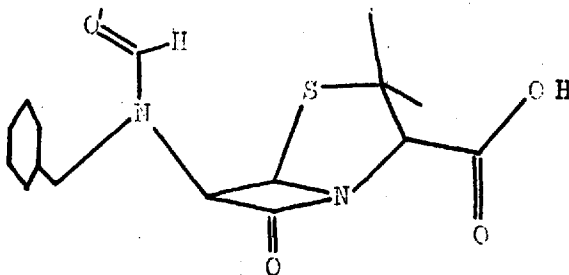
London, S.W. 7.

September 1966.

## Abstract

The crystal structures of three natural-product derivatives have been examined by three-dimensional X-ray diffraction techniques.

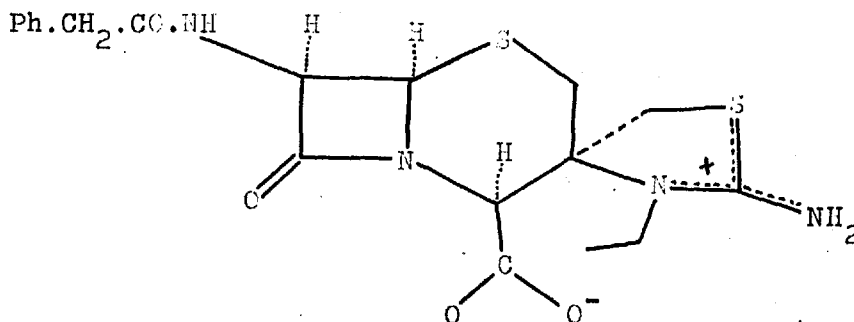
6-(N-Benzylformamido)penicillanic acid ( $C_{16}H_{18}O_4N_2S$ ) is an isomer of the antibiotic, benzylpenicillin, but possesses only one ten-thousandth part of its antibacterial activity. The crystals are monoclinic with  $a = 19.58 \text{ \AA}$ ,  $b = 6.427 \text{ \AA}$ ,  $c = 13.98 \text{ \AA}$ ,  $\beta = 108^\circ$  and spacegroup  $C2$ , with four molecules in the unit cell. The structure, which is shown below was determined with the aid of a graphical Patterson



superposition technique. It is similar to those found by previous X-ray studies on the penicillins except for the position of one of the possible hydrogen-bonding groups ( $O'$ ). This difference is consistent with current explanations for the antibiotic properties of the penicillins.

The crystal structure of a spiro-cyclic derivative of another antibiotic series, the cephalosporins, has been

determined. This spiro compound ( $C_{19}H_{22}N_4O_4S_2 \cdot 3H_2O$ ) crystallizes in the monoclinic system with  $a = 8.063$  Å,  $b = 7.184$  Å,  $c = 19.72$  Å and  $\beta = 100.3^\circ$ . The spacegroup is  $P2_1$  with two molecules per cell. The molecule, represented by



the diagram above, forms a novel tricyclic system and presents many interesting aspects of structure and conformation, which are discussed in some detail.

Attempts have also been made to determine the crystal structure of zeorin acetate ( $C_{32}H_{54}O_3$ ), a member of the triterpene series. The crystals are orthorhombic with  $a = 8.78$  Å,  $b = 11.59$  Å,  $c = 29.15$  Å and belong to the spacegroup  $P2_12_12_1$ , with four molecules in the unit cell. This compound presents substantial crystallographic problems and efforts have been made to interpret its Patterson function mainly with the aid of a relatively modern Patterson searching technique.

## Acknowledgements

I would like to express my thanks to Professor D.Rogers, whose enthusiastic supervision during the course of this work has been much appreciated.

I am also grateful to all my friends at Imperial College, and especially Roger Diamand, Mike Drew and Mick Hursthouse for the interest they have shown in this work.

Computing has been carried out at the Institute of Computer Science, University of London and at the Imperial College Computer Unit. In each case, the use of the facilities and the cooperation of the staff are gratefully acknowledged.

The Science Research Council is thanked for financial support in the form of a Research Studentship.

To  
Gloria

## Contents

Chapter 1	The Phase Problem and an Introduction to the Patterson Function	7
Chapter 2	Data Treatment and General Crystallographic Methods Used	22
Chapter 3	Chemistry of the Penicillins and Cephalosporins	28
Chapter 4	The Crystal Structure of 6-(N-Benzylformamido)penicillanic Acid	46
Chapter 5	The Crystal Structure of (3S,4S,6R,7R)-2'-Amino- 3'-ethyl-2'-thiazolinium-4'-spiro-3-(7-phenylacet- amidocepham-4-carboxylate) Trihydrate	84
Chapter 6	The Chemistry of Zeorin	129
Chapter 7	The Interpretation of the Patterson for Complex Structures	143
Chapter 8	An X-Ray Investigation of the Crystal Structure of Zeorin Acetate	158
	References	198

CHAPTER 1

The Phase Problem and an  
Introduction to the Patterson Function

One of the first stages in the X-ray analysis of a crystal structure is the measurement of the intensities of the spectra that arise from the diffraction of X-radiation by the three-dimensional crystal lattice. Each diffracted beam can be regarded as the 'reflexion' of X-rays by a particular set of parallel crystal planes. Directionally, a diffracted beam will depend only upon the orientation and separation of its reflecting planes with respect to the 'unit cell' of the crystal lattice. The intensity, however, depends upon the type and arrangement of the atoms with regard to these planes.

If there are  $N$  atoms in the unit cell, the diffraction pattern of the crystal lattice can be regarded as made up from the patterns of  $N$  atomic lattices and the total wave diffracted from the unit cell can be described by the equation

$$F(hkl) = \sum_r^N f_r \exp i\phi_r \quad \dots\dots (1)$$

where  $F(hkl)$  is the 'Structure Factor' for the particular reflexion and  $f_r$  is the 'form factor' of the  $r$ th. atom. The

form factor describes the power with which atoms of type  $r$  'reflect' X-rays and it depends upon the atomic number and decreases with increasing Bragg angle,  $\theta$ .  $\phi_r$  is the phase angle of the diffracted beam from the  $r$ th. atomic lattice.

Since a crystal is periodic in three dimensions, Bragg (1929) has shown that the electron density ( $\rho$ ) at any point  $x, y, z$  can be represented by a three-dimensional Fourier series of the form

$$\rho(xyz) = \frac{1}{V} \sum_{h,k,l} F(hkl) \exp(-2\pi i(hx + ky + lz)) \dots (2)$$

where  $V$  is the volume of the unit cell and the function is everywhere continuous. A good and convenient approximation to the structure factor is obtained assuming that all the electron density in the crystal occurs in spherically symmetrical atoms. The structure factor (equation 1) can then be written as

$$F(hkl) = \sum_{r=1}^N f_r \exp 2\pi i(hx_r + ky_r + lz_r) \dots (3)$$

where  $x_r, y_r, z_r$  are the coordinates of the  $r$ th. atom expressed as fractions of unit-cell edges. Thus the expression (2) for the electron density can be written as

$$\rho(xyz) = \frac{1}{V} \sum_{h,k,l} \left\{ \sum_{r=1}^N f_r \exp -2\pi i (h(x-x_r) + k(y-y_r) + l(z-z_r)) \right\} \dots (4)$$

The Fourier series (4) will consist of  $N$  resolved, spherically symmetrical peaks at the positions of the atoms  $x_r, y_r, z_r$  and



the number of electrons in each peak will be equal to  $Z_r$ , the atomic number. (The Fourier in the form of equation (4) is pertinent to the discussion of the Patterson in later sections).

Crystal structure analysis involves substituting the values of the structure factors,  $F(hkl)$ , into equation (2) in order to obtain a representation of the electron density distribution in the unit cell. However, the structure factors are, in general, complex quantities and the X-ray crystallographer observes intensities, which are proportional to the square of the modulus of the structure factors,  $|F(hkl)|^2$ . It is the determination of the phases that constitutes the 'phase problem' in X-ray crystallography.

One of the most successful methods proposed to overcome this problem is due to Patterson (1935). He derived a Fourier series with the coefficients,  $F(hkl)$ , replaced by  $|F(hkl)|^2$  and related the series to the inter-atomic vectors in the unit cell. The rest of this chapter is devoted to a description of this 'Patterson series' as it has been used extensively throughout the thesis. Some of the simpler applications are also described here.

Using for simplicity the one-dimensional series of period 'a' the equation

$$\rho(x) = \frac{1}{a} \sum_{h=-\infty}^{\infty} F(h) \exp -2\pi i(hx) \quad \dots\dots (5)$$

gives the electron density at any point  $x$ . The density distribution about  $x$  can also be expressed as a function of a parameter  $u$ , i.e.  $\rho(x + u)$ . The total amount of material between  $x$  and  $x + dx$  is  $\rho(x)dx$ , which gives the weighted distribution about  $x$  as  $\rho(x) \rho(x + u)dx$  and the weighted average distribution as

$$A(u) = \int_0^1 \rho(x) \rho(x + u) dx \quad \dots\dots (6)$$

Thus from equation (5) and utilising the property that

$$\int_0^1 \exp -2\pi i(m + n)x dx = 1 \text{ if } n = -m \text{ and is otherwise}$$

zero, equation (6) gives

$$A(u) = a^{-2} \sum_{h=-\infty}^{\infty} |F(h)|^2 \exp 2\pi i hu \quad \dots\dots (7)$$

This is the one-dimensional Patterson series and the derivation can be extended to three dimensions to give

$$A(uvw) = V^{-2} \sum_{h,k,l=-\infty}^{\infty} |F(hkl)|^2 \exp 2\pi i(hu + kv + lw) \quad \dots (8)$$

where the distribution is now a function of the three parameters  $u, v, w$  about the point  $x, y, z$ . The general form of the three-dimensional function is usually written as

$$P(uvw) = \frac{1}{V} \sum_{h,k,l=-\infty}^{\infty} |F(hkl)|^2 \cos 2\pi(hu + kv + lw) \quad \dots (9)$$

Equation (9) differs from equation (8) for  $A(uvw)$  by a factor of  $1/V$  and in the use of the cosine. The former factor is merely a result of defining the function as an average value of the electron density product, and the latter because in the absence of fluorescence,  $F(hkl) = F^*(\bar{h}\bar{k}\bar{l})$ , so that their imaginary components cancel. As the cosine function is even, it follows that the Patterson function is centrosymmetric.

The physical meaning of the Patterson can be readily seen by considering it in the form of equation (6). Thus  $A(u)$  will only be large when both  $\rho(x)$  and  $\rho(x + u)$  are large, so that peaks appear in the Patterson corresponding to peaks in the electron density distribution separated by a vector 'u'. The Patterson function, then, will consist of a large, multiple peak at the origin (ie. the sum of the product  $\rho(x)\rho(x)$  for all  $x$ ), and peaks whose vectors from the origin represent inter-atomic vectors in the crystal. Although a Fourier series is a continuous function it is sometimes useful to describe the Patterson as the vector set of the electron density.

### Properties of the Patterson

Writing the one-dimensional structure factor in the form of equation (3), it follows that

$$|F(h)|^2 = \sum_{r,s=1}^N f_r f_s \exp 2\pi i h(x_r - x_s) \dots (10)$$

Substituting equation (10) in (7) gives

$$\begin{aligned} A(u) &= a^{-2} \sum_{h=-\infty}^{\infty} \left\{ \sum_{r,s=1}^N f_r f_s \exp 2\pi i h(u - (x_s - x_r)) \right\} \\ &= a^{-2} \sum_{h=-\infty}^{\infty} \sum_{r=1}^N f_r^2 \exp 2\pi i h u + a^{-2} \sum_{h=-\infty}^{\infty} \sum_{\substack{r,s=1 \\ r \neq s}}^N f_r f_s \exp 2\pi i h(u - (x_s - x_r)) \dots (11) \end{aligned}$$

The Patterson peaks thus correspond to the Fourier representation of artificial atoms with specific 'form factors'.  $N$  of these, represented by the first term on the right hand side of equation (11) coincide at the origin with 'form factors' of  $f_r^2$ ; the remaining  $N(N-1)$  are situated at points  $\pm(x_s - x_r)$  with 'form factors' of  $f_r f_s$ .

Thus the total number of 'electrons' in the origin peak is  $\sum_{r=1}^N Z_r^2$ , and peaks corresponding to a vector between two atoms at  $x_r$  and  $x_s$  respectively will contain  $Z_r Z_s$  'electrons' and the peak height will be roughly proportional to this product in the three-dimensional case. It can also be noted that the volume of a three-dimensional Patterson peak is roughly eight times that of a corresponding peak in  $\rho(xyz)$ . Coupled with the fact

that the Patterson contains  $N^2$  peaks in the same volume as the electron density contains  $N$ , this means that the resolution of the former is poor compared to that of the latter.

Also, the origin peak can be removed by using as coefficients in the summation,  $|F_o(h)|^2$ , where

$$|F_o(h)|^2 = |F(h)|^2 - \sum_{r=1}^N f_r^2$$

The new series will retain all the information regarding interatomic vectors and may also show peaks that were previously obscured by the large origin peak.

### Sharpening

Patterson (1935) suggested a method of improving the resolution of the Patterson series, which in effect attempts to transform the observed  $|F(h)|^2$  terms into what they would be if the crystal were composed of point atoms. As the different form-factor curves are, in fact, very similar when scaled to unity, he suggested setting up an average f-factor per electron of

$$\hat{f}(h) = \frac{\sum_{r=1}^N f_r(h)}{\sum_{r=1}^N Z_r}$$

and the sharpened synthesis is then computed by dividing each  $|F(h)|^2$  term by the appropriate  $\hat{f}(h)$ .

Another factor to be taken into account is the thermal

motion of the atoms. This, if isotropic and uniform for all atoms, tends to reduce the observed values of  $|F(h)|$  by a factor of

$$\exp ( -B \sin^2 \theta / \lambda^2 )$$

where  $\lambda$  is the wavelength of the X-radiation and B a constant for the particular crystal, which can be estimated from the intensity data by the method of Wilson (1942). Thus, division of each  $|F(h)|^2$  by

$$\hat{F}^2(h) \exp ( -2B \sin^2 \theta / \lambda^2 )$$

will give a Patterson function sharpened to represent point atoms at rest.

An undesirable result of sharpening the Patterson is the appearance of false peaks. Equation (2) indicates that a Fourier series is ideally the sum of an infinite number of terms. In practice the number of terms is limited but the unsharpened series converges rapidly because of the thermal attenuation of the terms. However, if sharpening is applied, the importance of these high-order terms will be greatly increased. The truncation of the data becomes obvious and produces series-termination ripples in the Fourier map.

In recent years, more empirical sharpening functions have been used which attempt to compromise between resolving power and freedom from non-convergence effects. For example, Shoemaker et al. (1953) have used the function

$$(2\sin \theta / \lambda)^4 \exp -\alpha^2 (2\sin \theta / \lambda)^2 \quad \text{with } \alpha = 2.2$$

in the structure analysis of DL-serine. The function had a maximum value at  $\sin \theta = 0.5 \sin \theta_{\max}$  and tended to reduce the Fourier ripple.

### The Use of Symmetry

Harker (1936) suggested that the use of the symmetry of the spacegroup could lead to a simplification in the interpretation of the Patterson.

For a diad, coincident with the b axis (for example), the coordinates of a pair of atoms related by the symmetry are

$$\begin{array}{ccc} x & y & z \\ -x & y & -z \end{array}$$

The vectors between them will have components

$$\pm (2x \quad 0 \quad 2z)$$

and the 'Harker section' in the Patterson at  $\psi = 0$  will contain peaks corresponding to vectors between all atoms related by this symmetry element. Equation (9) takes the form

$$\begin{aligned} P(uOw) &= \frac{1}{V} \sum_{h,k,l=-\infty}^{\infty} \sum_{k=-\infty}^{\infty} |F(hkl)|^2 \cos 2\pi(hu + lw) \\ &= \frac{1}{V} \sum_{h,l=-\infty}^{\infty} \left\{ \sum_{k=-\infty}^{\infty} |F(hkl)|^2 \cos 2\pi(hu + lw) \right\} \\ &= \frac{1}{V} \sum_{h,l=-\infty}^{\infty} C_{h,l} \cos 2\pi(hu + lw) \quad \dots \dots (12) \end{aligned}$$

where  $C_{h,1} = \sum_{k=-\infty}^{\infty} |F(hk1)|^2$ . Use of equation (12) reduces computation to that of the two-dimensional case but as three-dimensional data are used the resolution of the Harker section will be far better than the corresponding two-dimensional projection. Analogous results can be derived for screw axes but the relevant Harker plane is then displaced along the screw. For mirror and glide planes, the summation reduces to one-dimensional Harker lines normal to the plane.

In any Harker region there are always some extra peaks which arise accidentally and arise from non-equivalent atoms. Such peaks confuse the impression and are not readily distinguishable from true Harker peaks.

### Interpretation of the Patterson

The complexity of this problem depends upon the nature of the substance being examined and consequently, the methods of solution provide one of the most diverse and interesting aspects of crystal structure analysis. This thesis is concerned with organic molecules which for convenience can be divided into two groups :

- (a) Molecules containing a relatively large number of atoms of low atomic number with only a few heavy scatterers.
- (b) Molecules containing only light-atom scatterers.



The interpretation of the Patterson of crystals containing type (a) molecules is reasonably straightforward. The initial step is the determination of the coordinates of the heavy atoms.

### The Heavy Atom Method

It has been shown (page 12) that the height of a Patterson peak representing a vector between two atoms of atomic number  $Z_r$  and  $Z_s$  respectively is roughly proportional to  $Z_r Z_s$ . If the crystal contains relatively few atoms of high scattering power, the Patterson peaks of these 'heavy' atoms will stand out against a background of smaller peaks. It is then usually a simple matter to determine the coordinates of the heavy atoms, especially by making use of Harker regions. If partial structure factors,  $F^H(hkl)$ , are then calculated from these positions, the total structure factor is given by

$$F(hkl) = F^H(hkl) + F^L(hkl)$$

where  $F^L(hkl)$  is the structure factor contribution from the light atoms. In general,  $F^H(hkl)$  will be much greater than  $F^L(hkl)$  and the computation of a Fourier series using the phases of  $F^H(hkl)$  applied to the observed structure amplitudes should enable the location of light atoms. In the computer program available here, a rejection test can be applied where  $F(hkl)$

is excluded from the Fourier synthesis if

$$|F^H(hkl)| < x |F_o(hkl)|$$

where  $x$  is normally 0.25 - 0.33 and  $|F_o(hkl)|$  is the observed structure amplitude. In this way, structure factors to which the heavy atoms contribute very little can be excluded from the summation because of uncertainties in phase. In most cases, the first Fourier map is not clear enough to locate all the light atom peaks. The above process must be repeated several times, using at each stage the atomic positions located in the preceding map to phase the structure factors for the next. Lipson and Cochran (1953) have suggested that the method works best when the sum of the squares of the atomic numbers of the heavy and light atoms are approximately equal, i.e. each group contributes approximately equally to the average intensity.

### Image Seeking

Clastre and Gay (1950), Garrido (1950), McLachlan (1950) and Beevers and Robertson (1950) simultaneously published methods for the interpretation of the Patterson which are classed as 'superposition' methods since they involve the superposition of one Patterson map on another. These methods can be applied when the proportion of heavy atoms in the crystal is insufficient to determine the phases of a majority of the

structure factors. Since then, superposition methods have been formalised and given a rigorous theoretical treatment as image-seeking methods by M.J.Buerger, whose work from 1950 onwards is presented in his book, Vector Space (1959).

Considering the Patterson as the vector set of the electron density (page 11), solution of the Patterson can be looked upon as identifying its fundamental set. That this can be done for discrete points was first shown by Wrinch (1939), who used the term 'image' to describe, say, the point  $ab$  at the end of the vector  $\vec{ab}$ , as the way point  $b$  looks from  $a$ . Thus the Patterson can be imagined as the superposition of the images of the structure as seen from each atom in turn, each image being translated to the origin of the Patterson. Searching for these images can be carried out graphically or by using a digital computer.

A single peak in the Patterson that represents a vector between two symmetry-related atoms is first selected, (it may be useful in this respect to predict the expected peak heights based upon the height of the origin peak). For instance, this may be a heavy-atom peak from which the heavy-atom positions can be found (at points  $r_1, \dots, r_j$ ). The values of the Patterson are then compared for the set of points ( $r_1+r, r_2+r, \dots, r_j+r$ ) and  $\vec{r}$  is regarded as a vector of the fundamental set only if the Patterson at all these points is large. Buerger

(1959) describes three types of functions for testing the 'vector-end' Patterson values; the product, sum and minimum functions. The product function is defined as the product of the weighted values of the Patterson at the ends of the vectors, and the other two functions are respectively the sum and the minimum of these Patterson values. This multiple comparison is carried out right through the cell by varying the common vector  $\vec{r}$ . In the above heavy-atom example, the weight of each Patterson value will be the same, but if other atomic species are included as 'image points', the vector-end Patterson values must be weighted according to their scattering powers. Buerger discusses the merits of each image-seeking function and their relation to the electron density. He recommends the minimum function as it is simple to use and the other two tend to give false maxima. Thus a contoured map of, say, the minimum function can be obtained for the unique part of the unit cell, and the peaks will represent possible atomic positions.

If two image points are used in the search, the resulting function is said to be of rank two. Normally, this is not enough to reveal the complete structure and a stepwise procedure has to be employed, whereby functions of higher rank are computed by using as image points, atomic positions that have been determined from lower-ranking functions.

Graphically, the procedure can be carried out by preparing

a duplicate contoured map of the Patterson on tracing paper and laying it on the original map with its origin on the selected single peak of the lower map. The minimum function can then be contoured on a perspex sheet superimposed on both maps. In practice it is difficult to prepare, by this method, minimum functions of rank higher than two.

For structures of type (b) (page 16), containing no heavy atoms, the solution of the Patterson is generally quite complex. The function normally consists of clusters of unresolved peaks, some of which may not be distinguishable from the background. Recognition of single peaks becomes extremely difficult and consequently, normal image-seeking methods are unsuitable. However, in recent years, modified image-seeking methods have been developed for specific use with light-atom structures. A description of these methods is deferred until later (Chapter 7), prior to the account of attempts to solve the crystal structure of zeirin acetate ( $C_{32}H_{54}O_3$ ) by a Patterson searching method.

## CHAPTER 2

### Data Treatment and

### General Crystallographic Methods Used

All intensity data were collected photographically by the Weissenberg method using filtered  $\text{CuK}\alpha$  radiation. Two four-film exposures on Ilford Industrial 'G' were carried out for each layer, the time ratio being approximately 60 : 1. Using the equi-inclination setting for non-zero layers, the bulk of the data was collected about the shortest crystallographic axis, and between one and three layers about a second axis for data correlation. Intensities were estimated visually using calibrated 'wedges', and inter-film scales were calculated by hand. No corrections were applied for absorption. Unless the mass absorption coefficient of the crystal is very high, it is expedient to try to avoid making absorption corrections by choosing a specimen of small enough dimensions. This was done in each case and the pertinent data are given in the relevant chapters. Primary extinction is due to the interference effects of out-of-phase rays that have been 'back-reflected' into the primary and reflected beams by the stack of planes in the particular reflecting position. A large reduction in intensity can occur for strong, low-order reflexions and consequently

any suspected primary extinction was dealt with by omitting the reflexions from the structure refinement.

A series of computer programs were used to obtain a complete set of data on one relative scale. All the programs mentioned form part of a crystallographic system for the Atlas computer. Formulated mainly by M.G.B.Drew (1966), and named ATSYS, this system facilitates the handling of data and enhances continuity by the option of storing both programs and data on magnetic tape. Further details can be obtained from the reference cited and the list of references therein. In each case, the programmer's name is given, and the author, who fully appreciates the exasperation sometimes involved, is grateful to them all.

LSCD.....R.D.Diamand.

The unit cell dimensions are calculated by a least-squares method outlined by Alexander and Klug (1954). The method assumes that any systematic errors are a function of the Bragg angle,  $\theta$ , so that an error term is added to the observational equations. In this work the data were derived from Weissenberg films.

FIFI..... R.D.Diamand.

Lorentz and polarisation corrections of the form

$$(L_p)^{-1} = 2\xi \cos \theta / (1 + \cos^2 2\theta)$$

are applied to a set of intensity data, where  $\xi$  is the radial cylindrical coordinate of the reciprocal lattice point.

POLO..... M.G.B.Drew.

Procedures can be carried out as follows:

- (a) Pick out common reflexions from separate lists of data and print out their ratios. Common reflexions will be used to calculate the inter-layer scales (b), and this list usually indicates mis-indexing and other trivial mistakes.
- (b) Calculate the inter-layer scales by the least-squares method of Hamilton, Rollett and Sparks (1965), and apply them to the data.
- (c) Sort a list into any order and modify parts of the list.

LOLA..... R.A.Sparks, modified by the author.

Inter-layer scales can be calculated by the method of Rollett and Sparks (1960), now superseded by the method in POLO.

Other ATSYS programs used for calculations in this thesis are :-

MATT..... the author.

Wilson's (1942) method is applied to estimate the absolute scale and overall temperature factor, from two or



three-dimensional data. The procedure used is analogous to that outlined by Rogers (1965). The data are output to facilitate the plotting of the graph of  $\log_e(\langle I \rangle / \sigma_2)$  against  $\sin^2 \theta / \lambda^2$ , where  $\langle I \rangle$  and  $\sigma_2$  are the average values of  $|F(hkl)|^2$  (on a relative scale) and  $\sum_{r=1}^N f_r^2$  for shells of the reciprocal lattice extending over equal intervals of  $\sin^2 \theta$ . The values of B, the overall isotropic temperature factor and K, the scale to be applied to  $|F(hkl)|$  are also calculated by a simple least-squares routine.

BOSS..... M.M.Harding, modified by M.G.B.Drew.

The program is basically for the calculation of Fourier series but includes a routine to calculate structure factors from a set of atomic positions. An agreement analysis can also be prepared, i.e. a list of  $\sum F_o(hkl)$  and  $\sum F_c(hkl)$  and R for various groups of reflexions where k

$$R = \frac{\sum k \left| |F_o| - |F_c| \right|}{\sum k |F_o|}$$

is the scale factor and  $F_c$  the calculated structure factor, (adopting the more convenient notation), and the summations are over the appropriate groups of reflexions.

DIDO..... R.A.Sparks, modified by the author.

Using the eigenvalue method outlined by Rollett (1965)

the best plane through a set of specified atoms is calculated together with the distances of other atoms from this plane.

BABA..... R.D.Diamand, modified by M.G.B.Drew.

The program calculates structure factors from input atomic coordinates and refines, by a block diagonal, least-squares method, positions, temperature factors and an overall scale. The anisotropic temperature factors are of the form  $\beta_{ij}$  where the contribution to the structure factor is

$$\exp. - (\beta_{11}h^2 + \beta_{22}k^2 + \beta_{33}l^2 + \beta_{12}hk + \beta_{13}hl + \beta_{23}kl)$$

The method is essentially that outlined by Cruickshank (1961). The scale, applied to  $F_o$ , is coupled with an overall temperature factor in a 2 x 2 matrix, and 3 x 3 and 6 x 6 matrices are computed for positions and anisotropic vibrations respectively. The function minimised is

$$\sum w (k |F_o| - |F_c|)^2$$

where  $\sqrt{w}$  is the weight applied to each observation. The weighting scheme used is that described by Rollett (1961) where

$$\sqrt{w} = F^+ / F_o \quad \text{if } F_o > F^+$$

$$\sqrt{w} = 1 \quad \text{if } F_o < F^+$$

The value of  $F^+$  can be chosen from the agreement analysis of

BOSS to give roughly constant values of  $\sum w (|F_o| - |F_c|)^2$  (i.e.  $w\Delta^2$ ) over ranges of  $|F_o|$ .

The program also optionally applies a 'fudge factor' for modification of parameter shifts. This is particularly useful to dampen the oscillation of non-centrosymmetric structures whose origin is not defined.

ELSI..... R.D.Diamand and M.G.B.Drew.

Bond distances and angles are calculated and their standard deviations. The variances of the normal equations obtained from BABA are used to calculate the standard deviations, which are thus lower than their true value as most of the off-diagonal terms are ignored. The formula used for the estimation of the standard deviation,  $\sigma$ , of a variable  $x_r$  is that of Cruickshank (1959) where

$$\sigma^2(x_r) = V_{rr} \sum w \Delta^2 / (m - n)$$

$V_{rr}$  is the variance of the parameter  $x_r$ ,  $m$  the number of observations and  $n$  the number of parameters refined.

A limited number of programs have been used from the 'X-Ray '63' system for the I.B.M. 7090. Thanks are extended to the authors (mentioned in the text) and especially J.Stewart who was chiefly responsible for making the programs available at Imperial College.

### CHAPTER 3

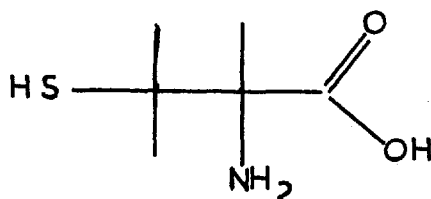
## Chemistry of the Penicillins and Cephalosporins.

### The Penicillins.

That the antibiotic penicillin is produced from a mould, later identified as a strain of *Penicillium notatum*, was first observed by Fleming (1929). Penicillin is active against a large number of organisms such as *Diplococcus pneumoniae* (pneumonia organism), *Streptococcus pyogenes* (associated with scarlet and rheumatic fevers) and *Staphylococcus aureus* (skin infections), but early clinical use was limited by its instability. This also complicated the chemical work on the structure of penicillin and a further difficulty was that certain bacteria secrete an enzyme, penicillinase, which inactivates the antibiotic. Nevertheless, the potentialities of penicillin for full-scale use against many infectious diseases led to some very intense work from 1940-45. During this period of the Second World War, chemical information was restricted and consequently, an historical account of the structure determination is complex. The following outline of the fundamental chemical points, for which no references are given, was taken from 'The Chemistry of Penicillin', edited by Clarke,

Johnson and Robinson (1949).

The first solid forms of penicillin, though stable when dry, were soon found to be inhomogeneous, and it was not until 1943 that a chemically pure compound possessing the properties of penicillin was isolated. Further studies showed that more than one such compound existed, and the chemical differences between them soon became evident. Hydrolytic degradation of the individual penicillins gave, in each case, the same sulphur-containing amino-acid, penicillamine (I), carbon dioxide and a penillo-

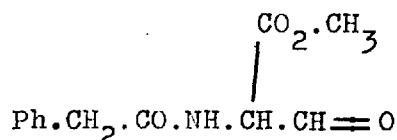


(I)

aldehyde ( $R.CO.NH.CH_2.CH:O$ ). The structure of (I) was confirmed by synthesis, its absolute configuration being D. The chemical differences between the penicillins were attributed to the identity of the group R in the penilloaldehydes. This provided a basis for nomenclature, so that with  $R = C_6H_5.CH_2$  the parent penicillin was given the name benzylpenicillin.

Although the penicillins are strong monobasic acids, the action of methanol on benzylpenicillin under mild conditions, gave a monomethyl ester of a dibasic acid, benzylpenicilloic acid.

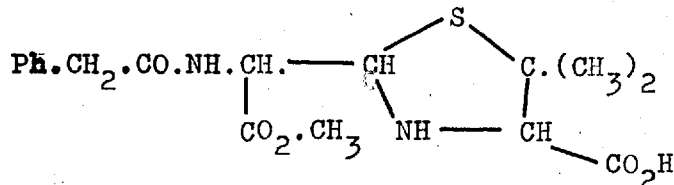
This indicated that the penicillins also contain a labile, but 'masked' carboxyl group, since esterification of free carboxyl groups normally takes place under more vigorous conditions. The monomethyl ester of benzylpenicilloic acid was further degraded to penicillamine (I) and the benzylpenaldic ester (II). Further hydrolysis of the latter compound gave benzylpenaldic acid which



(II)

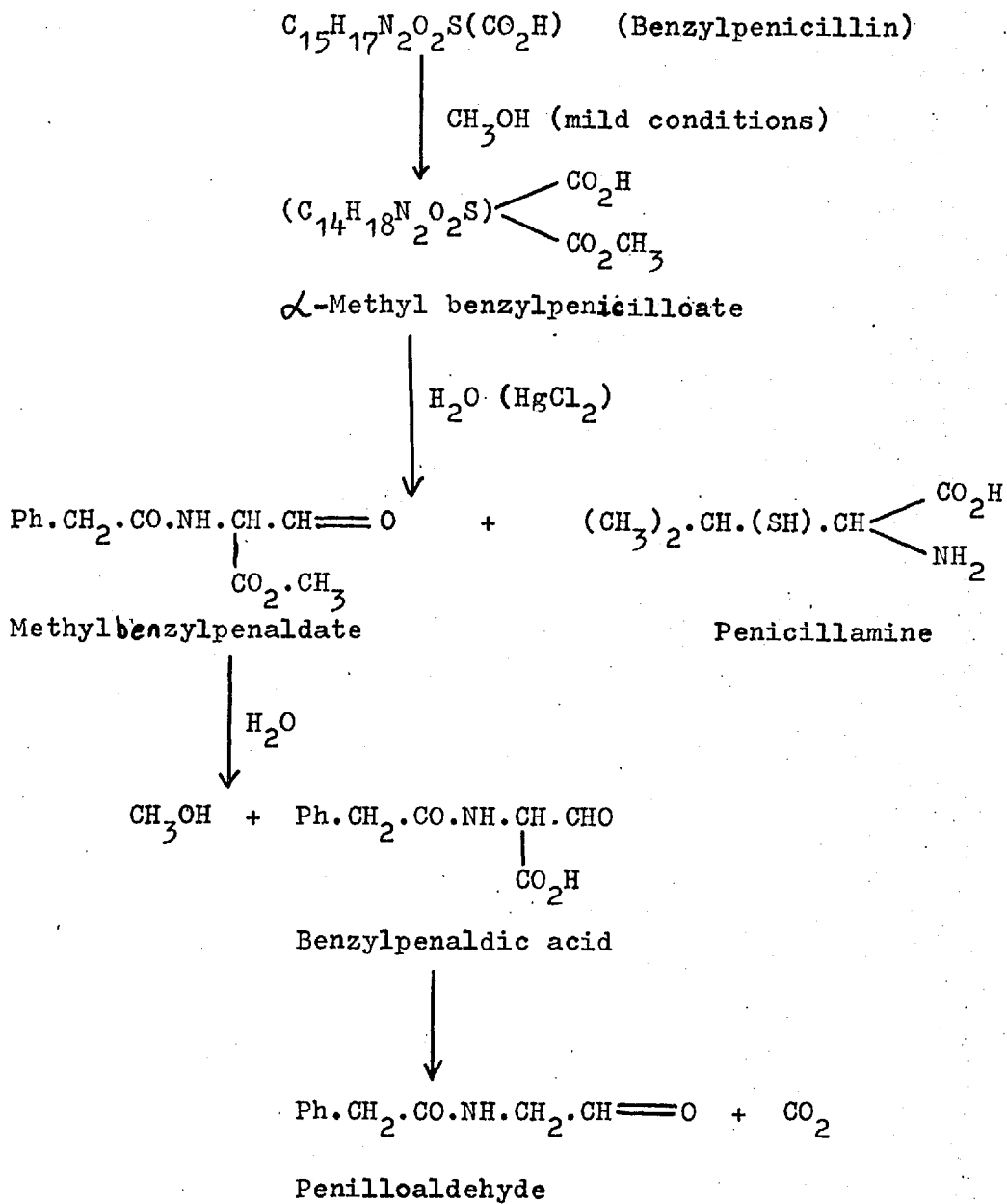
loses carbon dioxide to give benzylpenilloaldehyde.

These reactions are indicated schematically in Figure 1, and showed the free carboxyl group to be associated with the penicillamine residue, and the masked group with the penilloaldehyde. It had also been demonstrated that penicillamine yielded thiazolidines on condensation with carbonyl compounds and consequently, the monomethyl ester of benzylpenicilloic acid was formulated as (III), which was supported by synthesis.

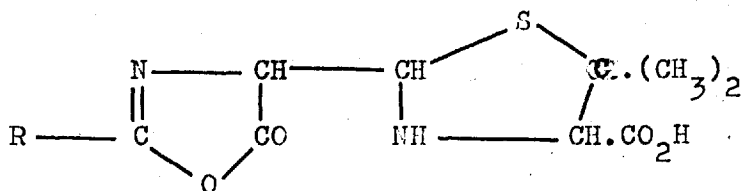


(III)

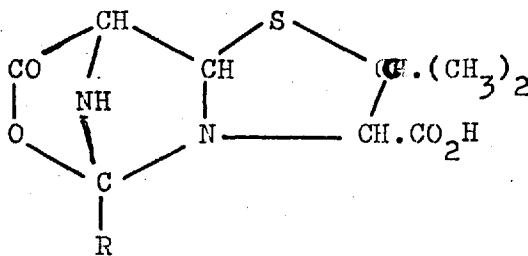
Figure 1.



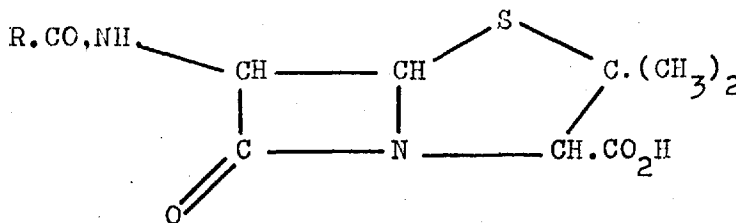
Thus, for the organic chemists, the problem was reduced to postulating a linkage, working from (III), that would explain the masked carboxyl group of the penicillins. However, any postulated structure also had to satisfy other criteria that had arisen during the very exhaustive chemical work. Three main structural formulae were proposed, namely the oxazolone (IV), tricyclic (V) and  $\beta$ -lactam (VI).



(IV) Oxazolone



(V) Tricyclic

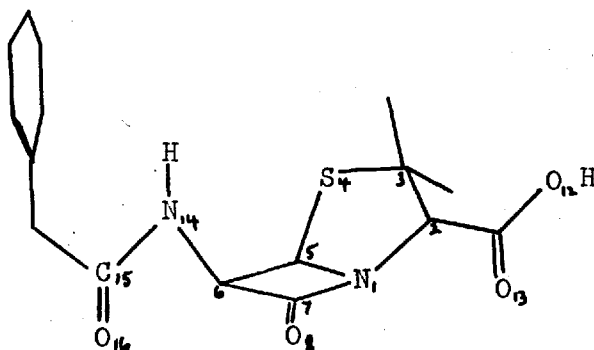
(VI)  $\beta$ -Lactam



The  $\beta$ -lactam structure gradually became the most popular, and was finally confirmed by an X-ray analysis by Crowfoot, Bunn, Rogers-Low and Turner-Jones (1949).

Two-dimensional X-ray investigations were carried out on the sodium, potassium and rubidium salts of benzylpenicillin. The latter two salts are isomorphous and the Patterson series was used to locate approximately, the metal ion positions. Unfortunately, it was found that the heavy atoms contributed to only a limited number of reflexions, so that the Fourier maps were difficult to interpret except that the sulphur atom was located. The sodium salt was examined by optical methods and the derived Fourier maps were little better than those from the isomorphous salts. However, by comparison of the two sets of Fouriers it became clear that the molecule existed as a 'curled' configuration, not extended as had previously been thought, and when the results were viewed without bias towards any of the proposed structures (the oxazolone structure was originally taken as model), the adoption of trial positions and subsequent refinement, led to the  $\beta$ -lactam structure (VI) for benzylpenicillin. The general configuration of the molecule is represented by (VII). The thiazolidine ring is not planar,  $C_2$  lies out of the plane of the other atoms on the opposite side to  $C_7$  and similarly,  $O_8$  projects out of the plane of the  $\beta$ -lactam ring system towards the sulphur atom. The amide group in the phenylacetyl side-chain

is planar and possesses dimensions of a normal amide.

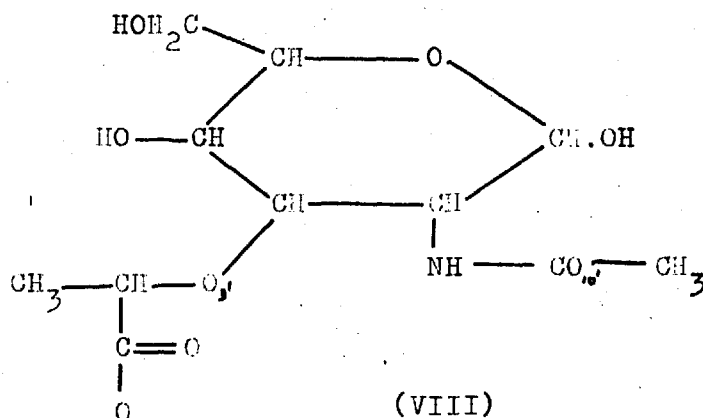


(VII)

The crystal structure of phenoxymethylpenicillin has been determined by Abrahamsson, Crowfoot Hodgkin and Maslen (1963). The molecule shows marked similarities in the general configurations of the thiazolidine and  $\beta$ -lactam rings to those in benzylpenicillin. The main difference is that in benzylpenicillin, the plane of the benzene ring is approximately parallel to the  $\beta$ -lactam-thiazolidine system, whereas in phenoxymethylpenicillin, the benzene ring is considerably inclined to this system. The differences may be largely due to packing considerations in the crystals.

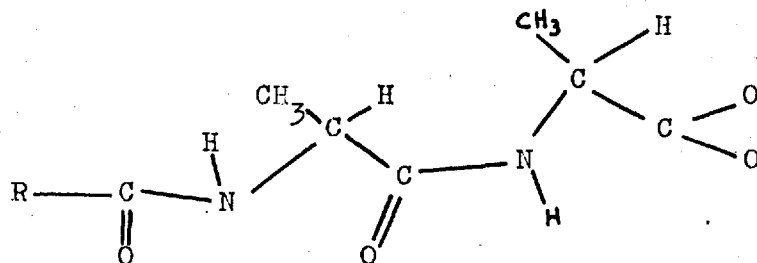
In 6-aminopenicillanic acid (6-APA), as determined by Diamand (1963), the out-of-plane atom in the thiazolidine ring is  $N_1$ , which is projected on the same side of the plane as  $N_{14}$ . This is in contrast to the situation in the other two penicillins where  $C_2$  deviates most from the best plane.

The mechanism by which penicillin kills bacterial cells is still not clear. Evidence has been presented by Park and Strominger (1957) that the antibiotic interferes with the synthesis of the bacterial cell wall, by reacting preferentially with an enzyme binding site that normally takes part in cell-wall synthesis. Collins and Richmond (1962) suggested that penicillin may bind to the enzyme in preference to some derivative of N-acetylmuramic acid (VIII). They point out that



in one of the permissible conformations of N-acetylmuramic acid, the carboxyl group can occupy the same position as that in benzylpenicillin and similarly  $O_3'$  and  $O_{10}'$  in N-acetylmuramic acid can occupy identical positions to  $N_1$  and  $O_{16}$  in benzylpenicillin. They further suggest that the binding of the N-acetylmuramic acid residue to an 'active centre' will depend primarily on ionic and hydrogen-bonding forces, and that the high affinity of penicillin for the active centre could be explained by the fact that the possible hydrogen-bonding group  $O_8$ , has no counterpart in N-acetylmuramic acid. Similar considerations can be applied to the cephalosporins.

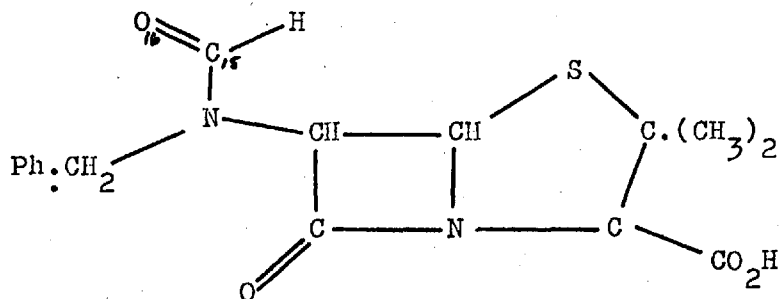
Tipper and Strominger (1965) have suggested that penicillin interferes with cell-wall synthesis by binding to an active centre in preference to an acyl-D-alanyl-D-alanine (IX), and



(IX)

not N-acetylmuramic acid. They show that similar spatial considerations apply as in Collins and Richmond's hypothesis described previously.

6-(N-Benzylformamido)penicillanic acid (6-NBF-PA) represented by (X), is an isomer of benzylpenicillin but Housley

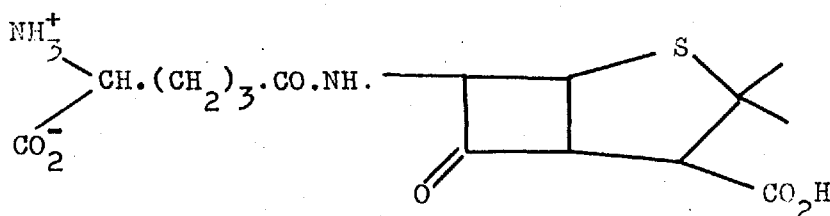


(X)

and Spooner (1965) have measured its antibiotic activity as less than one ten-thousandth of that of benzylpenicillin. A three-dimensional X-ray study (described in Chapter 4) has been undertaken mainly to determine the positions of the hydrogen-bonding groups. These studies have, in fact, shown that the carbonyl group  $C_{15} - O_{16}$  is on the 'wrong' side of the molecule, in terms of Collins and Richmond's explanation, to participate in possible hydrogen bonding to an active centre, and hence its low antibiotic activity is consistent with their theory.

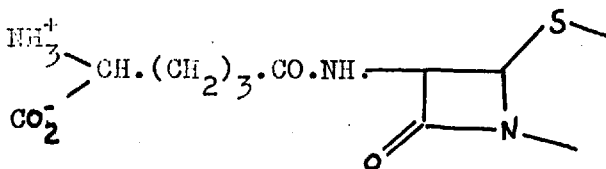
## The Cephalosporins

The isolation of cephalosporin C (ceph. C) has been described by Newton and Abraham (1955). A species of the mould 'cephalosporium' produced a mixture of penicillin N (XI), and



(XI)

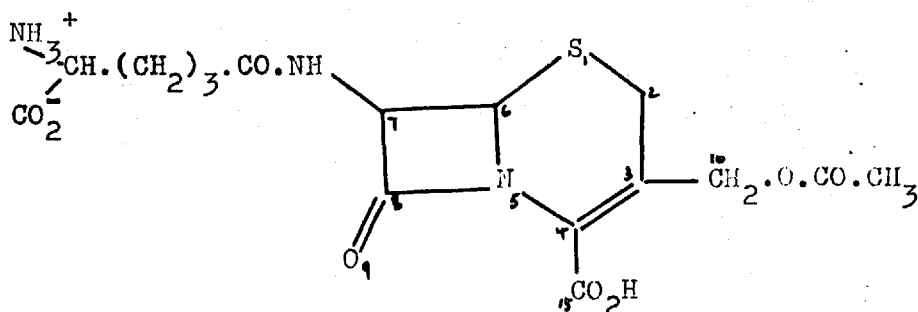
another antibiotic, ceph. C. Chemical evidence given by Abraham and Newton (1961) for the structure of ceph. C indicated a monoamino dicarboxylic acid present as a residue of  $\alpha$ -amino-adipic acid linked to the rest of the molecule by its  $\delta$ -carboxyl group. The infra-red absorption spectrum of the sodium salt showed a maximum at  $5.62\mu$ , which is close to the carbonyl stretching frequency of the  $\beta$ -lactam ring in the penicillins. This fact and the results of hydrogenolysis experiments indicated the presence of the part structure (XII).



(XII)

These initial lines of enquiry were based on the assumption that ceph. C contained the characteristic skeleton of the penicillins, although the ultra-violet absorption spectrum of ceph. C showed a maximum at  $260\text{ m}\mu$ , which could not be explained in terms of the fused four and five-membered ring system. Further chemical work and nuclear magnetic resonance spectroscopy threw more doubts on this hypothesis, which was thus rejected.

Abraham and Newton then proposed the structure (XIII),



(XIII)

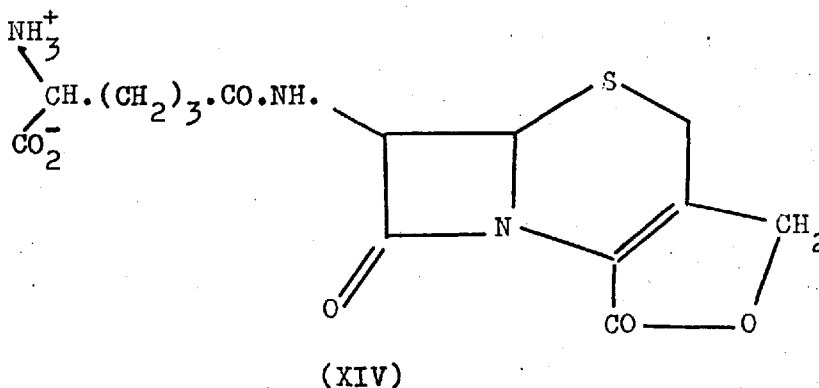
which was consistent with all the chemical reactions, while the 3-4 double bond would account for the U.V. maximum at  $260\text{ m}\mu$ . However, the possibility of other structures, especially those with a 2-3 double bond were not excluded.

Before any further chemical evidence became available regarding this structure, the X-ray analysis by Crowfoot Hodgkin and Maslen (1961) indicated the presence of a six-membered ring containing sulphur. Thenceforward, the chemical and X-ray crystallographic progress was rapid, and both finally substantiated the structure (XIII) for ceph. C.

The full X-ray analysis was complicated by the low

reflecting power and rapid deterioration of the crystals. Consequently, the accuracy achieved was limited but the analysis showed that the atoms  $C_2$ ,  $C_3$ ,  $C_4$ ,  $N_5$ ,  $C_{10}$  and  $C_{15}$  form a plane with  $S_1$  about 0.6 Å above the plane, and  $C_6$  about 0.6 Å below it. The length of the bond  $C_3 - C_4$  (1.31 Å) is in agreement with its formulation as a double bond. The carbonyl group of the amide is nearly normal to the  $\beta$ -lactam ring and the protons at  $C_6$ ,  $C_7$  are cis and in the same configuration as in the penicillins.

Lactonisation of ceph. C by hydrochloric acid at room temperature produces another antibiotic, ceph. Cc, represented by (XIV). The X-ray analysis of ceph. Cc (carried out by

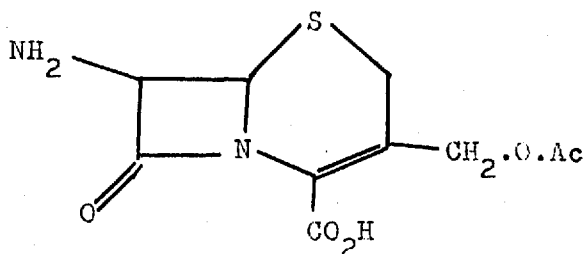


Diamand (1963)) has confirmed the general configuration of the molecule and provided quite accurate bond lengths, the true standard deviations probably being 0.02 - 0.03 Å.

The biological activity of the cephalosporins has been studied by Newton and Abraham (1956). Ceph. C shows only 0.1 %

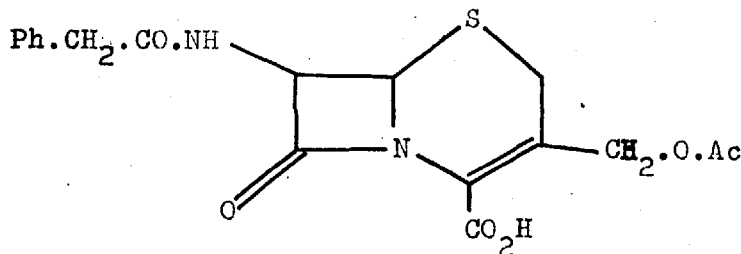


of the activity of benzylpenicillin against *Staph. aureus*, but is relatively stable to penicillinase. By analogy with the penicillins Loader, Newton and Abraham (1961) suggested that the substitution of, say, a phenylacetyl group for the  $\alpha$ -aminoadipic acid residue in cephalosporin C might produce more active compounds that would still be stable to penicillinase. Treatment of cephalosporin C with dilute acid at room temperature produced the cephalosporin C nucleus, 7-aminocephalosporanic acid (XV), which although



(XV)

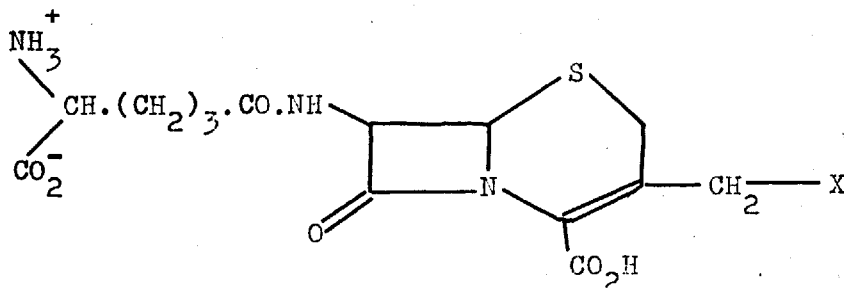
biologically inactive itself, was acylated to give 7-phenylacetamidocephalosporanic acid (XVI). This possesses approximately



(XVI)

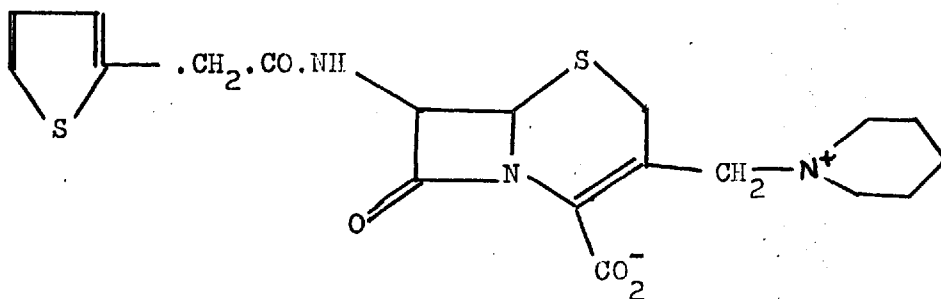
one hundred times the activity of ceph. C against *Staph. aureus*, i.e. similar to benzyl penicillin but more stable to penicillinase.

Another interesting reaction of ceph. C was observed by Hale, Newton and Abraham (1961). The acetoxy group in ceph. C can be displaced by nucleophiles, especially hetero tertiary bases such as pyridine. The resulting compounds, known as the ceph. C<sub>A</sub> family, show increased antibacterial activity and are represented by (XVII), X = pyridine etc.



(XVII)

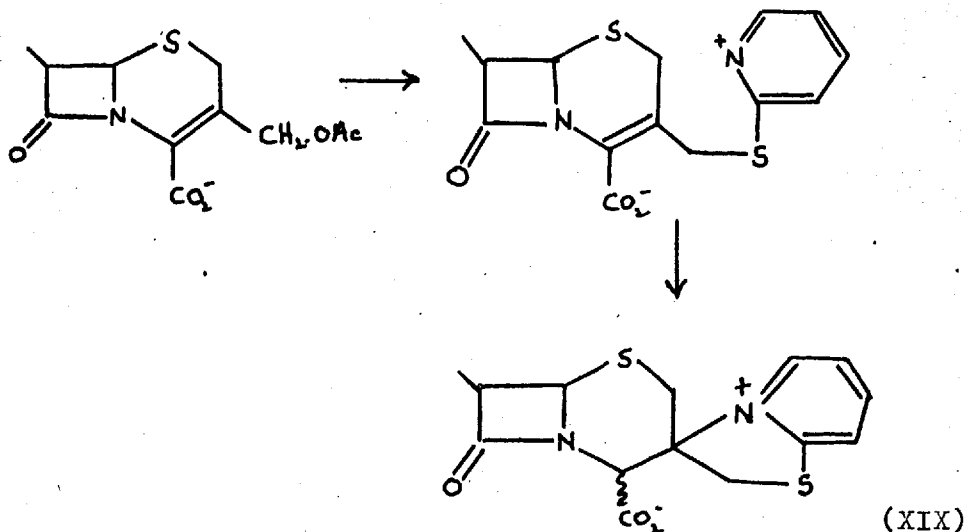
Muggleton, O'Callaghan and Stevens (1964) have prepared many analogues of ceph. C, in which both the  $\alpha$ -amino adipic acid side-chain and the acetoxy group were replaced. Their work led to the production of cephaloridine (XVIII) (Trade name 'Ceporin')



(XVIII)

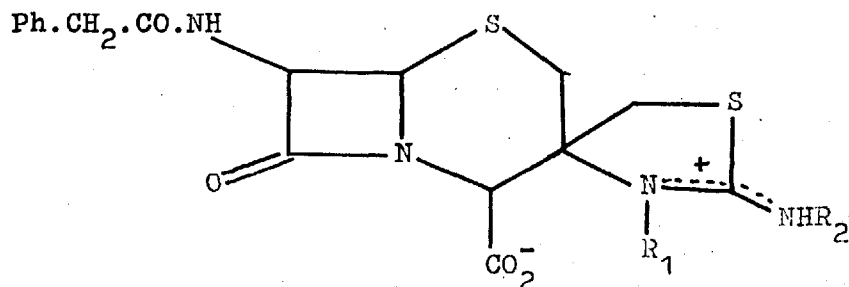
Glaxo Ltd.), a highly active antibiotic of low toxicity.

Cocker et al. (1965) have replaced the acetoxy group in ceph. C with sulphur nucleophiles such as thiourea, and Fazakerly et al. (1965) produced spirocyclic compounds by the reaction of certain bidentate nucleophiles with 7-phenylacetamido cephalosporanic acid. Nucleophiles such as pyrid-2-thione and thio-uracil give products that lack the U.V. absorption maximum at  $260\text{ m}\mu$ , and it was suggested that the reaction, which is illustrated below for pyrid-2-thione, is a two-stage process.



First, the acetoxy group is displaced from the cephalosporanic acid derivative by the sulphur end of the nucleophile, followed by internal Michael addition by the nitrogen atom giving compounds of type (XIX), with a spiro atom at the 3 position. The spiro compounds are dextrorotatory and possess weak antibacterial activity. A substance thought to be the thiazolinium

derivative (XX),  $R_1, R_2 = Et, H$  or  $H, Et$  was formed when

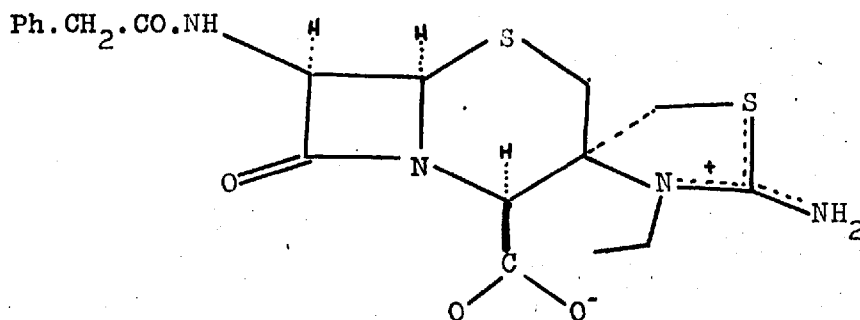


(XX)

7-phenylacetamidocephalosporanic acid and N-ethylthiourea were mixed in aqueous solution at  $37^{\circ}$  for several days. Electrophoresis experiments, together with an I.R. absorption maximum at  $1610 - 1630 \text{ cm}^{-1}$  due to an ionized carboxyl group, indicated that it occurred as a zwitter-ion. The compound possesses only one fifteenth of the anti-bacterial activity of 7-phenylacetamidocephalosporanic acid against *Staph. aureus* (Long (1966)). If (XX) is correct it contains two new centres of asymmetry.

The prospects of determining the detailed stereochemistry of this molecule by any means other than X-rays seemed poor. Thus, as a three-dimensional X-ray determination has been carried out to determine the stereochemistry at the asymmetric centres, and to study the conformations of this new tricyclic system. The results, which are reported in Chapter 5, indicate that (XX)

is essentially correct, but should be written more precisely as (XXa).



(XXa)

CHAPTER 4

The Crystal Structure of  
6-(N-Benzylformamido)penicillanic Acid

Preliminary Data

The crystals were prepared and the compound characterized by J.R.Housley and D.F.Spooner of the Boots Pure Drug Co. Ltd., Nottingham and supplied to the author by J.F.Collins of the Medical Research Council, Mill Hill, London. After treating 6-benzylaminopenicillanic acid at room temperature with an ethereal solution of acetic formic anhydride, 6-NBF-PA was crystallized from ether/light petroleum (40° - 60°) at 0° C mainly as clusters of ill-formed, monoclinic needles, elongated along [010]. The solution in dioxan is dextrorotatory with  $[\alpha]_D^{25} = +351^\circ$ . The structural formula and numbering scheme are shown in the pull-out diagram inside the back cover.

Formula  $C_{16}H_{18}O_4N_2S$  Molecular Weight (formula) = 335

Mass absorption coefficient for  $CuK\alpha, \mu = 1.85 \text{ cm}^{-1}$

Unit-cell dimensions

$a = 19.58$  (0.01 Å),  $b = 6.427$  (0.003) Å,  $c = 13.98$  (0.006) Å  
 $\beta = 108.0^\circ$  (0.1),  $V = 1673 \text{ Å}^3$ ,  $Z = 4$   $F(000) = 704$  electrons.

$$D_{\text{obs}} (\text{by flotation}) = 1.33 \text{ g.cm}^{-3} \quad D_{\text{calc}} = 1.33 \text{ g.cm}^{-3}$$

Absent Spectra:

only among hkl for  $h + k = 2n + 1$

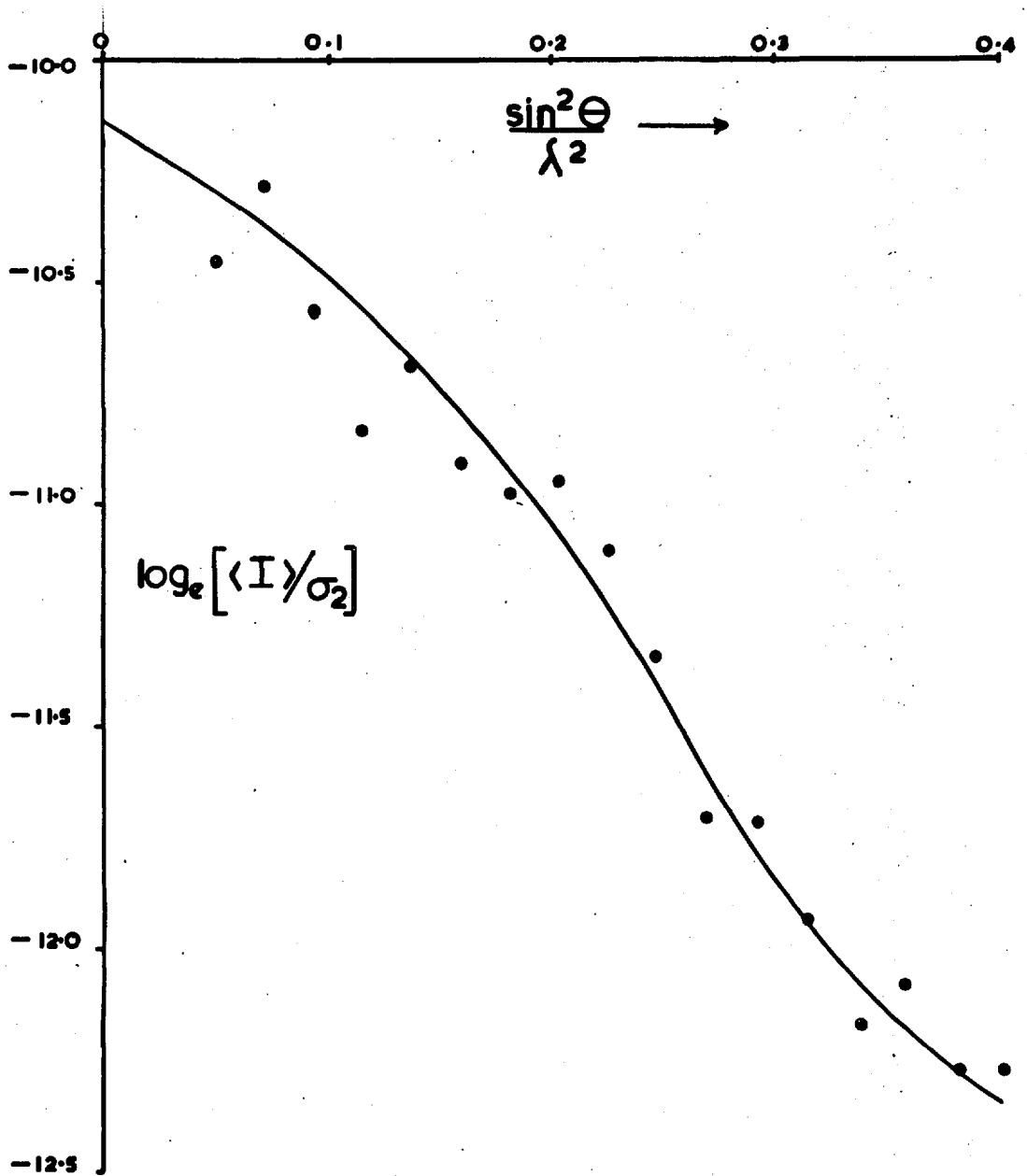
The compound is optically active, so that the spacegroup is uniquely determined as C2. 1580 independent reflexions were estimated visually and correlated from six layers collected about the b axis and reflexions from the zero layer about the c axis. The crystal used for the collection of the main axis data had the approximate dimensions 0.50 x 0.15 x 0.10 mm. and in view of the value of the absorption coefficient ( $18.5 \text{ cm}^{-1}$ ) absorption corrections were considered unnecessary.

A Wilson plot based on three-dimensional data was calculated by MATT and is shown in Figure 1. The data were divided into 17 shells, each containing 90 - 110 reflexions. Unobserved reflexions were included as  $|F_{\text{unobs}}| = 2/3 |F_{\text{min}}|$ , where  $|F_{\text{min}}|$  is the minimum observable value of  $|F|$  at the appropriate point in reciprocal space. The least-squares method gave  $B = 2.98$ ,  $K = 145.9$  and the results from the graph are  $B = 2.64$ ,  $K = 159.2$ . (After structure refinement the final scale was found to be 131.4.)

### Structure Determination

The four sulphur atoms in the unitcell give rise to  $\frac{1}{2}$  six S - S inter-vectors which overlap to give  $\frac{1}{2}$  three

Figure 1. 6-NBF-PA Wilson plot based on three-dimensional data.





distinct peaks in the three-dimensional Patterson. In terms of the coordinates  $x, y, z$  of one of the sulphur atoms their positions are given by

$$\pm \begin{cases} 2x, 0, 2z \\ \frac{1}{2}, \frac{1}{2}, 0 \\ 2x + \frac{1}{2}, \frac{1}{2}, 2z \end{cases}$$

Only the first peak need be considered as the second and third are merely related to the origin and first peaks respectively by the C-face centering of the spacegroup.

The  $[010]$  Patterson projection was computed with each  $|F|^2$  term modified by its value of  $(Lp)^{-1}$  as a crude sharpening function. The position of the S - S peak could not be unambiguously assigned, and of the four most likely peaks, the highest was chosen to give the tentative sulphur position of  $x = 0.205, y = 0.0, z = 0.208$  (Coordinates of the peak were estimated by Booth's (1948) method.).

A solution of the crystal structure directly from the sulphur position was attempted using the FATAL program written by J. Rollett for the Mercury computer. The program was used to calculate structure factors from the above sulphur position, then compute a three-dimensional Fourier map and finally to search the Fourier map for peaks above a certain height. Six additional peaks were recognised possessing geometry reasonably consistent with that of a fused  $\beta$ -lactam-thiazolidine ring system. However, when the additional positions were input to

a second FATAL run, the R value increased from 0.58 to 0.62 and the resulting peaks showed no indication of any further structural details. The method was therefore abandoned (Only two of the additional peaks were near final atomic positions).

In order to check the position of the sulphur atom, a three-dimensional Patterson function was computed using as sharpening function

$$1/f^2 \exp(-3 \sin^2 \theta / \lambda^2)$$

where  $f$  is the form factor for sulphur and the resulting Patterson is specifically sharpened for sulphur peaks. The S - S peak was easily located in the Harker section  $P(u, 0, w)$  and gave the position of the sulphur atom as  $x = 0.206$ ,  $y = 0.0$ ,  $z = 0.214$ , which is close to that derived from the  $[010]$  Patterson projection. It was thought that the FATAL method may have failed because the sulphur atom was not heavy enough to determine unambiguously enough of the phases, the ratio  $\sum Z_H^2$  to  $\sum Z_L^2$  being only 0.27. Even though Fourier methods, applied carefully, may have led to the solution of the structure, it was felt that superposition methods would provide a simpler route.

Duplicate copies of the  $(u, w)$  sections of the sharpened, three-dimensional Patterson were prepared on tracing paper and contoured at arbitrary but uniform intervals. The origin of the zero section was then laid on the S - S peak of the duplicate

and the minimum function plotted on a perspex sheet by drawing the minimum contours of coincident peaks in the superposed Pattersons. The other sections were paired off with their duplicates using an identical  $u, w$  displacement. The resulting minimum function was of rank two as the procedure was equivalent to selecting as image points the two sulphur atoms at  $x = 0.206$ ,  $y = 0$ ,  $z = 0.214$  and  $x = -0.206$ ,  $y = 0$ ,  $z = -0.214$ , i.e. related by a diad. Thus the origin of the minimum function was situated half-way along the  $u, w$  displacement.

Figure 2 is a composite diagram derived from all the sections of the minimum function. The mirror plane of the Patterson spacegroup,  $C2/m$ , is not eliminated in this function, which contains a pseudo mirror plane through  $y = 0$ . Although this rendered the  $y$  coordinates ambiguous, the main structural features of the molecule were recognisable, as shown in Figure 2. However, the structure near  $N_{14}$  was ambiguous, though the cluster of peaks to the left of this strongly suggested the location of the benzene ring, giving the molecule a curled conformation as in benzylpenicillin. (This was in fact later vindicated).

Three-dimensional structure factor and Fourier calculations were carried out including the fourteen positions marked in Figure 2. The Fourier map, in which the pseudo mirror plane was now eliminated, gave unambiguous peaks for all 23 atoms, and

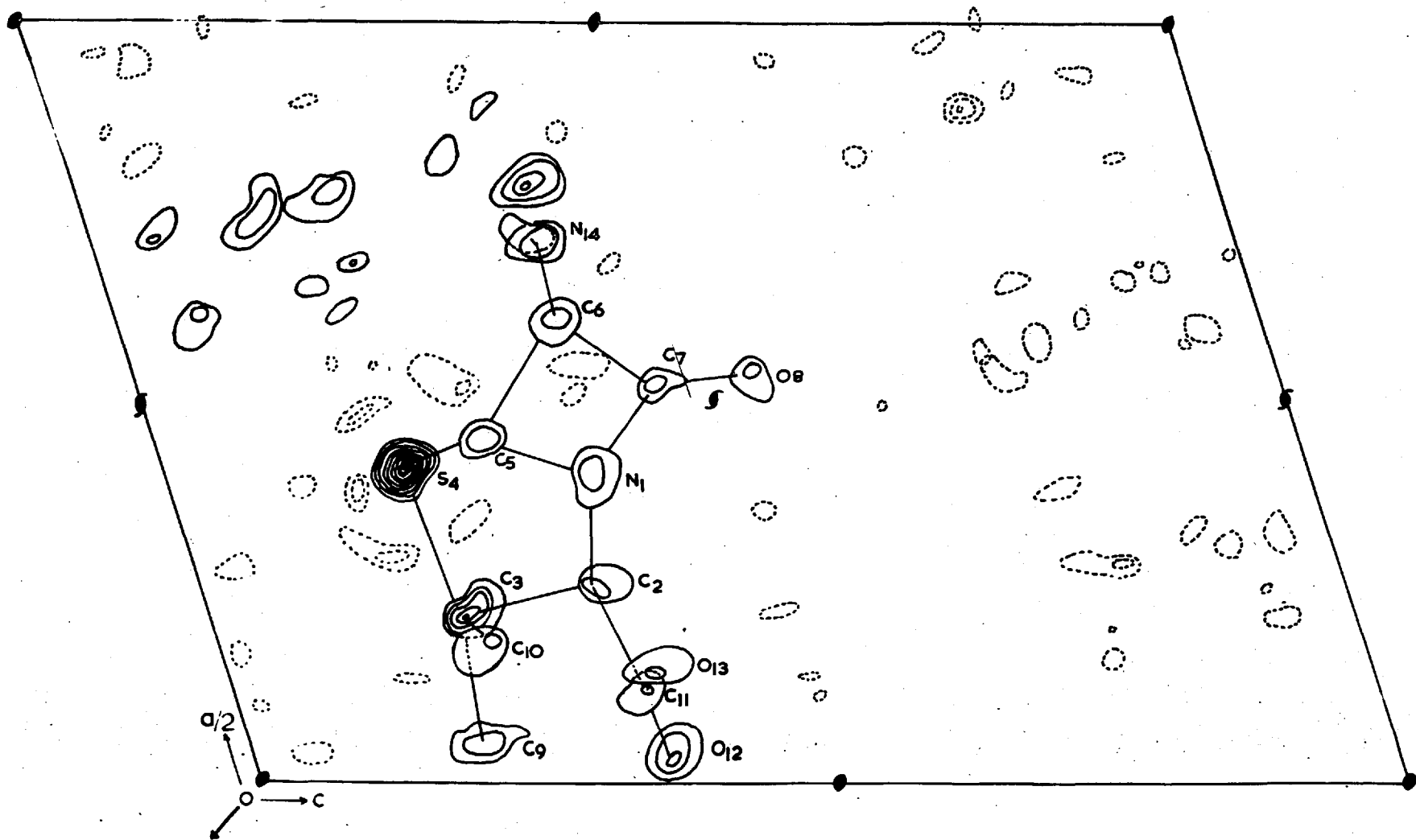


Figure 2. Composite diagram derived from sections of the minimum function.

indicated that C<sub>9</sub> and C<sub>10</sub> had been misplaced. The details near N<sub>14</sub> were clarified and showed that C<sub>15</sub> and O<sub>16</sub> (diagram inside back cover) were projecting 'down' as seen in Figure 2. The suggested position of the benzene ring was confirmed. Before starting least-squares refinement, a Fourier map phased on all 23 atomic positions was calculated and when deriving the revised atomic positions, double shifts were applied to the observed peak positions as recommended by Donohue (1950).

### Refinement

Rollett's Mercury program for the least-squares refinement of parameters was now used to refine the atomic coordinates and isotropic temperature factors for all 23 atoms. The method is essentially that used in BABA and described briefly in Chapter 2. Rollett's weighting scheme 2 was used and checks were made at various stages of refinement with an agreement analysis program written by G.A.Mair and the bond distances and angles program of R.A.Sparks.

The course of the refinement is shown in Table 1. At cycle A6, all the thermal parameters were converted into their anisotropic form but only the sulphur coordinates and thermal parameters refined. The anisotropic refinement was then continued including all atoms and switched to the Atlas program

Table 1. The refinement process for 6-NBF-PA

Cycle	R	$\sum w\Delta^2 \times 10^{-4}$
I1	0.308	16419
I2	0.225	10393
I3	0.188	8184
I4	0.179	7134
I5	0.167	5838
A6	0.154	4622
A7	0.140	3544
A8	0.105	1314
A9	0.099	990
A10	0.127	3177
A11	0.102	2154
A12	0.096	1951
A13	0.095	1912
A14	0.095	1894
A15	0.109	2398
A16	0.106	2197
A17	0.106	2179
A18	0.106	2169
A19	0.103	2038
A20	0.101	1989
A21	0.100	1984
A22	0.100	1982
A23	0.100	1981
A24	0.100	1981
A25	0.100	1980
A26	0.100	1980
A27	0.100	1980

I = isotropic refinement

A = anisotropic refinement

BABA at A8. (The  $F^+$  value in the weighting scheme was inadvertently decreased at A8 but corrected again at A10). During cycles A12, A13 and A14 it was noted that little convergence was taking place and that the refinement was oscillatory. Thus 164 unobserved reflexions were included at  $\frac{2}{3}F_{\min}$  and a fudge factor of 0.75 applied. The process was again disturbed at A18 when the calculated positions of the 18 hydrogen atoms were included in the structure factor calculations but not refined. Hydrogen atom positions were calculated on an X-Ray '63 program written by D.F.High, assuming staggered conformations for the C<sub>9</sub> and C<sub>10</sub> methyl groups. An earlier difference Fourier showed peaks at or near the calculated hydrogen atom positions varying in height from 0.1 to 0.6 e/A<sup>3</sup> but the difference map exhibited ripple as high as 0.5 e/A<sup>3</sup> and cannot be taken as conclusive evidence for the hydrogen atom positions - the positions of the methyl hydrogens were especially ill-defined.

Subsequent refinement was extremely slow, and at A27 the coordinate shifts were less than one tenth of their standard deviations, so that refinement was ceased.

### Results and Discussion

The final atomic coordinates are shown in Table 2, together with their standard deviations, and the anisotropic

Table 2. Atomic coordinates and standard deviations for  
6-(N-benzylformamido) penicillanic acid (fractional values).

	X	Y	Z	$\sigma_x$	$\sigma_y$	$\sigma_z$
N1	0.19398	0.19816	0.36500	0.00027	0.00135	0.00042
C2	0.12891	0.06769	0.34228	0.00035	0.00140	0.00056
C3	0.11559	-0.01477	0.23186	0.00035	0.00200	0.00056
S4	0.20502	-0.00849	0.21308	0.00009	0.00058	0.00014
C5	0.23075	0.21859	0.28823	0.00036	0.00160	0.00054
C6	0.30337	0.22048	0.37611	0.00034	0.00161	0.00054
C7	0.25648	0.16794	0.41425	0.00033	0.00163	0.00055
O8	0.26642	0.12197	0.52951	0.00027	0.00123	0.00038
C9	0.08592	-0.22774	0.22020	0.00057	0.00203	0.00087
C10	0.06584	0.13802	0.15406	0.00051	0.00232	0.00066
C11	0.06760	0.19723	0.35791	0.00034	0.00166	0.00057
O12	0.01415	0.07078	0.36209	0.00030	0.00118	0.00058
O13	0.06669	0.38004	0.36511	0.00031	0.00127	0.00056
N14	0.35902	0.07255	0.37699	0.00029	0.00116	0.00047
C15	0.35506	-0.12767	0.39730	0.00041	0.00166	0.00064
O16	0.39630	-0.26675	0.38916	0.00030	0.00122	0.00050
C17	0.41454	0.14853	0.33327	0.00036	0.00157	0.00060
C18	0.38742	0.15183	0.21828	0.00043	0.00177	0.00070
C19	0.38852	-0.02767	0.16578	0.00066	0.00256	0.00079
C20	0.36315	-0.03048	0.06097	0.00089	0.00299	0.00085



Table 2 continued

	X	Y	Z	$\sigma_x$	$\sigma_y$	$\sigma_z$
G21	0.33591	0.15432	0.01082	0.00090	0.00327	0.00096
G22	0.33318	0.33570	0.06531	0.00077	0.00299	0.00100
G23	0.36263	0.33517	0.16991	0.00064	0.00219	0.00090

Table 3. Anisotropic temperature factor coefficients for  
6-NBF-PA.

	$\beta_{11}$	$\beta_{22}$	$\beta_{33}$	$\beta_{23}$	$\beta_{13}$	$\beta_{12}$
N1	0.00076	0.02892	0.00363	-0.00141	0.00102	0.00000
C2	0.00126	0.01857	0.00476	-0.00145	0.00197	-0.00075
C3	0.00141	0.02953	0.00482	-0.00397	0.00060	0.00063
S4	0.00172	0.03483	0.00469	-0.00725	0.00226	-0.00134
C5	0.00152	0.02347	0.00402	0.00054	0.00170	-0.00120
C6	0.00120	0.02536	0.00431	-0.00098	0.00205	-0.00169
C7	0.00098	0.02762	0.00436	-0.00276	0.00128	-0.00011
O8	0.00184	0.03298	0.00399	-0.00110	0.00168	0.00392
C9	0.00359	0.02473	0.00924	-0.01337	0.00471	-0.00704
C10	0.00269	0.04859	0.00430	-0.00059	-0.00052	0.00300
C11	0.00106	0.02594	0.00489	-0.00133	0.00132	-0.00227
O12	0.00162	0.02382	0.01028	-0.00654	0.00458	-0.00344
O13	0.00176	0.02437	0.00946	-0.00154	0.00332	0.00069
N14	0.00124	0.01738	0.00475	-0.00050	0.00186	-0.00105
C15	0.00172	0.02048	0.00591	0.00442	0.00222	-0.00121
O16	0.00218	0.02204	0.00804	0.00320	0.00501	0.00384
C17	0.00130	0.02296	0.00553	-0.00036	0.00255	-0.00156
C18	0.00217	0.02514	0.00696	0.00902	0.00442	0.00236
C19	0.00529	0.03373	0.00658	0.00307	0.00461	0.00438
C20	0.00867	0.04386	0.00607	0.00664	0.00731	-0.00130

Table 3 continued

	$\beta_{11}$	$\beta_{22}$	$\beta_{33}$	$\beta_{23}$	$\beta_{13}$	$\beta_{12}$
C21	0.00713	0.06227	0.00677	0.00839	0.00559	-0.00320
C22	0.00495	0.06718	0.00829	0.02674	0.00268	0.00124
C23	0.00408	0.03213	0.00831	0.01258	0.00387	0.00236

All temperature factors in this Table are positive-definite.

Table 4. 6-NBF-PA observed and calculated structure factors  
( x 100) in the order

\* h k  
l  $|F_o|$   $|F_c|$   $\alpha$  (radians)

Unobserved reflexions are marked † , and the reflexions  
not included are :-

0 0 1  
0 0 2  
1 1  $\bar{1}$   
1 1 1  
1 3  $\bar{1}$   
1 3 1  
2 0  $\bar{2}$   
2 0  $\bar{1}$   
2 0 1  
2 0 2

as they were all obscured by the backstop.











0	946	857	0.068	2	1895	1599	0.000	-3	255	337	0.219
1	3472	3295	-3.048	3	957	901	0.000	-2	509	620	-2.359
2	1115	992	0.764	4	197	124	3.142	-1	680	453	-1.911
3	1428	1191	-0.086	5	1759	1593	3.142	0	1552	1603	-3.039
4	667	584	-0.471	6	657	555	3.142	1	2371	2054	0.501
5	286	268	1.615	7	1734	1609	0.000	2	1391	1303	-1.059
6	1972	1841	-3.063	8	131	54	3.142	3	613	588	2.382
7	114	196	2.503	9	131	27	3.142	4	966	893	-2.906
8	1554	1614	0.277	10	764	770	3.142	5	950	806	-1.930
9	228	252	-3.115	11	263	280	0.000	6	1052	994	0.252
10	301	317	-2.800	12	228	305	0.000	7	580	558	-0.809
11	263	247	-2.784	12	12	2	0.000	8	634	624	2.780
12	66	117	-2.539	-17	360	397	1.320	9	546	598	3.096
	11	3		-16	421	510	-0.222	10	93	176	-0.991
-16	335	378	0.470	-15	329	334	-2.181	11	354	430	-0.863
-15	431	429	-0.559	-14	558	520	2.822		13	3	
-14	492	440	-1.237	-13	664	613	-2.621	-16	66	37	-2.394
-13	617	584	2.280	-12	1066	979	1.551	-15	93	176	-2.999
-12	606	498	-1.213	-11	1513	1540	-0.142	-14	591	592	2.761
-11	617	549	1.248	-10	752	698	-2.497	-13	465	415	-0.287
-10	813	827	0.102	-9	1257	1391	2.603	-12	496	441	-0.638
-9	689	661	-2.643	-8	714	734	-0.619	-11	400	371	-0.610
-8	780	854	2.705	-7	315	266	0.635	-10	1119	1107	3.809
-7	651	579	0.099	-6	1642	1893	0.697	-9	161	71	2.572
-6	847	920	-0.214	-5	1425	1532	-2.404	-8	1163	1183	0.229
-5	131	76	0.259	-4	1368	1542	2.267	-7	1022	962	-1.486
-4	1259	1481	2.672	-3	941	1037	0.060	-6	147	98	1.586
-3	530	427	2.864	-2	692	668	-1.279	-5	1403	1370	2.378
-2	746	758	-1.705	-1	1016	991	-0.397	-4	580	489	-1.920
-1	2167	2085	-0.196	0	1981	2019	2.917	-3	1276	1326	0.091
0	538	499	1.963	1	1651	1684	3.107	-2	1201	1114	-0.424
1	869	885	-3.070	2	2166	2231	0.380	-1	2077	1833	2.887
2	973	858	2.867	3	896	849	-0.684	0	469	345	-3.089
3	1049	1025	-0.468	4	884	880	-3.025	1	228	178	-0.993
4	1001	988	0.359	5	927	855	2.852	2	1464	1314	0.803
5	522	479	-3.018	6	538	495	-2.526	3	161	121	-2.908
6	237	234	2.633	7	1305	1334	0.908	4	1194	1135	-3.122
7	329	328	-1.521	8	416	424	-0.069	5	329	300	1.641
8	383	290	0.366	9	692	784	2.858	6	808	787	-0.712
9	131	82	0.294	10	174	178	-1.898	7	637	649	0.243
10	400	433	2.860	11	66	53	-0.309	8	431	539	2.849
11	93	151	2.379	12	12	4		9	372	460	2.775
	11	5		-15	147	185	-0.838	10	301	246	-0.575
-13	378	369	3.338	-14	431	561	2.471		13	5	
-12	573	507	1.981	-13	426	418	2.602	-13	66	453	-0.217
-11	487	428	-1.093	-12	360	402	-1.080	-12	66	11	0.542
-10	114	175	-0.081	-11	93	93	2.706	-11	93	73	2.760
-9	114	42	-2.201	-10	487	458	-0.983	-10	255	204	-2.357
-8	460	442	2.405	-9	114	236	2.710	-9	460	388	2.532
-7	522	399	2.549	-8	1027	1039	2.660	-8	602	562	-0.219
-6	696	630	-0.528	-7	1417	1444	-0.565	-7	421	408	0.589
-5	389	308	-0.304	-6	114	136	2.509	-6	546	478	3.134
-4	644	539	-2.754	-5	451	430	-1.762	-5	577	465	-2.043
-3	1199	1157	2.142	-4	573	511	2.261	-4	492	360	2.167
-2	874	744	-0.521	-3	522	463	-3.049	-3	673	604	-0.475
-1	844	698	-0.381	-2	1337	1322	-0.701	-2	839	721	1.308
0	469	392	2.922	-1	1228	1092	1.305	-1	816	719	-2.667
1	348	185	-2.245	0	1240	1195	3.115	0	114	187	-0.061
2	744	648	2.509	1	562	486	-1.480	1	114	118	1.090
3	627	446	-0.183	2	366	326	1.993	2	478	412	-1.124
4	764	823	-0.970	3	823	684	-0.731	3	400	349	1.561
5	595	644	1.882	4	279	264	1.144	4	383	357	2.182
6	436	405	3.060	5	906	935	2.252	5	383	408	-2.208
7	348	336	-1.432	6	634	633	-1.676	6	538	540	0.088
8	66	169	1.667	7	246	273	-0.488	7	66	122	0.408
	12	0		8	501	562	0.123		14	0	
-17	446	380	0.500	9	513	557	-2.812	-17	66	106	0.000
-16	505	449	0.000	10	308	422	2.074	-16	620	626	3.142
-15	186	205	3.142		12	6		-15	114	193	3.142
-14	558	495	3.142	0	114	237	-2.587	-14	651	730	0.000
-13	505	466	3.142		13	1		-13	131	46	0.000
-12	913	1012	0.300	-17	335	309	-0.174	-12	886	693	3.142
-11	465	385	0.000	-16	66	121	2.680	-11	591	573	0.000
-10	131	131	3.142	-15	720	763	-2.759	-10	1231	1288	3.142
-9	831	701	3.142	-14	348	273	0.812	-9	286	295	0.000
-8	534	416	3.142	-13	372	348	0.052	-8	1313	1413	0.000
-7	1300	1200	0.300	-12	1076	1153	-0.189	-7	1503	1497	3.142
-6	1819	1619	0.000	-11	591	590	-2.428	-6	717	474	3.142
-5	1587	1480	3.142	-10	1094	1187	2.050	-5	1305	1208	0.000
-4	580	665	3.142	-9	977	953	-1.873	-4	1467	1270	3.142
-3	831	889	0.000	-8	483	400	0.280	-3	1131	966	0.000
-2	2746	2700	0.000	-7	1306	1455	0.506	-2	1106	1004	3.142
-1	1080	998	3.142	-6	1443	1511	-2.225	-1	1523	1308	3.142
0	1117	969	3.142	-5	1697	1841	2.386	0	1744	1599	0.000
1	114	163	3.142	-4	294	321	0.615	1	834	729	0.000

2	1064	926	3.142	4	887	892	-0.919	-9	513	563	-3.132
3	354	271	0.000	5	786	776	0.450	-8	492	648	-2.779
4	1142	960	3.142	6	558	575	1.648	-7	775	809	-0.496
5	421	339	0.000	7	623	653	-2.231	-6	436	396	1.183
6	1648	1466	0.000	8	237	223	-2.755	-5	436	417	-2.938
7	657	640	3.142	9	702	787	0.455	-4	573	539	-1.454
8	455	417	3.142	10	315	462	-1.576	-3	839	893	-3.110
9	114	148	3.142 †		15	J		-2	308	280	-0.114
10	613	722	0.000	-15	416	356	0.564	-1	831	885	-0.023
11	246	341	3.142	-14	416	472	0.177	0	538	524	1.673
	14	2		-13	660	662	-3.068	1	620	564	-2.497
-16	131	153	-2.633	-12	301	352	2.849	2	580	503	3.102
-15	197	2.6	2.851	-11	147	188	2.401 †	3	664	644	-0.292
-14	348	3.7	0.418	-10	823	821	-0.212	4	534	534	-0.064
-13	670	690	-0.544	-9	147	139	0.973 †	5	400	435	2.063
-12	421	4.1	-2.603	-8	660	602	-2.754	6	294	318	-2.441
-11	1010	1291	2.397	-7	469	468	3.097	7	66	96	2.685 †
-10	879	9.1	-1.662	-6	660	639	1.981	8	66	125	-1.029 †
-9	831	870	0.061	-5	988	1110	-0.495		16	4	
-8	647	645	-0.170	-4	522	437	-2.356	-13	66	103	-0.397 †
-7	821	871	-2.617	-3	522	532	1.675	-12	496	446	1.750
-6	1172	1221	2.549	-2	657	649	-2.756	-11	569	576	-0.702
-5	294	248	-0.256	-1	522	480	-0.540	-10	246	206	1.092
-4	913	9.6	-0.808	0	894	849	1.319	-9	263	195	-2.947
-3	1642	1739	0.285	1	813	755	-1.356	-8	378	365	-2.599
-2	936	951	-2.878	2	872	865	2.628	-7	421	394	1.039
-1	1305	1388	2.870	3	147	95	2.664 †	-6	534	528	-0.185
0	1041	1078	-0.492	4	708	745	-0.408	-5	455	352	-2.144
1	766	685	0.442	5	301	170	0.376	-4	1027	992	2.262
2	550	489	0.016	6	441	431	-3.034	-3	366	293	-0.964
3	1188	1160	2.926	7	354	407	2.667	-2	322	191	-0.543
4	599	500	-2.872	8	93	82	1.468 †	-1	599	514	-0.011
5	1416	1436	-0.676		15	5		0	436	363	-2.637
6	492	308	1.497	-12	66	393	2.104 †	1	580	501	2.527
7	487	517	2.666	-11	301	277	0.960	2	263	218	-0.989
8	341	424	2.789	-10	486	529	-1.162	3	246	259	0.822
9	114	226	-2.106 †	-9	255	308	1.483	4	441	462	-0.287
10	416	552	0.963	-8	228	207	-1.745	5	237	268	-2.057
	14	4		-7	483	420	-2.757	6	378	429	2.455
-14	580	645	0.176	-6	400	386	1.503		16	6	
-13	66	93	1.269 †	-5	849	827	-0.342	0	366	292	1.352
-12	308	2.1	3.140	-4	237	191	-2.768		17	1	
-11	554	578	2.862	-3	580	493	2.816	-16	465	488	-0.166
-10	93	141	1.694 †	-2	410	308	-1.503	-15	478	473	-1.897
-9	906	830	0.234	-1	620	577	1.689	-14	778	832	-2.362
-8	366	2.2	-1.479	0	952	812	-0.991	-13	505	495	-2.325
-7	400	394	-2.819	1	354	291	1.210	-12	986	996	-0.322
-6	680	620	2.607	2	644	662	3.016	-11	114	119	1.606 †
-5	738	721	2.727	3	378	376	-0.979	-10	1243	1151	-2.236
-4	1644	1989	-0.289	4	341	387	1.867	-9	929	887	2.112
-3	372	379	2.427	5	542	471	-0.603	-8	114	109	-0.915 †
-2	738	745	-2.562		16	0		-7	904	921	-0.687
-1	400	316	-0.035	-16	436	410	0.000	-6	1486	1592	1.265
0	630	611	2.149	-15	93	150	0.000 †	-5	1901	1872	-2.300
1	696	763	-0.717	-14	550	481	0.000	-4	1140	1141	-2.354
2	400	3.7	0.979	-13	1226	1212	3.142	-3	2767	2809	0.807
3	844	791	-2.968	-12	131	193	0.000 †	-2	2316	2412	-1.762
4	93	120	-0.246 †	-11	943	998	0.000	-1	1170	1174	1.196
5	436	435	0.915	-10	360	214	3.142	0	738	719	2.372
6	301	357	-0.952	-9	294	125	3.142	1	1242	1257	-2.260
7	174	144	2.332	-8	906	860	3.142	2	1206	1123	0.479
8	558	717	2.767	-7	874	810	3.142	3	573	529	-0.509
	14	6		-6	2503	2709	0.000	4	874	848	-2.798
0	93	181	1.905 †	-5	131	20	3.142 †	5	657	710	1.620
	15	1		-4	2157	2123	3.142	6	237	306	-2.525
-16	446	415	-2.925	-3	131	38	0.000 †	7	271	332	-0.132
-15	410	354	0.131	-2	573	359	0.000	8	509	610	0.634
-14	329	280	0.321	-1	577	493	0.000		17	3	
-13	354	347	2.868	0	1012	1070	0.000	-14	480	429	-3.053
-12	469	487	2.512	1	1865	1685	3.142	-13	161	233	-0.309
-11	451	371	0.347	2	513	472	3.142	-12	455	454	1.231
-10	1208	1247	-1.576	3	934	773	0.000	-11	573	511	-9.589
-9	1569	16.3	0.655	4	131	213	3.142 †	-10	478	387	-2.635
-8	922	882	2.768	5	279	329	0.000	-9	441	483	2.363
-7	968	12.1	-2.627	6	623	573	3.142	-8	389	366	-0.621
-6	1499	1653	1.280	7	383	417	3.142	-7	450	429	3.346
-5	758	821	-1.446	8	859	940	0.000	-6	147	236	2.129 †
-4	1286	1284	0.589	9	174	206	0.000	-5	465	364	-2.723
-3	1054	872	2.994		16	2		-4	465	347	-0.435
-2	1692	1633	2.927	-15	714	766	-0.118	-3	657	639	3.026
-1	847	8.2	-0.661	-14	431	480	2.616	-2	1037	1120	-0.207
0	1710	16.9	0.574	-13	378	414	-2.901	-1	613	576	2.331
1	372	380	-2.611	-12	451	469	0.391	0	496	539	-2.980
2	509	443	2.666	-11	93	213	-1.185 †	1	147	183	-1.200 †
3	1197	1139	3.018	-10	378	393	0.040	2	308	216	0.023

3	465	446	0.861	3	66	114	0.371 †	-6	669	899	-0.307
4	436	457	-1.471	4	394	357	3.030	-5	455	407	-0.538
5	400	409	2.588	5	19	1		-4	558	580	0.291
6	161	199	2.009	-15	714	673	1.220	-3	1041	1158	2.910
7	66	348	-0.931 †	-14	761	687	-1.236	-2	530	486	-3.068
-10	17	5		-13	657	660	0.226	-1	1197	1215	-0.051
-9	66	412	2.957 †	-12	538	454	-2.902	0	93	92	-0.845 †
-8	210	191	2.411	-11	966	905	3.075	1	218	207	3.000
-7	93	110	1.038 †	-10	492	445	0.554	2	478	534	2.752
-6	588	543	-1.415	-9	723	785	-0.356	3	186	231	-1.654
-5	569	480	0.599	-8	114	144	0.434 †	4	630	722	-0.288
-4	667	588	3.098	-7	501	468	-2.856		20	4	
-3	335	227	2.084	-6	966	937	2.881	-10	474	460	-0.640
-2	580	511	-0.008	-5	478	411	0.583	-9	174	162	-1.073
-1	421	366	-1.636	-4	877	942	-0.056	-8	478	442	2.469
0	93	73	1.250 †	-3	1027	1083	-2.566	-7	627	557	-3.008
1	577	484	2.068	-2	602	618	1.293	-6	441	392	0.865
2	550	486	-2.127	-1	526	484	-2.926	-5	1078	1074	-0.477
3	460	463	0.494	0	696	730	0.284	-4	431	436	2.747
-15	66	164	-1.511 †	1	677	616	-1.149	-3	509	530	3.097
-14	18	0		2	554	563	2.816	-2	294	242	-0.540
-13	93	116	3.142 †	3	208	229	3.123	-1	255	248	1.937
-12	702	612	0.000	4	301	238	-0.665	0	492	516	-0.517
-11	664	555	0.000	5	360	397	0.245	1	66	124	1.488 †
-10	699	531	3.142	6	66	131	-0.175 †	2	383	534	2.953
-9	1174	1170	3.142	-13	348	351	-0.457		21	1	
-8	1144	1166	0.000	-12	441	424	-3.048	-13	1070	943	-2.670
-7	416	264	0.000	-11	550	532	2.760	-12	228	218	1.907
-6	513	466	0.000	-10	114	151	-0.670 †	-11	829	788	-0.421
-5	360	272	3.142	-9	595	691	0.067	-10	542	388	0.935
-4	2184	2279	3.142	-8	286	350	-1.269	-9	378	462	2.369
-3	2184	2182	0.000	-7	791	733	2.972	-8	934	884	-2.506
-2	887	865	0.000	-6	711	681	2.035	-7	400	371	0.354
-1	1895	1895	3.142	-5	894	932	-1.106	-6	908	899	0.062
0	1604	1478	0.000	-4	720	716	0.267	-5	93	156	0.931 †
1	964	944	3.142	-3	483	453	0.555	-4	975	1021	-3.016
2	131	171	0.000 †	-2	1630	1617	-3.040	-3	460	478	2.339
3	1522	1485	0.000	-1	469	482	0.293	-2	602	612	-0.484
4	1484	1410	3.142	0	469	329	-0.247	-1	1076	1091	0.383
5	114	17	0.000 †	1	436	424	-0.558	0	813	857	-2.889
6	341	383	0.000	2	366	404	1.541	1	329	340	2.643
7	93	64	3.142 †	3	711	822	-2.719	2	348	286	-2.928
8	436	473	0.000	4	93	173	0.497 †	3	366	465	-0.413
-15	66	319	3.142 †	5	66	378	0.155 †	4	705	761	0.606
-14	18	2		6	19	5			21	3	
-13	802	815	2.573	-8	255	146	0.008	-11	389	408	-0.165
-12	66	114	-2.450 †	-7	341	487	2.328	-10	329	318	-0.769
-11	522	592	0.253	-6	329	607	-2.168	-9	538	577	2.822
-10	542	536	-0.100	-5	66	488	0.843 †	-8	463	491	2.848
-9	711	729	-2.496	-4	66	205	-0.103 †	-7	436	388	0.182
-8	744	712	2.630	-3	66	136	-2.041 †	-6	606	697	-0.710
-7	741	681	0.581	-2	66	216	2.977 †	-5	315	245	2.547
-6	522	659	-1.038	-1	66	94	1.603 †	-4	416	431	2.402
-5	702	766	1.254	0	301	233	-1.346	-3	627	603	-2.887
-4	595	614	-2.652		20	0		-2	886	747	-0.113
-3	271	268	-2.468	-14	441	321	0.000	-1	237	271	0.746
-2	872	94	1.269	-13	93	38	0.000 †	0	279	304	-1.911
-1	818	874	-1.045	-12	680	617	3.142	1	641	702	2.547
0	308	303	-2.183	-11	522	400	3.142	2	66	290	-0.781 †
1	1082	1211	2.288	-10	1066	913	0.000		22	0	
2	322	353	-1.631	-9	271	203	0.000	-13	378	248	3.142
3	591	580	-0.015	-8	335	292	3.142	-12	990	975	0.000
4	246	245	0.293	-7	769	746	3.142	-11	93	62	3.142 †
5	599	625	-2.262	-6	400	348	0.000	-10	218	238	3.142
6	446	484	2.602	-5	755	710	0.000	-9	460	429	3.142
7	286	311	1.267	-4	451	452	3.142	-8	651	560	3.142
8	301	389	-0.241	-3	197	152	3.142	-7	1632	1638	0.000
-12	66	60	2.338 †	-2	772	712	3.142	-6	114	59	3.142 †
-11	18	4		-1	920	811	0.000	-5	1480	1468	3.142
-10	492	457	-0.053	0	580	593	0.000	-4	501	403	0.000
-9	400	299	-3.001	1	1121	1105	3.142	-3	301	272	0.000
-8	246	241	-2.987	2	301	318	0.000	-2	831	790	0.000
-7	372	403	2.334	3	487	419	3.142	-1	400	241	3.142
-6	723	754	-0.756	4	294	206	0.000	0	752	898	3.142
-5	322	266	0.355	5	1196	1084	0.000	1	93	38	3.142 †
-4	589	495	2.766	6	546	889	3.142	2	341	429	0.000
-3	301	244	-2.479		20	2		3	606	531	0.000
-2	335	297	-0.945	-13	670	649	3.111		22	2	
-1	474	452	0.512	-12	627	613	3.081	-11	647	686	0.192
0	208	125	1.493	-11	354	330	-0.401	-10	599	657	-2.863
1	764	648	3.039	-10	492	602	-0.046	-9	446	520	2.870
2	237	210	-1.599	-9	378	410	-0.331	-8	441	509	0.107
3	329	293	-0.647	-8	899	951	2.964	-7	66	192	-1.087 †
4	348	334	1.101	-7	647	626	2.993	-6	383	349	0.720
								-5	501	471	-2.036

-4	1024	1122	3.120
-3	872	897	0.343
-2	651	723	-0.242
-1	329	422	3.078
0	416	457	2.904
1	394	390	-2.165
2	558	607	0.031
.	22	4	
-5	686	712	1.923
-4	565	501	-1.801
*	23	1	
-11	186	176	-2.190
-10	831	820	-3.102
-9	421	397	0.654
-8	723	741	-0.266
-7	405	403	2.254
-6	394	420	-2.070
-5	797	789	-2.756
-4	1007	1103	0.964
-3	1058	1108	-0.897
-2	469	530	2.202
-1	595	676	2.911
0	410	419	-1.575
1	197	249	0.270
.	23	3	
-8	308	254	-0.495
-7	496	526	-1.024
-6	492	553	1.698
-5	758	578	-2.559
-4	308	292	2.788
-3	869	899	0.192
-2	335	329	-2.470
*	24	0	
-10	66	147	0.000 †
-9	1339	1201	0.000
-8	908	725	3.142
-7	93	163	3.142 †
-6	400	352	3.142
-5	93	59	0.000 †
-4	1166	996	0.000
-3	400	405	3.142
-2	496	431	3.142
0	208	256	3.142
.	24	2	
-8	522	495	-0.995
-7	228	309	2.804
-6	394	376	2.354
-5	186	150	2.937
-4	602	652	-0.479
-3	308	318	0.691

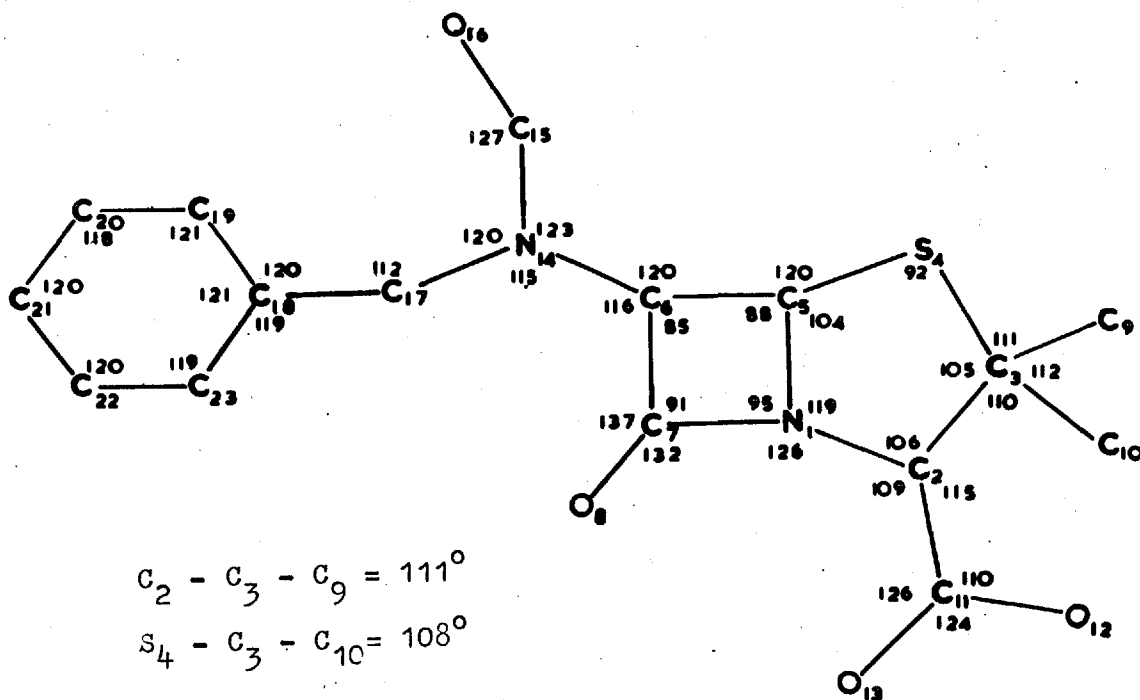
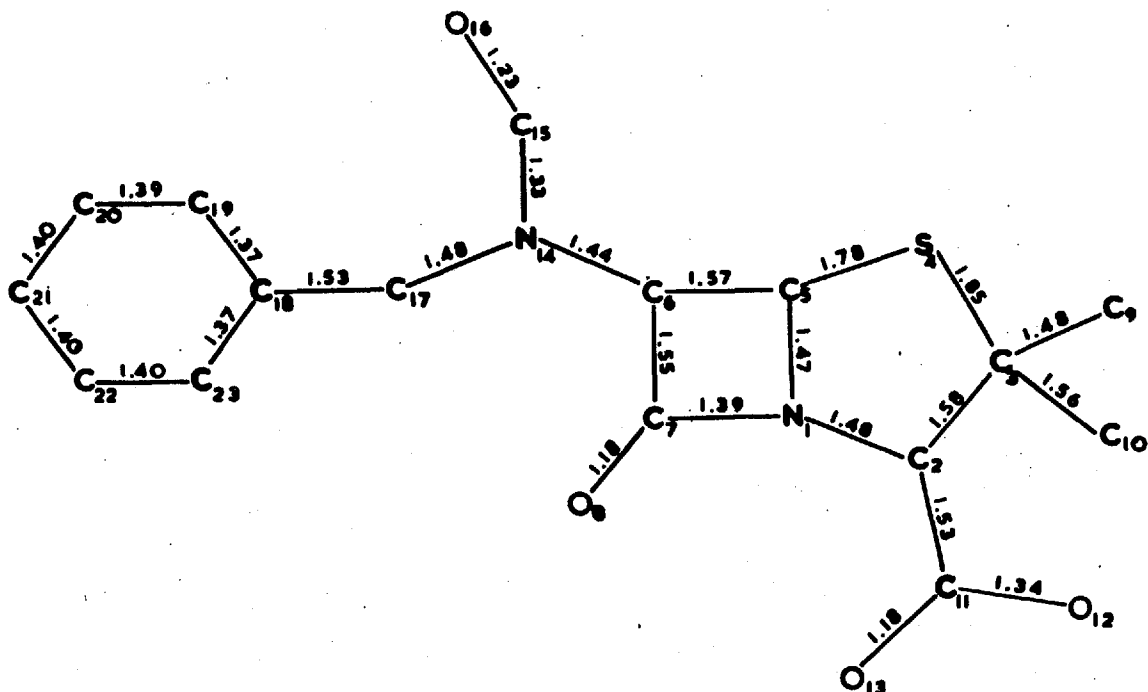
Table 5. 6-NBF-PA intra-molecular bond distances and their estimated standard deviations in Angstrom units.

Bond		Bond	
N1 - C2	1.476 (0.009)	N14 - C17	1.485 (0.008)
N1 - C5	1.471 (0.008)	C15 - O16	1.233 (0.011)
N1 - C7	1.387 (0.008)	C17 - C18	1.529 (0.012)
C2 - C3	1.576 (0.011)	C18 - C19	1.371 (0.018)
C2 - C11	1.529 (0.009)	C18 - C23	1.371 (0.017)
C3 - S4	1.850 (0.005)	C19 - C20	1.394 (0.015)
C3 - C9	1.476 (0.017)	C20 - C21	1.398 (0.026)
C3 - C10	1.563 (0.014)	C21 - C22	1.403 (0.026)
S4 - C5	1.778 (0.010)	C22 - C23	1.396 (0.018)
C5 - C6	1.566 (0.009)		
C6 - C7	1.551 (0.008)		
C6 - N14	1.443 (0.009)		
C7 - O8	1.184 (0.009)		
C11 - O12	1.342 (0.009)		
C11 - O13	1.180 (0.013)		
N14 - C15	1.325 (0.013)		

Table 6. 6-NBF-PA intra-molecular bond angles and their standard deviations in degrees.

C2 - N1 - C5	118.6 (0.6)	C6 - N14 - C15	123.2 (1.1)
C2 - N1 - C7	125.6 (0.7)	C6 - N14 - C17	115.3 (0.5)
C5 - N1 - C7	94.9 (0.5)	C15 - N14 - C17	120.4 (0.9)
N1 - C2 - C3	105.8 (0.7)	N14 - C15 - O16	126.9 (1.5)
N1 - C2 - C11	108.9 (0.5)	C2 - C11 - O12	109.5 (0.5)
C3 - C2 - C11	114.9 (0.8)	C2 - C11 - O13	126.1 (1.3)
C2 - C3 - S4	104.7 (0.5)	O12 - C11 - O13	124.4 (1.4)
C2 - C3 - C9	111.1 (1.1)	N14 - C17 - C18	112.1 (0.8)
C2 - C3 - C10	110.5 (0.8)	C17 - C18 - C19	119.6 (1.3)
S4 - C3 - C9	111.2 (0.7)	C17 - C18 - C23	119.1 (1.3)
S4 - C3 - C10	107.5 (0.6)	C19 - C18 - C23	121.4 (1.7)
C9 - C3 - C10	111.5 (1.4)	C18 - C19 - C20	120.9 (1.7)
C3 - S4 - C5	92.4 (0.4)	C19 - C20 - C21	118.2 (1.7)
N1 - C5 - S4	104.2 (0.6)	C20 - C21 - C22	120.4 (2.6)
N1 - C5 - C6	87.6 (0.4)	C21 - C22 - C23	119.6 (1.9)
S4 - C5 - C6	119.5 (0.8)	C18 - C23 - C22	119.2 (1.7)
C5 - C6 - C7	85.1 (0.5)	N1 - C7 - C6	91.3 (0.4)
C5 - C6 - N14	120.1 (0.7)	N1 - C7 - O8	132.0 (1.1)
C7 - C6 - N14	116.1 (0.6)	C6 - C7 - O8	136.7 (1.1)

Figure 3. 6-NBF-PA bond distances and angles.



temperature factor coefficients are shown in Table 3. The observed and calculated structure factors are listed in Table 4, the final R value being 0.100. Bond distances and angles and their estimated standard deviations were calculated by ELSI and are shown in Tables 5 and 6, and in Figure 3.

#### Configuration of the Molecule

Figure 4 is a projection of the 6-(N-benzylformamido)-penicillanic acid molecule down the b axis, as determined by the analysis. The projection down the c axis is shown in Figure 5. With the exception of the N-benzylformamido side-chain, the structure of the molecule is similar to those found for the other penicillins mentioned in Chapter 3.

The benzyl group in the side-chain is curled round towards the fused ring system as in benzyl penicillin, but its position in 6-NBF-PA is slightly different. It can be expressed as an imaginary rotation, of approximately  $90^\circ$ , of the benzyl group about the bond N14 - C17 in the direction of the sulphur atom. The least-squares planes through the groups of atoms in the molecule have been calculated with DIDO and are shown in Table 7. The amide group in the side-chain is planar, although the deviations are not as low as would be expected (Table 7a), and orientated approximately normal to the plane of the  $\beta$ -lactam ring. The dimensions of the group are consistent with those



Figure 4. 6-NBF-PA projected down the b axis

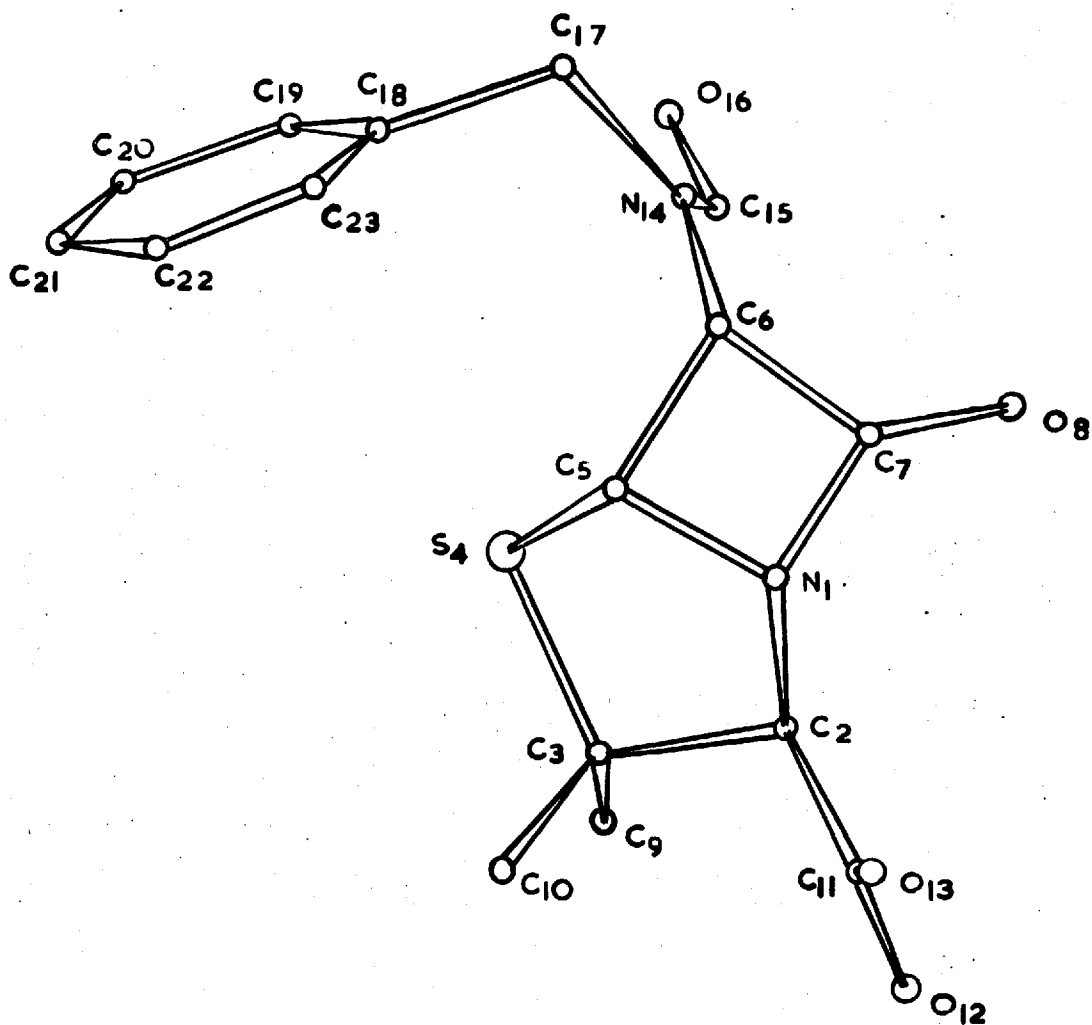
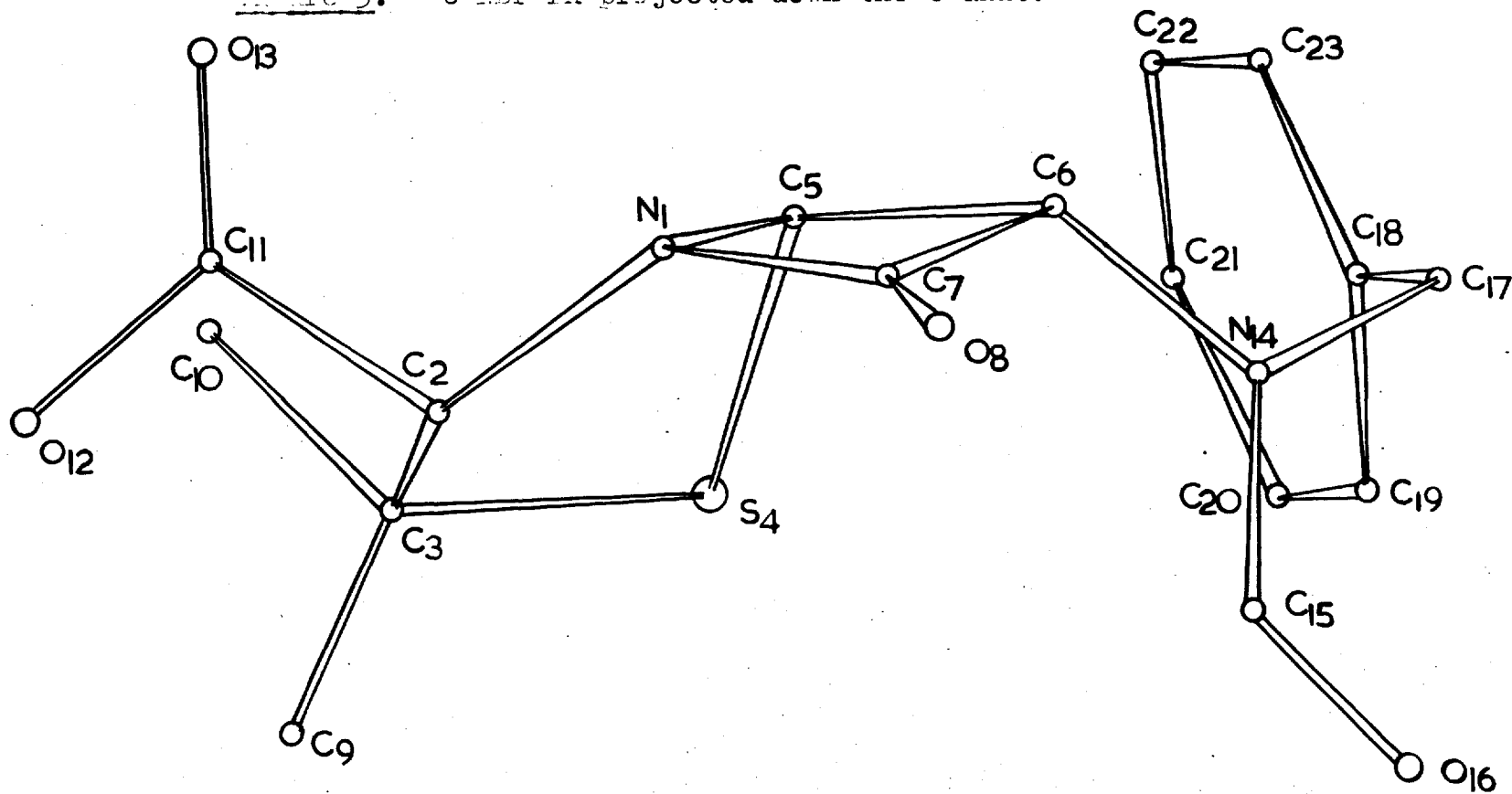


Figure 5. 6-NBF-PA projected down the c axis.



Scale 0 1 Å

Table 7. Deviations ( $\text{\AA}$ ) of the atoms in 6-NBF-PA from the calculated least-squares planes. Atoms marked with \$ were not included in the calculation of the plane.  $\sum d^2$  is the sum of the squares of the deviations from the plane (in  $\text{\AA}^2$ )

## a. Amide

$$\sum d^2 = 0.00943$$

Atom	Deviation
C6	-0.043
C15	0.017
O16	-0.033
N14	0.075
C17	-0.015

## b. Benzene Ring

$$\sum d^2 = 0.00297$$

Atom	Deviation
C17	-0.020
C18	0.007
C19	0.002
C20	0.005
C21	0.000
C22	-0.032
C23	0.040

## c. Thiazolidine Ring

$$\sum d^2 = 0.00014$$

Atom	Deviation
C3	-0.004
C2	0.007
N1	-0.008
C5	0.004
S4 \$	0.729

d.  $\beta$ -lactam

$$\sum d^2 = 0.01858$$

Atom	Deviation
N1	0.072
C5	-0.089
C6	0.057
C7	0.008
O8	-0.047

e.  $\beta$ -lactam

$$\sum d^2 = 0.00002$$

Atom	Deviation
N1	-0.001
C6	-0.001
C7	0.004
O8	-0.002
C5 \$	0.209

of a normal resonating amide. O16 is cis to the benzyl group and C15 is trans to the proton at C6, which is opposite to the analogous position in the other penicillins.

In terms of Collins and Richmond's explanation of the biological activity of the penicillins, O16 is on the 'wrong' side of the molecule with respect to the other polar groups (N1, O13, O8) to form a possible hydrogen-bonding system with a protein substrate similar to that postulated for N-acetylmuramic acid and the penicillins. As pointed out by Hunt and Rogers (1964), O16 can only be brought into the required position by rotation about C6 - N14 followed by cis-trans isomerization of the amide group. This combination seems improbable even in physiological solutions; the rotation would be hindered by the size of the benzyl group and the isomerization would require energy equal to the resonance energy of the amide. (Wheland (1955) estimates this value as 17 - 60 K cal./mole but with a large degree of uncertainty). Hence, the low antibacterial activity of 6-NBF-PA is consistent with Collins and Richmond's theory, and, it should be noted, with Tipper and Strominger's view that penicillin binds to the active centre in preference to a substituted D-alanyl-D-alanine.

#### Packing

The unitcell contents and the adjacent molecules in the 6-NBF-PA crystal are shown projected down the b axis in

Figure 6 and down the c axis in Figure 7. Some inter-molecular distances are shown in both diagrams and distances less than 3.25 Å are shown in Table 8. Atoms related to those in Table 2 by the symmetry of the spacegroup are referred to by terms in parentheses following the atom name.

The distances between the atoms O16 and O12 ( $x + \frac{1}{2}$ ,  $y - \frac{1}{2}$ ,  $z$ ) of 2.665 Å strongly suggests a hydrogen bond between these two atoms. This is supported by the bond lengths in the carboxyl group, C11 - O12 (1.342 Å) and C11 - O13 (1.180 Å) which agree quite well with the values of 1.358 Å and 1.233 Å given by Sutton (1965) for the unionized form. The result is that the molecules related by centering form an approximately linear hydrogen-bonding system roughly along the ab diagonals. That this is a 'criss-cross' arrangement can be seen from Figure 7.

The general packing arrangement is similar to that described for potassium benzylpenicillin by Crowfoot et al. (1949) and for phenoxymethylpenicillin by Abrahamsson et al. (1963). The polar groups are on one side of the molecule and the hydrocarbon parts on the other, so that the molecules make contact with one another in alternate polar and non-polar layers, which in 6-NBF-PA are parallel to the a axis.

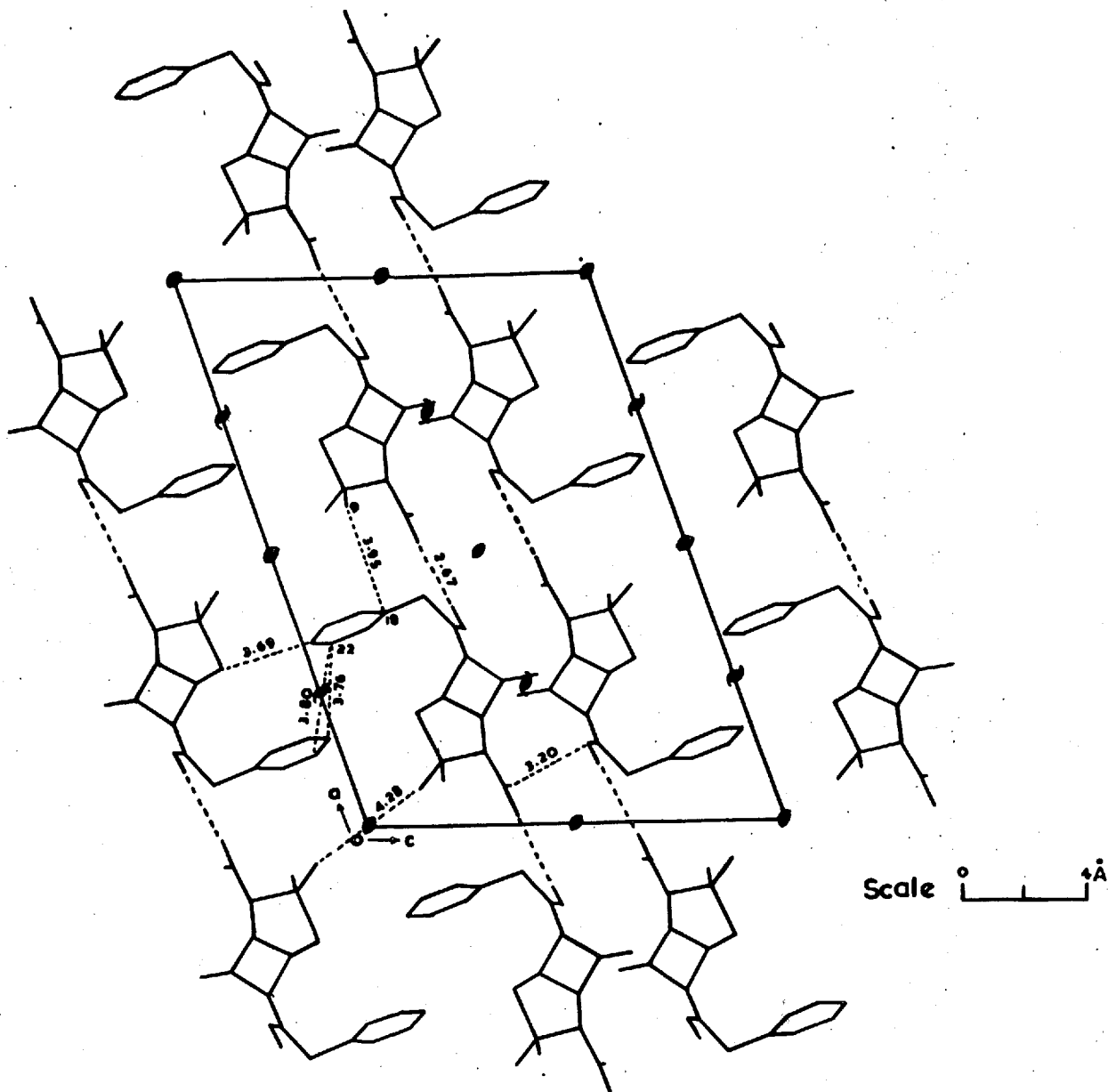


Figure 6. Crystal structure of 6-NBF-PA projected down the b axis

Figure 7. The crystal structure of 6-NBF-PA projected down the c axis.

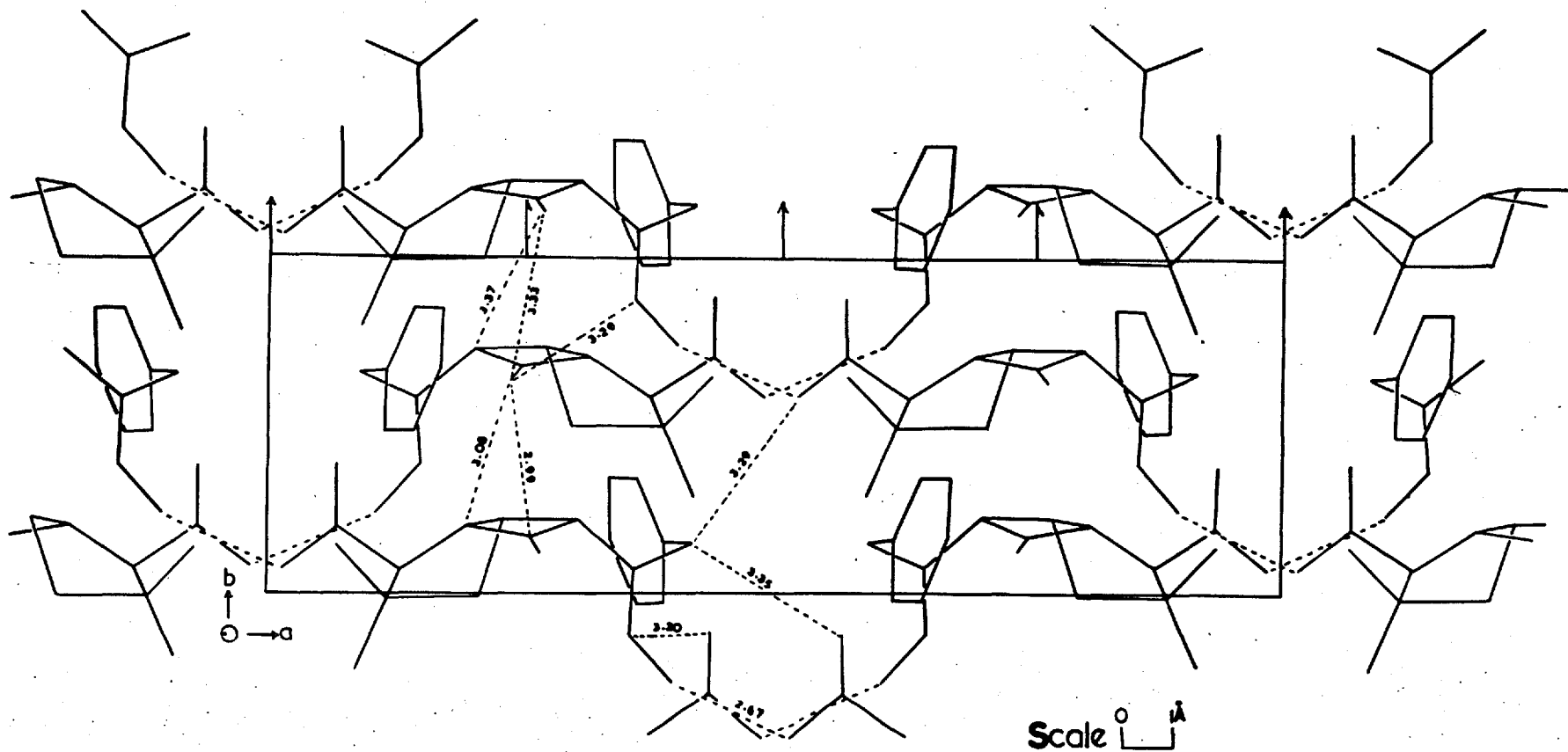


Table 8. Inter-molecular distances in 6-NBF-PA in A.

The atomic positions are related to those in Table 2 by the terms in parentheses which are :-

$$(1) = \frac{1}{2} - x, y + \frac{1}{2}, 1-z$$

$$(2) = x + \frac{1}{2}, y - \frac{1}{2}, z$$

$$(3) = x + \frac{1}{2}, y + \frac{1}{2}, z$$

N1 - 08 (1)	3.080	C11 - 016 (1)	3.398
C6 - 08 (1)	3.374	013 - C15 (1)	3.200
C7 - 08 (1)	2.992	013 - 016 (1)	3.417
08 - 08 (1)	3.331	016 - 012 (2)	2.665
08 - C15(1)	3.286	C17 - 012 (3)	3.293
C11 - C15(1)	3.479	C17 - 013 (2)	3.351



## The Thiazolidine and $\beta$ -Lactam Rings

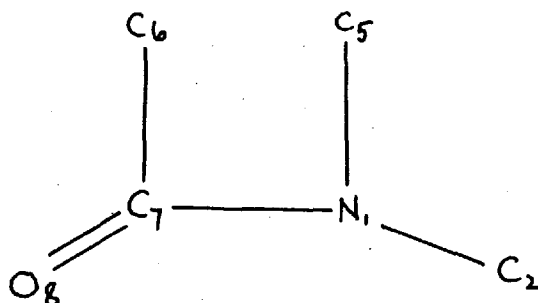
Diamand (1963) has tabulated the bond lengths and angles of the penicillin nucleus from the determination of the crystal structures of 6-APA, potassium benzylpenicillin refined by Rollett and Vaciago, phenoxymethylpenicillin and p-bromo-phenoxymethylpenicillin by Watson. Most of the values are in good agreement with those listed in Tables 5 and 6 for 6-NBF-PA. The shortening of the bond C3 - C9 (1.476 (0.017 Å)) is probably not significant in terms of the real standard deviations, and there is no apparent reason for the distortion of the angle C3 - C2 - C11 (114.9°) from the tetrahedral value of 109° 28'.

The thiazolidine ring has four atoms, N1, C2, C3 and C5 in a plane (Table 7c) with S4 0.729 Å below this plane viewing the molecule down the b axis as in Figure 4. This conformation is different to that of the thiazolidine rings in the other penicillins. As mentioned in Chapter 3, in benzylpenicillin and phenoxymethylpenicillin C2 is the out-of-plane atom, in the latter case by 0.51 Å on the opposite side of the plane to C7. In 6-APA, N1 deviates from the best plane through the other four atoms by 0.42 Å, on the same side of the plane as N14. The smaller value for the angle C3 - S4 - C5 (92.4°) compared with 96° - 97° in the other penicillins probably results from this conformational difference.

Although the bond S4 - C5 (1.778 Å) is only 4 e.s.d.'s lower than the average value of 1.817 Å, given by Sutton (1965) for a single C - S bond, S4 - C3 (1.850 Å) is 7 e.s.d.'s higher. This agrees with the values for the other penicillins except potassium benzylpenicillin for which Rollett and Vacicago give S4 - C5 (1.85 Å) and S4 - C3 (1.82 Å). The lengthening of the bond S4 - C3 has been discussed by Diamand (1963). By considering the mean value for this bond length and its true standard deviation from previous determinations, he tentatively suggests S4 - C3 has a bond length in the range 1.84 Å to 1.87 Å. The value in 6-NBF-PA lies in this range.

The non-planarity of the  $\beta$ -lactam ring can be seen from Table 7d, the deviation of C5 from the calculated plane being as high as 0.089 Å. Table 7e shows that by excluding C5 from the least-squares calculation, the 'cyclic amide' atoms N1, C6, C7 and O8 lie in a plane well within the limits of experimental accuracy, with C5 0.204 Å out of the plane on the same side as S4. This is similar to the arrangement in 6-APA, phenoxymethylpenicillin, cephalosporin C and the 3-spiro-thiazolinium derivative (Chapter 5) where the deviations of the out-of-plane atom vary from approximately 0.14 Å to 0.25 Å. In each case it is the atom bonded to the sulphur atom that lies out of the plane.

As Diamand (1963) has mentioned, the tendency of the group



to be planar, so that resonance can occur in the cyclic amide, is probably opposed to some extent by the tendency of the five- (or six) membered ring to adopt its most stable conformation. This will result in C5 being pulled out of the plane of the  $\beta$ -lactam ring. That resonance occurs to some extent in 6-NBF-PA is indicated by the length of the bond N1 - C7 (1.387 Å), which is nearer to the value of the C - N bond length in amides (1.333 Å) than the accepted value of 1.472 Å for a C - N single bond. The angle C2 - N1 - C5 (118.6°) suggests that N1 is tending to planarity.

CHAPTER 5

## The Crystal Structure of

(3S,4S,6R,7R)-2'-Amino-3'-ethyl-2'-thiazolinium-4'-spiro-3-(7-phenylacetamidocepham-4-carboxylate) trihydrate

Preliminary Data

The crystals, which were supplied by Dr.A.G.Long of Glaxo Ltd., and prepared as indicated on page 44, were colourless monoclinic needles. The crystallographically unique axis, b, was parallel to the needle axis and the crystal selected for data collection had the approximate dimensions 0.6 x 0.2 x 0.13 mm. The structural formula and numbering scheme are shown in the diagram inside the back cover.

Formula  $C_{19}H_{28}N_4O_7S_2$  Molecular Weight (formula) = 488

Mass absorption coefficient for  $CuK\alpha$ ,  $\mu = 25.5 \text{ cm}^{-1}$

## Unit-cell dimensions

$a = 8.063 (0.008) \text{ \AA}$ ,  $b = 7.184 (0.008) \text{ \AA}$ ,  $c = 19.72 (0.02) \text{ \AA}$   
 $\beta = 100.3^\circ (0.2)$   $V = 1123 \text{ \AA}^3$ ,  $Z = 2$ ,  $F(000) = 516$  electrons

$D_{\text{obs}}$  (by flotation) =  $1.45 \text{ g.cm}^{-3}$   $D_{\text{calc}} = 1.44 \text{ g.cm}^{-3}$

Absent Spectra: only among  $0k0$  for  $k = 2n + 1$

As the compound is dextrorotatory (page 43), the space-group is uniquely determined as  $P2_1$ . 2269 independent reflexions were estimated visually using three intensity wedges to accommodate spot-shape changes from layer to layer. The data were correlated from six layers collected about the b axis and three about the a axis, using LOLA for the determination of the inter-layer scale factors. It was considered that the value of  $\mu$  and the crystal dimensions rendered absorption corrections unnecessary (for data collected about the a axis, a crystal was sliced normal to the needle axis to give a rough cube of side 0.3 mm).

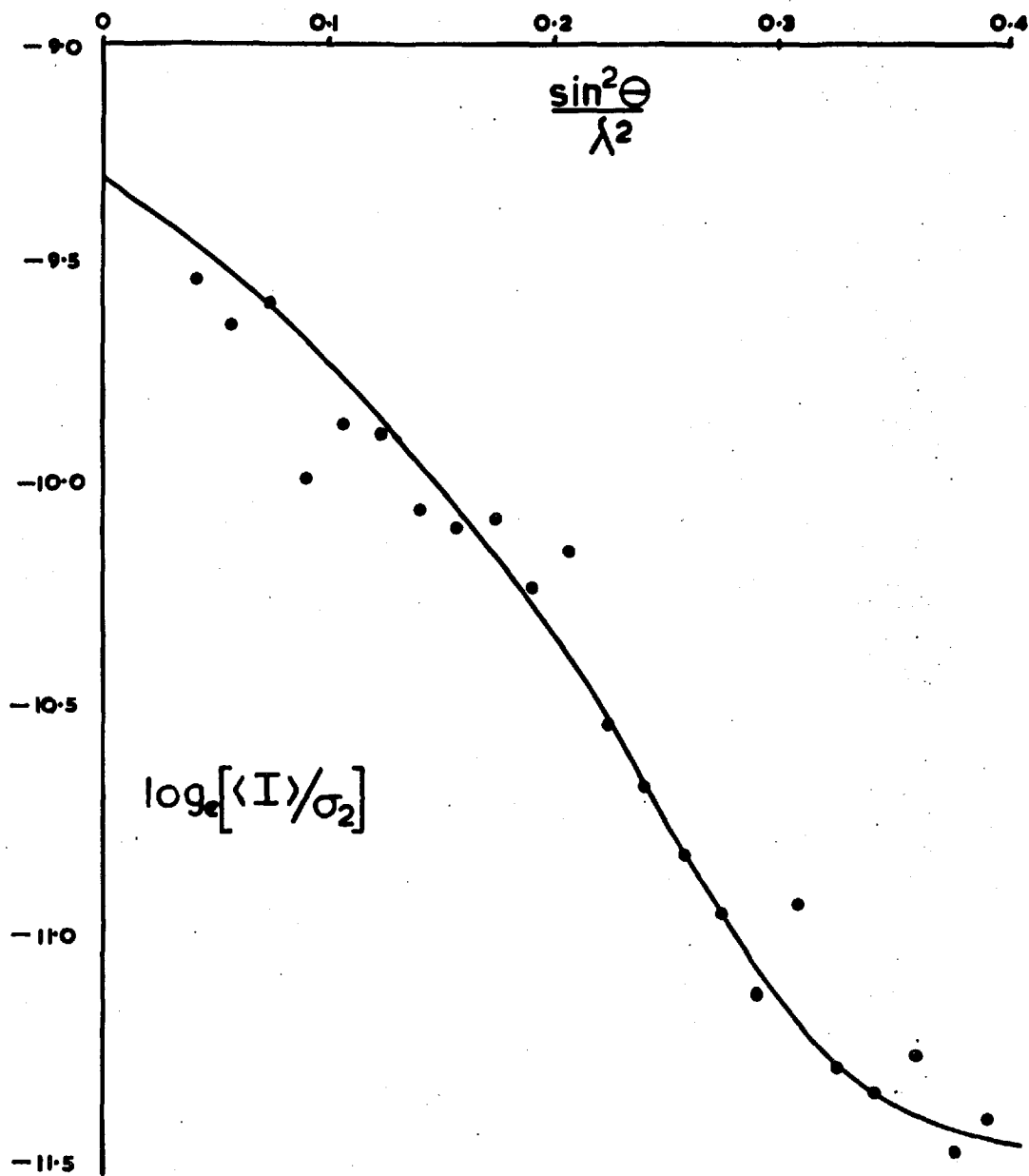
Figure 1 shows the Wilson plot calculated for three-dimensional data including the unobserved reflexions at  $\left| F_{\text{unobs}} \right| = \frac{2}{3} \left| r_{\text{min}} \right|$ . The data were divided into 22 shells each containing 80 - 120 reflexions. The least-squares method gave  $B = 2.95$ ,  $K = 100.4$ . From the graph, the best line through the points in the middle of the  $\sin^2 \theta / \lambda^2$  range gave  $B = 2.91$ , and the intercept gave  $K = 104.6$  (The final scale after structure refinement was 101.2)

### Structure Determination

#### 1. Location of the Sulphur Atoms

The four sulphur atoms in the unit cell give rise to

Figure 1. 3-Spiro-thiazolinium derivative Wilson plot based on three-dimensional data.



six centrosymmetrically related pairs of S - S inter vectors. In each six, two correspond to peaks in the three-dimensional Patterson, occurring in the Harker section at  $v = \frac{1}{2}$ , and the remaining four correspond to two peaks of double weight at

$$x_1 - x_2, y_1 - y_2, z_1 - z_2$$

$$x_1 + x_2, y_1 - y_2 + \frac{1}{2}, z_1 + z_2$$

where  $x_1, y_1, z_1$  and  $x_2, y_2, z_2$  are the positions of the two independent sulphur atoms. A three-dimensional Patterson was computed with coefficients sharpened by the function

$$1/\hat{f}^2 \cdot \exp(3\sin^2 \theta / \lambda^2)$$

where  $\hat{f}$  is the formfactor for sulphur. Four peaks were recognised which complied with the conditions described above and gave the following fractional coordinates for the sulphur atoms :

x	y	z
0.155	0	0.069
0.395	0.182	0.293

The distance between these two positions, 4.7 Å, seemed reasonable assuming the approximate geometry of ceph. Cc as determined by Diamand (1963).

## 2. Location of the Light Atoms

The ratio of the sum of the squares of the scattering powers of the sulphur atoms to that of the light atoms is 0.39

and Fourier methods were used to locate the positions of the light atoms. The first Fourier map, phased on the coordinates of the sulphur atoms revealed five additional peaks, one of which was subsequently found to have been misplaced. Three further Fouriers enabled the assignment of all thirty-two positions and the calculated and observed structure factors showed an overall agreement factor, R, of 0.29. During the course of the analysis, reflexions for which

$$|F_o| < 0.25 k |F_c| \quad \text{where } k = \frac{\sum |F_o|}{\sum |F_c|}$$

were omitted from the Fourier calculations, and double shifts were applied to the estimated coordinates before input to the next stage, as recommended by Donohue (1950)

### Refinement

Four cycles of isotropic, block-diagonal, least-squares refinement reduced R to 0.114 and a maximum coordinate shift of 0.03 Å. At this stage a bond-distance calculation indicated sensible bond lengths and a difference Fourier confirmed that the postulated structure was substantially correct. An agreement analysis was used to check the validity of the inter-layer scaling and that the choice of  $F^{\dagger} = 1500$  in the weighting scheme produced fairly constant values of  $\sum w\Delta^2$  over ranges



of  $|F_o|$ .

The progress of the structure refinement is shown in Table 1. It should be noted that the R value associated with a particular cycle was calculated from atomic coordinates before refinement. Agreement analyses and molecular geometry calculations were used to check the course of the refinement after cycles I8, A10 and A16.

Four further cycles of isotropic least squares (I5 to I8) produced very little convergence and so for input to A9, the individual isotropic temperature factors were converted to the equivalent anisotropic form and refinement continued on all 32 atoms, applying a fudge factor of 0.8 to all parameter shifts. At cycle A11, two reflexions ( $1\ 0\ \bar{2}$  and  $1\ 0\ \bar{1}$ ) were omitted for suspected extinction and 214 unobserved reflexions included at  $\frac{2}{3}F_{\min}$ , where  $F_{\min}$  is the minimum observed value of F at the relevant  $\sin^2 \theta$ . After cycle A16, a difference Fourier was calculated and suggested the positions of all hydrogen atoms except one bonded to C6, two bonded to C15, the three methyl-group hydrogens at C23 and the six of the three water molecules. The location of two peaks near N29 in approximately the correct orientation suggested the presence of the group  $=NH_2^+$ . However, the peak heights in the difference map varied from 0.13 to  $0.3\ eA^{-3}$ , and as the difference Fourier still exhibited ripple of the order  $0.2\ eA^{-3}$  these positions were not taken as

Table 1. The refinement process for the 3-spiro-thiazolinium-7-PAC derivative. I = isotropic, A = anisotropic refinement.

Cycle Number	Agreement Factor, R	$\sum w\Delta^2 \times 10^{-4}$	Maximum coord- inate shift (Å)
I1	0.289	35503	0.15
I2	0.175	14427	0.20
I3	0.133	7340	0.05
I4	0.114	5991	0.03
I5	0.113	5485	0.01
I6	0.112	5370	0.01
I7	0.112	5357	0.005
I8	0.112	5353	0.002
A9	0.112	5366	
A10	0.089	3487	0.014
A11	0.082	3034	0.008
A12	0.083	2634	0.014
A13	0.081	2441	0.007
A14	0.081	2420	0.004
A15	0.081	2411	0.002
A16	0.081	2408	0.002
A17	0.077	2073	0.009
A18	0.075	1963	0.003
A19	0.075	1955	0.0015
A20	0.075	1950	0.0008

conclusive proof of hydrogen atom positions.

Using a program written by D.F.High for the I.B.M. 7090, hydrogen positions were calculated assuming the staggered conformation for the methyl group at C23. The observed and calculated positions are shown in Table 2, excluding those of the water molecules. They show good agreement except for the atom bonded to C20. All the calculated hydrogen positions listed in Table 2 were included in subsequent structure-factor calculations with isotropic temperature factors 1.5 times those to which the hydrogen atoms are bonded. The hydrogens of the water molecules were not included as it was considered that their positions could not be well enough defined by stereochemical considerations.

Refinement was considered complete after cycle A20 when the position shifts were about one tenth of their standard deviations. Structure factors were calculated from the positions output from A20 to give a final R value of 0.075. The calculated and observed structure factors are listed in Table 3a.

A difference Fourier was calculated from the structure factors listed in Table 3a, in an attempt to locate the hydrogen atoms of the water molecules. The map exhibited a ripple up to about  $0.17 \text{ eA}^{-3}$  and the areas around the oxygen atom positions gave no indication of the hydrogen atoms.

Table 2. Observed and calculated hydrogen positions(in fractional coordinates) for the 3-spiro-thiazolinium-7-PAC derivative.

Atom.	Bonded to-	Calculated			Observed		
		x	y	z	x	y	z
H1	C2	0.475	0.632	0.201	0.491	0.625	0.200
H2	C2	0.453	0.872	0.178	0.438	0.883	0.167
H3	C4	0.052	0.674	0.235	0.054	0.675	0.233
H4	C6	0.271	0.608	0.363			
H5	C7	0.460	0.331	0.374	0.417	0.350	0.383
H6	C9	0.167	1.012	0.186	0.167	1.000	0.183
H7	C9	-0.017	0.882	0.152	0.000	0.875	0.150
H8	N13	0.674	0.586	0.311	0.646	0.600	0.308
H9	C15	0.979	0.488	0.317			
H10	C15	1.050	0.368	0.397			
H11	C17	1.090	0.540	0.485	1.083	0.500	0.500
H12	C18	1.329	0.387	0.567	1.375	0.450	0.550
H13	C19	1.444	0.090	0.539	1.438	0.000	0.542
H14	C20	1.319	-0.073	0.428	1.542	-0.150	0.400
H15	C21	1.089	0.080	0.346	1.125	0.133	0.367
H16	C22	0.199	0.407	0.033	0.167	0.350	0.067
H17	C22	0.248	0.364	0.124	0.250	0.350	0.117
H18	C23	0.495	0.284	0.067			
H19	C23	0.484	0.449	0.038			
H20	C23	0.544	0.537	0.123			
H21	N29	0.248	0.612	-0.041	0.229	0.600	-0.027
H22	N29	0.191	0.849	-0.054	0.188	0.850	-0.050

Table 3a. The 3-spiro-thiazolinium-7-PAC derivative observed and calculated structure factors ( x 100) in the order

*	h	k			
1			$ F_o $	$ F_c $	$\alpha$ (radians)

Unobserved reflexions are marked † , and 0 0 1 and 0 0 2 were obscured by the backstop. The two reflexions omitted for suspected extinction were

h	k	l	$ F_o $	$ F_c $	$\alpha$
1	0	$\bar{2}$	6003	8419	0.000
1	0	$\bar{1}$	5789	8266	0.000















Table with 10 columns: Index, Col 2, Col 3, Col 4, Col 5, Col 6, Col 7, Col 8, Col 9, Col 10. The table contains numerical data with various positive and negative values and upward-pointing arrows.





7	864	789	-1.582	2	545	543	3.033	1	899	1010	2.648
8	143	192	-2.014 +	3	143	175	-1.863 +	10	365	432	0.092
9	268	243	-0.941	4	965	1135	-0.633	8	506	578	1.185
-15	392	421	-0.207	5	336	210	2.162	-7	417	446	-0.842
-14	656	795	-1.487	6	429	447	2.272	-6	350	346	-0.667
-13	615	611	1.752	7	572	591	-0.595	-5	464	611	3.116
-12	268	361	0.975	9	2	2		-4	656	882	-3.107
-11	268	347	-1.554	-14	320	279	-3.009	-3	101	128	-2.224 +
-1	115	286	0.687 +	-13	526	579	2.538	-2	392	477	-1.677
-9	392	338	-2.570	-12	516	587	3.122	-1			
-8	1012	1096	-2.653	-11	581	612	-2.054				
-7	485	445	2.545	-10	764	843	-1.504				
-6	615	633	1.319	-9	429	412	1.837				
-5	526	563	0.843	-8	379	327	-0.073				
-4	840	892	-0.587	-7	496	531	-0.598				
-3	124	261	-0.045 +	-6	143	217	-0.461 +				
-2	417	465	0.900	-5	916	947	1.082				
-1	554	570	-0.431	-4	392	422	0.017				
1	111	215	0.873 +	-3	143	155	-1.544 +				
2	624	714	2.324	-2	640	732	2.783				
3	648	718	3.068	-1	392	356	-0.895				
4	506	461	-2.793	0	535	548	-1.185				
5	526	579	2.810	1	1046	1256	2.848				
6	336	403	-2.365	2	922	1042	3.077				
7	581	634	-1.888	3	392	413	-2.247				
8	76	200	2.843 +	4	365	409	-1.913				
9	554	580	0.452	5	474	561	2.485				
-1	268	251	2.788	6	143	172	1.641 +				
-9	226	278	-1.465	7	143	202	0.875 +				
-8	268	335	-1.964	9	607	645	-0.275				
-7	202	195	0.960 +	-12	1001	957	-0.737				
-6	516	456	-0.673	-11	598	241	0.783				
-5	286	260	-2.200	-10	248	237	2.617				
-4	809	773	0.937	-9	535	429	-1.985				
-3	485	505	-0.377	-8	101	46	0.561 +				
-2	320	313	-1.969	-7	392	358	2.319				
-1	516	550	1.993	-6	405	360	-1.664				
1	624	792	1.395	-5	143	69	2.218 +				
2	379	385	1.609	-4	694	651	1.627				
3	248	246	-1.218	-3	392	380	1.163				
4	452	408	-0.724	-2	143	144	-1.451 +				
9	441	485	-0.198	-1	379	410	2.218				
-16	764	698	0.000	0	797	816	2.565				
-15	78	154	3.142 +	1	554	466	-1.623				
-14	1113	980	3.142	2	143	84	2.613 +				
-13	101	65	3.142 +	3	320	278	2.057				
-12	708	708	0.000	4	101	620	-1.534 +				
-11	474	472	3.142	5	9	4					
-1	777	761	3.142	9	516	609	-1.569				
-9	365	356	0.000	-8	303	405	-0.512				
-8	365	323	3.142	-7	648	797	1.027				
-7	143	227	3.142 +	-6	379	386	0.454				
-6	976	873	0.000	-5	392	372	-0.078				
-5	876	805	0.000	-4	679	779	1.085				
-4	143	146	3.142 +	-3	268	271	0.248				
-3	143	260	3.142 +	-2	429	368	-1.822				
-2	784	679	0.000	-1	563	594	2.608				
-1	715	615	0.000	0	405	376	2.221				
1	143	116	3.142 +	1	336	331	-1.095				
2	624	519	0.000	10	590	548	0.000				
3	452	247	3.142	-10	78	91	0.000				
4	797	726	3.142	-9	303	259	3.142				
5	640	488	3.142	-8	750	687	0.000				
6	736	489	3.142	-7	101	284	0.000 +				
7	679	622	0.000	-6	101	33	3.142 +				
8	1037	911	0.000	-5	101	138	0.000 +				
-12	496	567	2.855	-4	852	703	3.142				
-11	485	601	-3.139	-3	615	549	3.142				
-10	101	206	-1.226 +	-2	563	544	0.000				
-9	632	677	-1.698	-1	101	127	0.000 +				
-8	679	740	-2.114	1	379	346	0.000				
-7	143	98	-3.076 +	10	303	352	-2.942				
-6	417	460	0.403	-10	429	441	-1.781				
-5	764	797	2.318	-9	516	534	0.284				
-4	143	201	-0.842 +	-8	90	28	0.567				
-3	790	809	-0.218	-7	365	313	2.416				
-2	954	974	1.396	-6	101	95	2.236 +				
-1	927	977	1.368	-5	545	486	-1.101				
1	496	507	-0.183	-4	365	347	1.093				
2	598	661	-1.779	-3	607	553	1.405				
3				-2	535	454	-0.914				
4				-1	816	803	3.033				

## Results and Discussion

The atomic coordinates of the non-hydrogen atoms and their standard deviations are shown in Table 3<sup>b</sup>, and Table 4 lists the anisotropic temperature factor coefficients. ELSI was used to calculate the intra-molecular bond distances and angles and their standard deviations shown in Tables 5 and 6. The intra-molecular bond distances and angles are also shown in Figure 2. That the estimated standard deviations are too low can be seen from the dimensions of the benzene ring, in which the C - C bond lengths range from 1.34<sup>o</sup> Å to 1.43<sup>o</sup> Å, indicating that the e.s.d.'s in Tables 5 and 6 have been underestimated by perhaps a factor of three. This is, no doubt due to the block-diagonal approximation of the least-squares program.

### The Configuration of the Molecule

The view of the molecule as shown in Figure 3 was derived from the final atomic coordinates by redefining their values with respect to the plane of the atoms S1, C6 and C4. Figure 3 shows that in the crystal at least, the molecule exists in a rather extended configuration as opposed to the curled forms of benzylpenicillin and 6-NBF-PA. The asymmetric centres at C6 and C7 are both R, (using the terms for chirality proposed and defined by Cahn, Ingold and Prelog (1966)), which is the



Table 3b. Atomic coordinates and standard deviations output from cycle A20 for the 3-spiro-thiazolinium-7-PAC derivative.

	(fractional values)			$\sigma_x$	$\sigma_y$	$\sigma_z$
	X	Y	Z			
S <sub>1</sub>	0.40182	0.81764	0.29429	0.00019	0.00027	0.00007
C <sub>2</sub>	0.39849	0.75748	0.20363	0.00066	0.00092	0.00028
C <sub>3</sub>	0.21655	0.71990	0.16468	0.00060	0.00088	0.00026
C <sub>4</sub>	0.12234	0.58335	0.20692	0.00062	0.00084	0.00026
N <sub>5</sub>	0.24289	0.48782	0.26052	0.00052	0.00077	0.00021
C <sub>6</sub>	0.33625	0.58921	0.32018	0.00073	0.00098	0.00026
C <sub>7</sub>	0.46553	0.42010	0.33023	0.00070	0.00098	0.00028
C <sub>8</sub>	0.36282	0.35330	0.25995	0.00066	0.00092	0.00027
C <sub>9</sub>	0.11601	0.90107	0.15082	0.00071	0.00091	0.00030
S <sub>10</sub>	0.15454	0.99421	0.06962	0.00021	0.00027	0.00008
C <sub>11</sub>	0.20262	0.77005	0.04416	0.00063	0.00096	0.00027
N <sub>12</sub>	0.23123	0.64606	0.09555	0.00056	0.00070	0.00021
N <sub>13</sub>	0.64054	0.46150	0.33197	0.00058	0.00090	0.00025
C <sub>14</sub>	0.76234	0.34013	0.35927	0.00078	0.00111	0.00034
C <sub>15</sub>	0.93905	0.40895	0.35974	0.00083	0.00156	0.00048
C <sub>16</sub>	1.07545	0.31144	0.41139	0.00081	0.00131	0.00033
C <sub>17</sub>	1.14044	0.40453	0.47206	0.00099	0.00140	0.00040
C <sub>18</sub>	1.27654	0.31844	0.51807	0.00106	0.00179	0.00036
C <sub>19</sub>	1.33923	0.15357	0.50272	0.00110	0.00164	0.00038
C <sub>20</sub>	1.27030	0.06257	0.44115	0.00107	0.00154	0.00042
C <sub>21</sub>	1.14061	0.14745	0.39573	0.00093	0.00130	0.00037

Table 3b continued

	X	Y	Z	$\sigma_x$	$\sigma_y$	$\sigma_z$
C <sub>22</sub>	0.27546	0.45226	0.08176	0.00067	0.00084	0.00028
C <sub>23</sub>	0.46137	0.42789	0.07739	0.00077	0.00116	0.00033
C <sub>24</sub>	-0.01397	0.45690	0.16453	0.00062	0.00088	0.00028
O <sub>25</sub>	-0.10451	0.53246	0.11447	0.00050	0.00068	0.00020
O <sub>26</sub>	-0.02332	0.29427	0.18508	0.00054	0.00072	0.00024
O <sub>27</sub>	0.38446	0.23180	0.21984	0.00051	0.00068	0.00020
O <sub>28</sub>	0.72824	0.18588	0.38048	0.00065	0.00099	0.00036
N <sub>29</sub>	0.21564	0.73742	-0.01975	0.00059	0.00082	0.00022
O <sub>30</sub>	0.70759	0.08559	0.19846	0.00062	0.00082	0.00029
O <sub>31</sub>	0.69064	-0.12790	0.08104	0.00069	0.00087	0.00024
O <sub>32</sub>	0.83998	-0.17257	0.30179	0.00080	0.00108	0.00036

Table 4. 3-Spiro-thiazolinium-7-PAC derivative anisotropic temperature factor coefficients

	$\beta_{11}$	$\beta_{22}$	$\beta_{33}$	$\beta_{23}$	$\beta_{13}$	$\beta_{12}$
S <sub>1</sub>	0.01324	0.01220	0.00187	-0.00206	0.00064	-0.00504
C <sub>2</sub>	0.00903	0.01125	0.00197	0.00026	0.00086	-0.00217
C <sub>3</sub>	0.00734	0.01075	0.00164	-0.00223	0.00090	-0.00045
C <sub>4</sub>	0.00786	0.00808	0.00158	-0.00056	0.00030	0.00101
N <sub>5</sub>	0.00926	0.00950	0.00148	-0.00042	0.00068	-0.00296
C <sub>6</sub>	0.01284	0.01448	0.00127	-0.00205	0.00099	-0.00650
C <sub>7</sub>	0.01100	0.01362	0.00160	0.00103	0.00022	-0.00552
C <sub>8</sub>	0.00975	0.01222	0.00166	0.00068	0.00067	-0.00319
C <sub>9</sub>	0.01071	0.00948	0.00217	-0.00085	0.00101	0.00188
S <sub>10</sub>	0.01699	0.00784	0.00258	0.00162	0.00185	0.00242
C <sub>11</sub>	0.00803	0.01461	0.00178	0.00190	-0.00030	-0.00442
N <sub>12</sub>	0.01089	0.00809	0.00134	-0.00034	0.00134	0.00126
N <sub>13</sub>	0.00968	0.01821	0.00186	0.00190	0.00021	-0.00072
C <sub>14</sub>	0.01317	0.01506	0.00264	0.00395	0.00071	0.00166
C <sub>15</sub>	0.00995	0.03357	0.00476	0.01460	0.00175	0.00231
C <sub>16</sub>	0.01310	0.02097	0.00245	0.00450	0.00145	-0.00224
C <sub>17</sub>	0.01874	0.02357	0.00293	-0.00231	0.00341	0.00332
C <sub>18</sub>	0.02237	0.03500	0.00215	-0.00224	0.00032	0.00438
C <sub>19</sub>	0.02146	0.03230	0.00236	0.00161	0.00001	0.00536
C <sub>20</sub>	0.02163	0.02569	0.00304	0.00097	0.00220	0.01332
C <sub>21</sub>	0.01679	0.02045	0.00264	-0.00189	0.00030	0.00571

Table 4 continued

	$\beta_{11}$	$\beta_{22}$	$\beta_{33}$	$\beta_{23}$	$\beta_{13}$	$\beta_{12}$
$C_{22}$	0.01081	0.00798	0.00185	-0.00108	0.00220	0.00277
$C_{23}$	0.01271	0.01931	0.00236	-0.00047	0.00400	0.00858
$C_{24}$	0.00816	0.01076	0.00194	-0.00154	0.00022	-0.00327
$O_{25}$	0.01222	0.01287	0.00195	-0.00138	-0.00012	-0.00492
$O_{26}$	0.01310	0.01081	0.00302	0.00097	0.00058	-0.00694
$O_{27}$	0.01206	0.01117	0.00211	-0.00107	0.00071	0.00150
$O_{28}$	0.01386	0.02159	0.00582	0.01169	0.00399	0.00008
$N_{29}$	0.01151	0.01258	0.00150	0.00179	0.00099	-0.00395
$O_{30}$	0.01459	0.01452	0.00415	-0.00168	0.00483	-0.00280
$O_{31}$	0.02132	0.01960	0.00238	-0.00145	0.00261	0.00092
$O_{32}$	0.02324	0.02141	0.00524	0.00452	0.00542	-0.00097

All temperature factors in this table are positive definite.

Table 5. 3-Spiro-thiazolinium-7-PAC derivative intra-molecular bond distances and estimated standard deviations in Angstroms.

Bond		Bond	
S1 - C2	1.835 (.005)	C14 - O28	1.233 (.010)
S1 - C6	1.825 (.007)	C15 - C16	1.529 (.011)
C2 - C3	1.553 (.007)	C16 - C17	1.389 (.010)
C3 - C4	1.568 (.007)	C16 - C21	1.348 (.012)
C3 - C9	1.532 (.009)	C17 - C18	1.433 (.012)
C3 - N12	1.487 (.006)	C18 - C19	1.343 (.016)
C4 - N5	1.472 (.007)	C19 - C20	1.403 (.011)
C4 - C24	1.550 (.008)	C20 - C21	1.390 (.011)
N5 - C6	1.471 (.007)	C22 - C23	1.527 (.008)
N5 - C8	1.369 (.008)	C24 - O25	1.243 (.006)
C6 - C7	1.590 (.009)	C24 - O26	1.243 (.008)
C7 - C8	1.558 (.007)		
C7 - N13	1.437 (.007)		
C8 - O27	1.211 (.007)		
C9 - S10	1.813 (.005)		
S10 - C11	1.751 (.007)		
C11 - N12	1.338 (.007)		
C11 - N29	1.306 (.006)		
N12 - C22	1.475 (.008)		
N13 - C14	1.351 (.009)		
C14 - C15	1.507 (.010)		

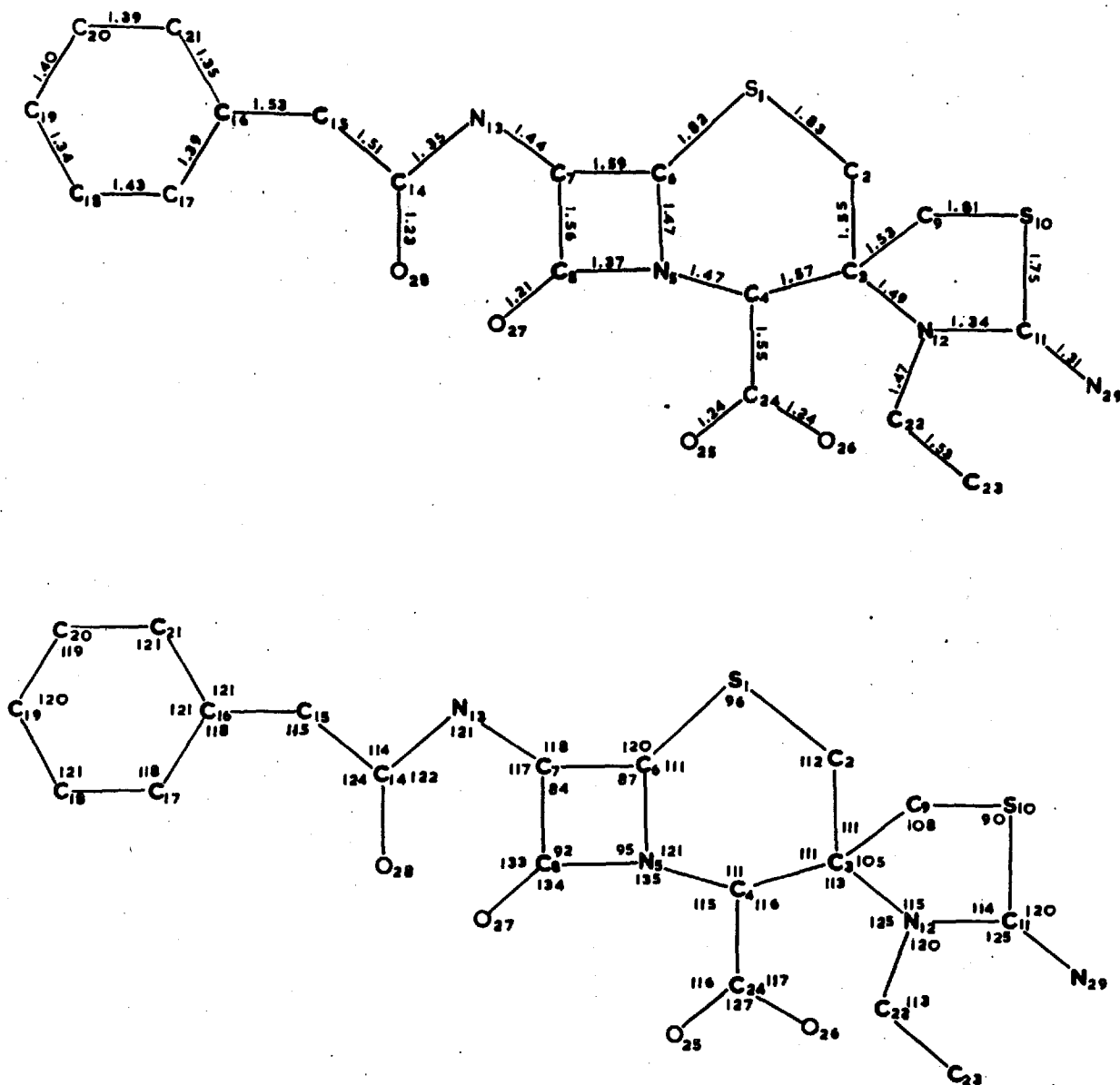
**Table 6.** 3-Spiro-thiazolinium-7-PAC derivative intra-molecular bond angles and standard deviations in degrees.

C2 - S1 - C6	96.1 (0.3)	C9 - S10 - C11	89.7 (0.3)
S1 - C2 - C3	111.8 (0.4)	S10 - C11 - N12	114.3 (0.7)
C2 - C3 - C4	110.5 (0.5)	S10 - C11 - N29	120.5 (0.6)
C2 - C3 - C9	111.3 (0.6)	N12 - C11 - N29	125.1 (0.7)
C2 - C3 - N12	107.0 (0.5)	C3 - N12 - C22	124.6 (0.6)
C4 - C3 - C9	109.6 (0.6)	C3 - N12 - C11	115.2 (0.5)
C4 - C3 - N12	112.9 (0.5)	C11 - N12 - C22	120.2 (0.7)
C9 - C3 - N12	105.4 (0.5)	C7 - N13 - C14	121.1 (0.7)
C3 - C4 - N5	110.7 (0.5)	N13 - C14 - C15	114.2 (0.7)
C3 - C4 - C24	116.4 (0.6)	N13 - C14 - O28	121.7 (1.1)
N5 - C4 - C24	115.3 (0.5)	C15 - C14 - O28	124.1 (1.1)
C4 - N5 - C6	121.4 (0.5)	C14 - C15 - C16	114.9 (0.7)
C4 - N5 - C8	134.5 (0.8)	C15 - C16 - C17	118.0 (0.8)
C6 - N5 - C8	95.5 (0.5)	C15 - C16 - C21	120.8 (1.1)
C6 - C7 - C8	83.8 (0.4)	C17 - C16 - C21	121.0 (1.1)
C6 - C7 - N13	117.7 (0.7)	C16 - C17 - C18	117.8 (0.9)
C8 - C7 - N13	116.7 (0.6)	C17 - C18 - C19	120.9 (1.4)
N5 - C8 - C7	92.3 (0.4)	C18 - C19 - C20	119.9 (1.3)
N5 - C8 - O27	134.3 (1.0)	C19 - C20 - C21	119.3 (1.0)
C7 - C8 - O27	133.4 (0.8)	C16 - C21 - C20	121.0 (1.2)
S10 - C9 - C3	107.6 (0.5)	N12 - C22 - C23	113.0 (0.6)

Table 6 continued

C4 - C24 - 025	115.6 (0.6)
C4 - C24 - 026	117.0 (0.7)
025 - C24 - 026	127.5 (0.9)

Figure 2. The 3-spiro-thiazolinium-7-PAC derivative bond lengths and angles.

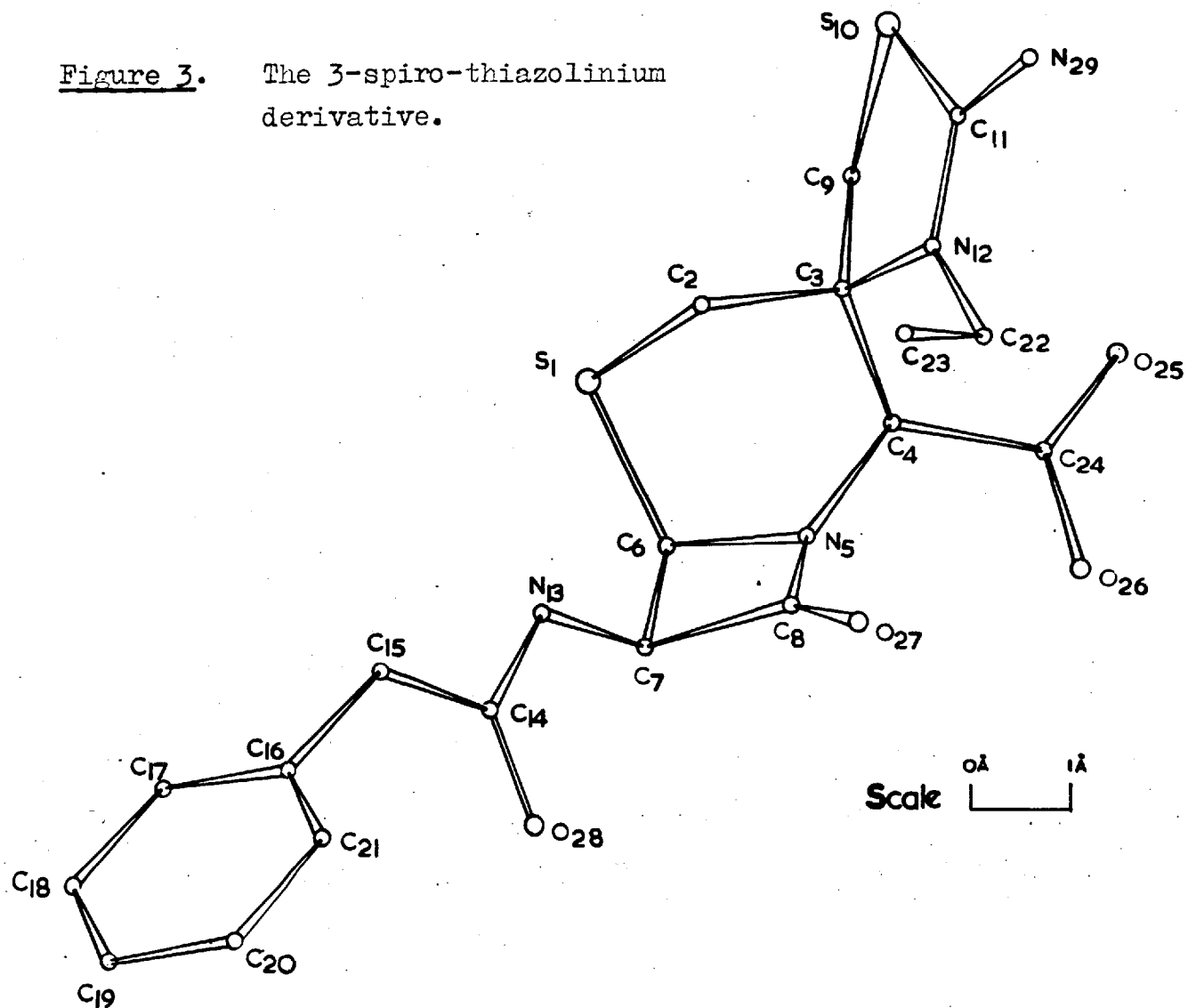


$$C_2 - C_3 - N_{12} = 107^\circ$$

$$C_4 - C_3 - C_9 = 110^\circ$$



Figure 3. The 3-spiro-thiazolinium derivative.



same as in all previously determined cephalosporins and penicillins. The asymmetric centre at C4 is S, whereas the corresponding centres in benzylpenicillin, phenoxymethylpenicillin and 6-NBF-PA possess the opposite chirality, R. Using the same notation, the spiro atom at C3 is S. It was the difficulty of describing the configuration at C3 that led the author, with the assistance of Dr.A.G.Long (1966), to adopt the Cahn-Ingold-Prelog notation which gives the name (3S,4S,6R,7R)-2'-amino-3'-ethyl-2'-thiazolinium-4'-spiro-3-(7-phenylacetamidocepham-4-carboxylate) trihydrate, where the 'cepham' system, suggested by Morin et al. (1962) is shown in Figure 4.

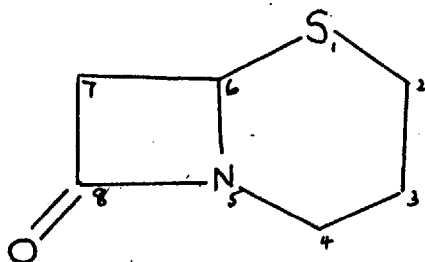


Figure 4. The cepham system

The analysis has shown that the ethyl group (C22, C23) is bonded to the cyclic nitrogen atom (N12) of the thiazolinium group.

## The Thiazolinium Ring

DIDO was used to calculate the least-squares planes through sets of atoms in the molecule, and the results are shown in Table 7.

The atoms C3, S10, C11, N12, C22 and N29 form a plane (Table 7a), the average deviation from the plane being 0.01 Å, and C9 lies 0.45 Å below the plane looking at the molecule as seen in Figure 3. The bond C9 - S10 (1.813 Å) is in good agreement with the average value of 1.817 Å for a single C - S bond given by Sutton (1965). However, S10 - C11 (1.751 Å) is approximately 9 e.s.d.'s shorter than this and nearer to the value of 1.718 Å in the conjugated, heterocyclic compound thiophen. Sutton gives the average C - N bond length in conjugated heterocyclics as 1.339 Å, with which the bond C11 - N12 (1.338 Å) is in good agreement, and C11 - N29 (1.306 Å) is approximately 5 e.s.d.'s shorter.

These results suggest that the thiazolinium system can be represented as in Figure 5, N29 being probably hydrogen

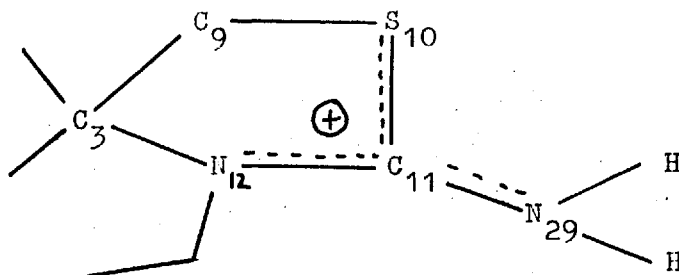


Figure 5. The thiazolinium ring.

bonded (see page 112). The bond lengths of the carboxyl group, C24 - O25 (1.243 Å) and C24 - O26 (1.243 Å) indicate that it is present in the ionized form (C - O = 1.26 Å (Sutton)), so that the analysis substantiates the electrophoresis and infrared data that suggested the compound occurs as a zwitter-ion. The carboxylate ion is also planar (Table 7e).

The bond angle C9 - S10 - C11 (89.7°) agrees quite well with the C - S - C angle in thiophen (91.3°), although the comparison is questionable as thiophen is completely conjugated. The angle N12 - C22 - C23 (113.0°) differs significantly from the equilibrium value of 109° 28'. This can be explained by repulsion between the C23 methyl group and the  $\pi$  electrons at N12, the distance N12 - C23 being 2.503 Å.

#### The Tetrahydrothiazine Ring

The atoms S1, C2, C3, C4, N5 and C6 form a distorted boat conformation with C2 and N5 at the prow and stern. The boat is distorted in that the bond S1 - C6 is far from parallel to C3 - C4. This can be seen in Figure 3; for an undistorted boat, the atoms S1, C3, C4 and C6 would be in a plane, whereas C3 actually lies 0.656 Å above the plane through the other three atoms.

The reasons for the preferred boat conformation in the crystal structure are difficult to assess. One explanation

may be that the chair form would separate the charges of the thiazolinium system and the carboxylate ion. Whether this is the case was difficult to decide by constructing models, especially as it is not known where the charge is concentrated in the thiazolinium group. The shortest inter-atomic distances relevant to this point are given below in A

C11 - O25	3.492
C11 - C24	3.902
N12 - C24	2.927
N12 - O25	2.915

Changing the model from the boat to the chair form moved O25 away from N12 but did not noticeably affect the N12 - C24 distance, though it did bring the exocyclic ethyl group into crowding with the  $\beta$ -lactam-tetrahydrothiazine ring system. Even in the boat conformation, the ethyl group is quite close to C2 and O27 as shown by the distances C2 - C23 (3.537 A), C2 - C22 (3.273 A), C22 - O27 (3.137 A) and C23 - O27 (3.299 A).

Another close contact that may affect the conformation of the six-membered ring is that between the group  $\begin{array}{c} \text{H} \\ \text{H} \end{array} > \text{C22}$  and the carboxylate ion. The distance C22 - C24 is 3.080 A, and one of the C22 hydrogen atoms points towards the carboxylate ion. This probably accounts for the fact that the angles C3 - C4 - C24 (116.4°) and N5 - C4 - C24 (115.3°) are both approximately 10 e.s.d.'s from the tetrahedral value and the

distortion may be favoured in that it results in a partial staggering of the bonds C3 - N12 and C4 - C24. It is also possible that the role of the water molecules in the crystal could contribute to the stability of a particular conformer. As will be described later, the water molecules enter into a hydrogen-bonding scheme that includes N29, O25 and O26.

The high degree of overcrowding that has been described may result in restricted rotation of the carboxylate ion around the bond C4 - C24 and possibly account for the low antibacterial activity of the spiro compound, in that it would be difficult for either O25 or O26 to acquire a 'penicillin-like' position. Rotation would be especially hindered by the close contacts between O25 and C22 (3.293 Å), O26 and O27 (3.267 Å) and C9 and O25 (3.199 Å).

The rest of the dimensions in the tetrahydrothiazine ring are unremarkable. The bonds S1 - C2 (1.835 Å) and S1 - C6 (1.825 Å) are not significantly different from the value given by Sutton (1.817 Å) for a C - S single bond and the value of 1.80 Å determined by Diamand (1963) for ceph. Cc. The dimensions of the ionized carboxyl group agree well with those listed by Sutton, for example in the tartaric acid ion and the zwitterion, L-threonine.

## The $\beta$ -Lactam Ring

The bond lengths and angles of the  $\beta$ -lactam ring in the 3-spiro-thiazolinium-7-PAC derivative are similar to those determined for 6-NBF-PA. The length of the bond C6 - C7 (1.590 Å) is possibly not significant in terms of the real standard deviations; previous crystallographic work has not indicated a bond significantly longer than the accepted value of 1.539 Å.

The least-squares plane through the atoms of the  $\beta$ -lactam ring including O27 shows deviations between 0.02 and 0.10 Å (Table 7b). However, the atoms N5, C7, C8 and O27 form a plane well within the experimental accuracy, with C6 projecting 0.245 Å out of the plane on the same side as S1. This arrangement agrees with that found for 6-NBF-PA.

That resonance takes place to a certain extent in the cyclic amide is shown by the bond length N5 - C8 (1.369 Å) and the angle C4 - N5 - C6 (121.4°) indicates the corresponding tendency for N5 to be planar. However, the nitrogen atom in the 3-spiro-thiazolinium-7-PAC derivative has achieved a greater degree of planarity than the corresponding atom in 6-NBF-PA, as shown by the sum of the angles round both atoms (351° and 340° respectively). This is probably because the six-membered ring in the spiro cephalosporin possesses more degrees of freedom than the thiazolidine ring, so that planarity at N5 can be achieved without exerting a great deal of strain at C6.

Table 7. DEviations (A) of the atoms from the calculated least-squares planes. Atoms marked with \* were not included in the calculation of the plane.  $\sum d^2$  is the sum of the squares of the deviations (A) from the plane.

## (a) Thiazolinium Ring

$$\sum d^2 = 0.00089$$

Atom	Deviation
S10	-0.001
C11	-0.020
N12	-0.008
N29	0.017
C3	0.013
C22	-0.002
C9 *	-0.451

(b)  $\beta$ -Lactam Ring

$$\sum d^2 = 0.02569$$

Atom	Deviation
N5	-0.080
C6	0.104
C7	-0.063
C8	-0.023
O27	0.062

(c)  $\beta$ -Lactam Ring

$$\sum d^2 = 0.00010$$

Atom	Deviation
N5	0.002
C7	0.002
C8	-0.009
O27	0.004
C6 *	0.245

## (d) Benzene Ring

$$\sum d^2 = 0.00040$$

Atom	Deviation
C16	-0.008
C17	0.000
C18	0.003
C19	0.003
C20	-0.011
C21	0.014
C15 *	0.091



Table 7 continued

(e) Carboxylate Ion

$$\sum d^2 = 0.00011$$

Atom	Deviation
O25	-0.003
C24	0.009
O26	-0.003
C4	-0.002

(f) Amide Group

$$\sum d^2 = 0.00107$$

Atom	Deviation
N13	0.025
C14	-0.002
O28	0.006
C15	-0.011
C7	-0.017

### The Phenylacetamido Side Chain

The amide group is planar (Table 7f) and the bond lengths are consistent with those of a normal resonating amide. The angle N13 - C14 - C15 ( $114.2^\circ$ ) is 8 e.s.d.'s from the expected value of  $120^\circ$ , and C14 - C15 - C16 ( $114.9^\circ$ ) is 7 e.s.d.'s above the tetrahedral value. These results can be explained by repulsive forces between the carbonyl electrons and the  $\pi$  electrons of the benzene ring, the distance C16 - O28 being 2.900 Å. The extended form of the side chain which results in this close contact is probably stabilized by packing conditions in the crystal.

### Packing and Hydrogen Bonding

In the following discussion, atoms that are related to those of Table 3b by the symmetry of the spacegroup are referred to by terms in parentheses following the atom symbol.

Some close-contact distances are shown in Figure 8 which is a projection of adjacent unit cells down the b axis. Inter-molecular distances less than 3.5 Å are listed in Table 8, including those between the oxygen atoms (O30, O31, O32) of the three water molecules.

The molecules of the spiro compound lie diagonally across the cell; the arrangements around the screw axes at

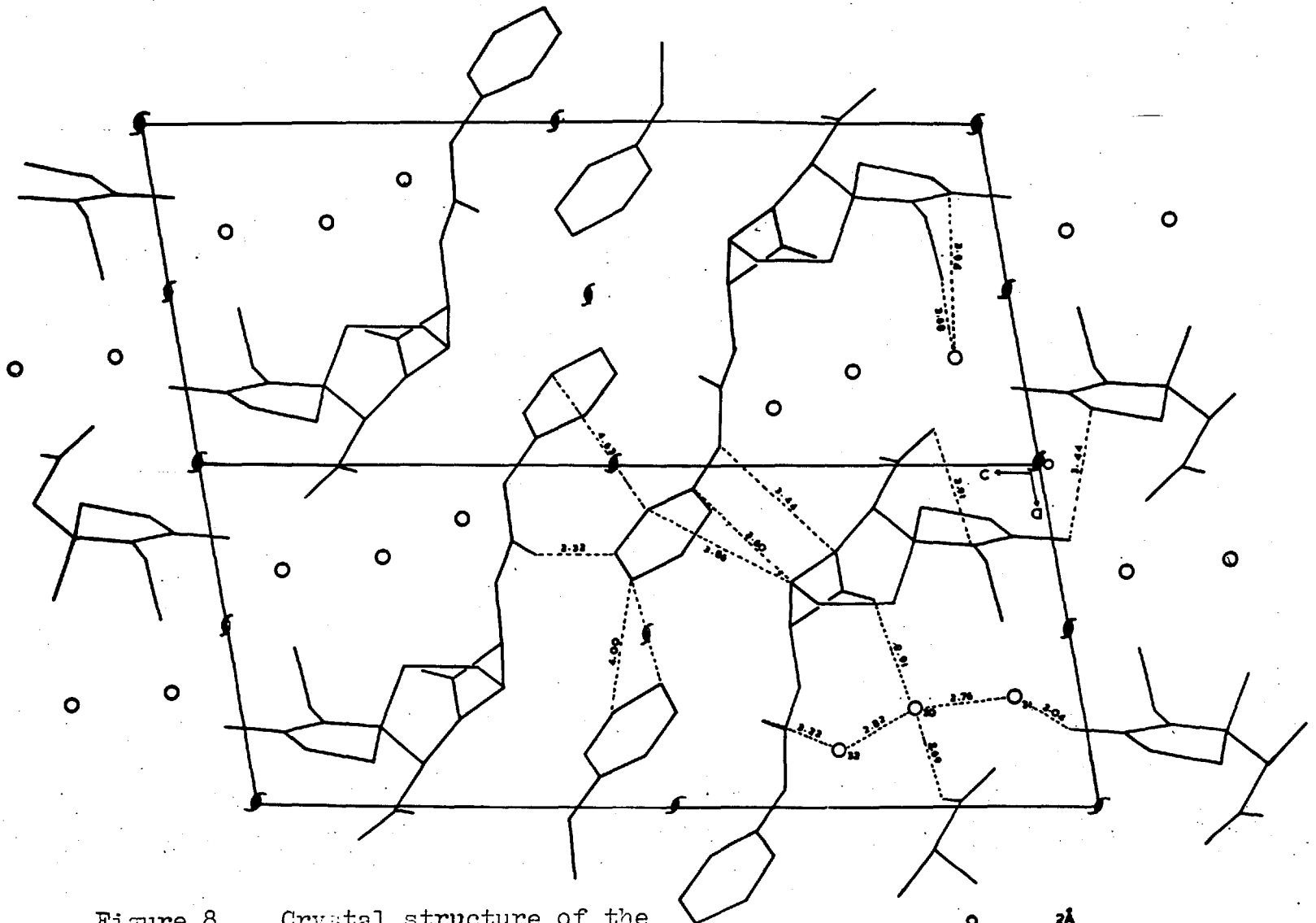


Figure 8. Crystal structure of the spiro compound projected down b.

Scale 2Å

Table 8. Inter-molecular distances ( $\overset{\circ}{\text{A}}$ ) less than 3.5  $\overset{\circ}{\text{A}}$  in the crystal of the 3-spiro-thiazolinium-7-PAC derivative. The terms in parentheses following the atom name relate the position of the atom to the values listed in Table 3b. The first term describes the symmetry relation where

$$\begin{aligned} 0/ &= x, \quad y, \quad z \\ 1/ &= -x, \quad y - \frac{1}{2}, \quad -z \end{aligned}$$

and the other terms give the number of cell translations in the directions x, y and z respectively.

Vector	Symmetry	Distance	Vector	Symmetry	Distance
S1 - O27	(0/0 1 0)	3.310	C24 - N29	(1/0 0 0)	3.412
C2 - O27	(0/0 1 0)	3.426	O25 - O31	(0/-1 1 0)	2.954
C2 - O30	(0/0 1 0)	3.445	O25 - N29	(1/0 0 0)	2.866
N5 - C15	(0/-1 0 0)	3.445	O26 - O30	(0/-1 0 0)	2.689
C9 - O26	(0/0 1 0)	3.157	O26 - N29	(1/0 0 0)	3.376
C9 - O27	(0/0 1 0)	3.336	O27 - O30		2.909
C9 - O31	(0/-1 1 0)	3.466	O28 - O32		3.217
S10 - C22	(0/0 1 0)	3.428	O30 - O31		2.760
S10 - N29	(1/0 1 0)	3.444	O30 - O32		2.820
N13 - O32	(0/0 1 0)	3.193	O31 - N29	(1/1 0 0)	3.035
C15 - O32	(0/0 1 0)	3.264	C18 - O28	(1/2 1 1)	3.317

$z = 0, 1$  etc. concern the polar groups, whereas the screw axes at  $z = 1/2, 3/2$  etc. are surrounded mainly by the non-polar benzyl groups. The close contacts around the screw axis at  $x = \frac{1}{2}, z = \frac{1}{2}$  are between the benzene rings and the  $\beta$ -lactam rings though the distances are quite large as shown in Figure 8.

The oxygen atoms of the three water molecules are located (Figure 8) such that the cephalosporin molecules in adjacent unit cells are linked in all three crystallographic directions by hydrogen bonds. The network so formed can be seen in Figure 9, which is a projection down the  $a$  axis. The positions of the atoms shown in Figure 9 are related to those in Table 3b as follows :

$$CB11 = C11 (1 - x, y - \frac{1}{2}, -z)$$

$$CC11 = C11 (1 - x, y + \frac{1}{2}, -z)$$

$$CA24 = C24 (1 + x, y, z)$$

$$OA25 = O25 (1 + x, y, z)$$

$$OA26 = O26 (1 + x, y, z)$$

$$NB29 = N29 (1 - x, y - \frac{1}{2}, -z)$$

$$NC29 = N29 (1 - x, y + \frac{1}{2}, -z)$$

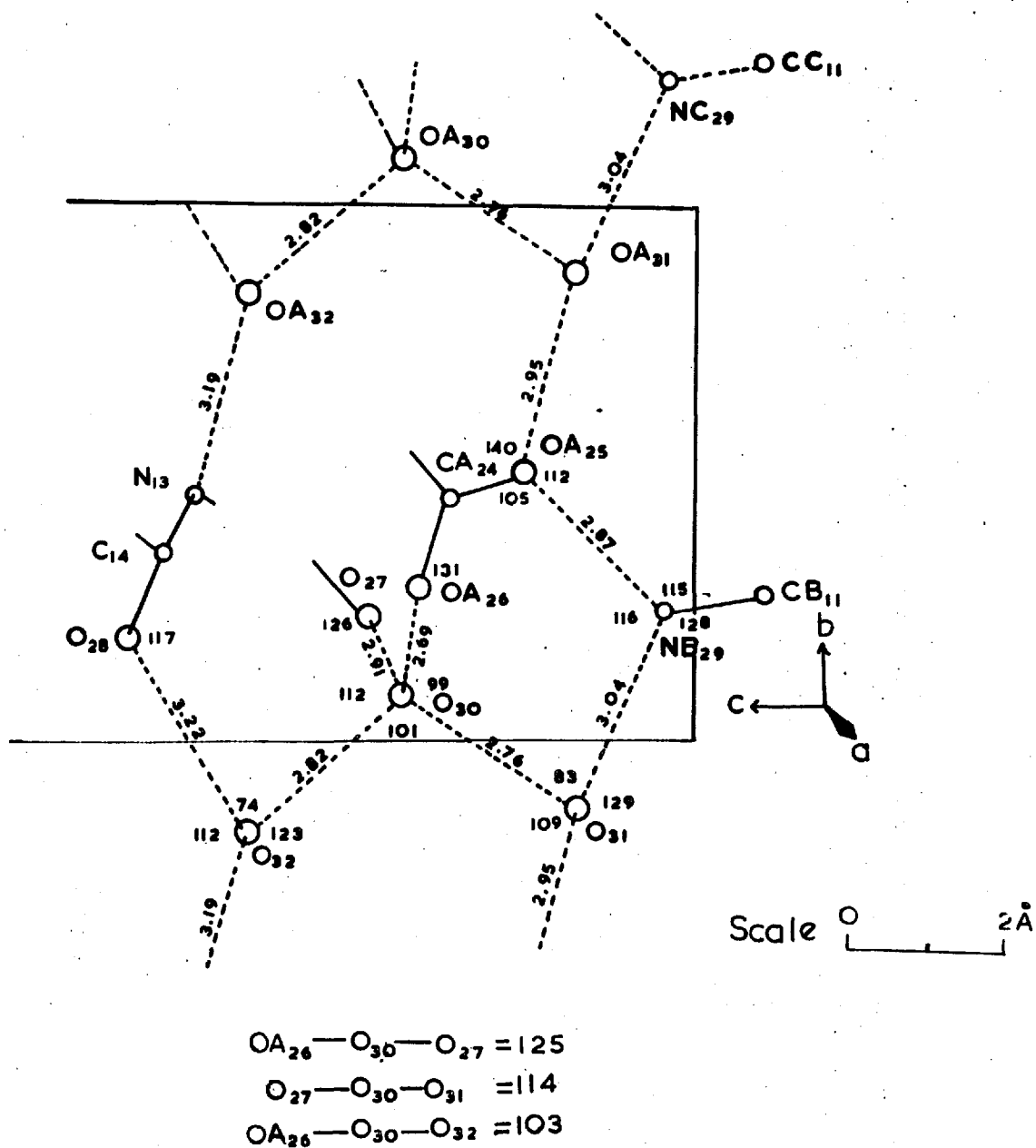
$$OA30 = O30 (x, y + 1, z)$$

$$OA31 = O31 (x, y + 1, z)$$

$$OA32 = O32 (x, y + 1, z)$$

$O30$  appears to be tetrahedrally bonded to  $O32$  (2.820 Å),  
 $O31$  (2.760 Å),  $O26$  (1 +  $x$ ,  $y$ ,  $z$ ) (2.689 Å) and  $O27$  (2.909 Å).

Figure 9. The 3-spiro-thiazolinium-7-PAC derivative hydrogen bonding system projected down the  $\alpha$  axis



The angles around O30 are shown in Figure 9. Pimental and McClellan (1960) have tabulated the known data for the O - H .....O distances and the O.....O.....O angles for water in organic crystals. The values vary over a wide range; the distances from 2.65 Å to 2.99 Å, and the angles from 83° to 120°, and the values associated with O30 are in good agreement with this range. If the hydrogen bonding is as suggested, the hydrogen atoms bonded to O30 must lie approximately in the directions of O27 and O26 (1 + x, y, z).

The atoms surrounding O31 are O25 (1 + x, y - 1, z) (2.954 Å), N29 (1 - x, y -  $\frac{1}{2}$ , -z) (3.035 Å) and O30 (2.760 Å). N12 (1 + x, y, z) is too far from O31 (4.101 Å) to take part in any hydrogen bonding. The location of two possible hydrogen atoms bonded to N29 has been described on page 89. For the calculation of the position of H21 (1 - x, y -  $\frac{1}{2}$ , -z) (Table 2), it was assumed that a linear hydrogen bond existed between O31 and N29 (1 - x, y -  $\frac{1}{2}$ , -z). The assumption for the calculation of H22 was that the atoms O31, C11(1 - x, y -  $\frac{1}{2}$ , -z) and the hydrogen atom would form a trigonal arrangement around N29 (1 - x, y -  $\frac{1}{2}$ , -z). The observed and calculated positions agree well, and the observed position of H21 (1 - x, y -  $\frac{1}{2}$ , -z) lies 19° off the line N29 (1 - x, y -  $\frac{1}{2}$ , -z) - O31 and that of H22 (1 - x, y -  $\frac{1}{2}$ , -z) is situated 7° from the line N29 (1 - x, y -  $\frac{1}{2}$ , -z) - O25 (1 + x, y, z). Thus, the hydrogen atoms bonded to O31 probably lie in the directions of O30 and

025 (1 + x, y, z).

The distances O32 - O28 (3.217 Å) and O32 - N13 (x, y - 1, z) (3.193 Å) suggest that weak hydrogen bonding may exist between these atoms. The angles around O32 are shown in Figure 9 and only O30 - O32 - O28 (74°) lies out of the range given by Pimentel and McClellan, and the two lone pair orbitals of O28 will not be pointing well towards O32, resulting in only a weak hydrogen bond. The calculated and observed positions of the hydrogen bonded to N13 (x, y - 1, z) are situated respectively 28° and 17° off the line O32 - N13 (x, y - 1, z), which indicates that the hydrogen atoms bonded to O32 are orientated towards O30 and O28.

The hydrogen-bonding network that has been described must contribute substantially to the stability of the crystal, and as mentioned on page 118 possibly plays an important part in stabilising the observed boat conformation of the tetrahydrothiazine ring.



CHAPTER 6

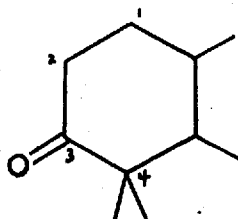
## The Chemistry of Zeorin

As mentioned at the end of Chapter 1, attempts have been made to solve the crystal structure of zeorin acetate, a compound containing only carbon, hydrogen and oxygen ( $C_{32}H_{54}O_3$ ) and derived from the natural product zeorin, a member of the triterpenoid series. The chemical work, which is briefly described in this chapter has established the structure of zeorin fairly well and shown that it is derived from a unique, saturated hydrocarbon zeorinane. The proposed structure of zeorin fits in well with the theory of squalene as the biogenetic precursor of the triterpenoids.

That zeorin is a component of foliaceous lichens was recognised by Hesse (1906) and Zopf (1909) but its chemistry received little attention until Asahina and Akagi (1938) demonstrated that it belongs to the triterpenoid series and has the formula  $C_{30}H_{52}O_2$ . Mild acetylation produced the mono-acetate, zeorin acetate, and Asahina and Yosioka (1940) showed that more vigorous acetylation gave anhydrozeorin acetate, by elimination of the elements of water from zeorin acetate. This indicated that zeorin contained a tertiary - OH group.

Zeorin, when heated with alcoholic hydrochloric acid gave a dehydration product, zeorinin, which also formed a monoacetate and when oxidised with dichromate gave a ketone, zeorininone ( $C_{30}H_{48}O$ ), indicating the presence in zeorin of a secondary - OH group.

These conclusions were substantiated and extended by Barton and Bruun (1952). Infra-red data for zeorinone (produced by chromic acid oxidation of zeorin) indicated a cyclohexanone part-structure, but the oxygen atom could not be at the  $C_3$  position, which is most common in the triterpenoids and shown in (I), as zeorinone is unreactive to normal carbonyl reagents



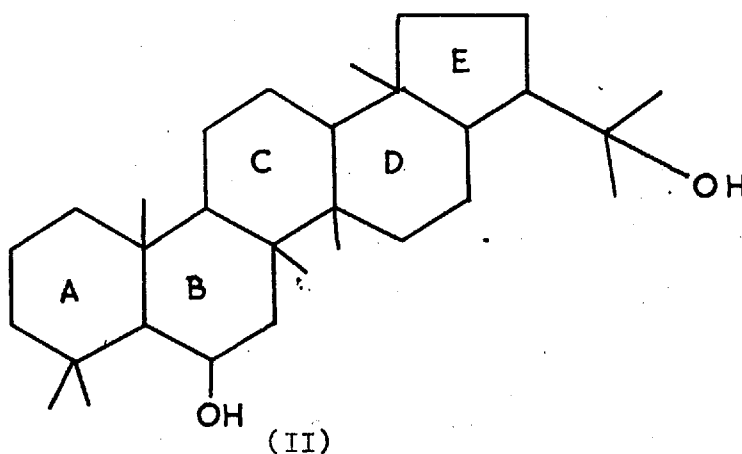
(I)

and reduction. Dehydration of zeorin acetate gave zeorinin acetate or an isomer, isozeorinin acetate, depending upon the reaction conditions. The infra-red absorption spectrum of isozeorinin acetate (probably equivalent to the anhydrozeorin acetate of Asahina and Yosioka) indicated the presence of a methylene group as  $\text{>CH}_2$ , hence the tertiary - OH of zeorin as  $\text{>CMe - OH}$ . That zeorin is not a simple derivative of a known triterpene was demonstrated by the preparation of

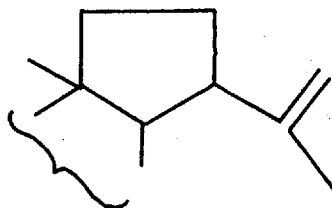
zeorinane, the unique and fully saturated hydrocarbon.

The above and other important reactions of zeorin and its derivatives are shown in Figure 1.

After further work, Barton, de Mayo and Orr (1958) proposed the structure (II) for zeorin.

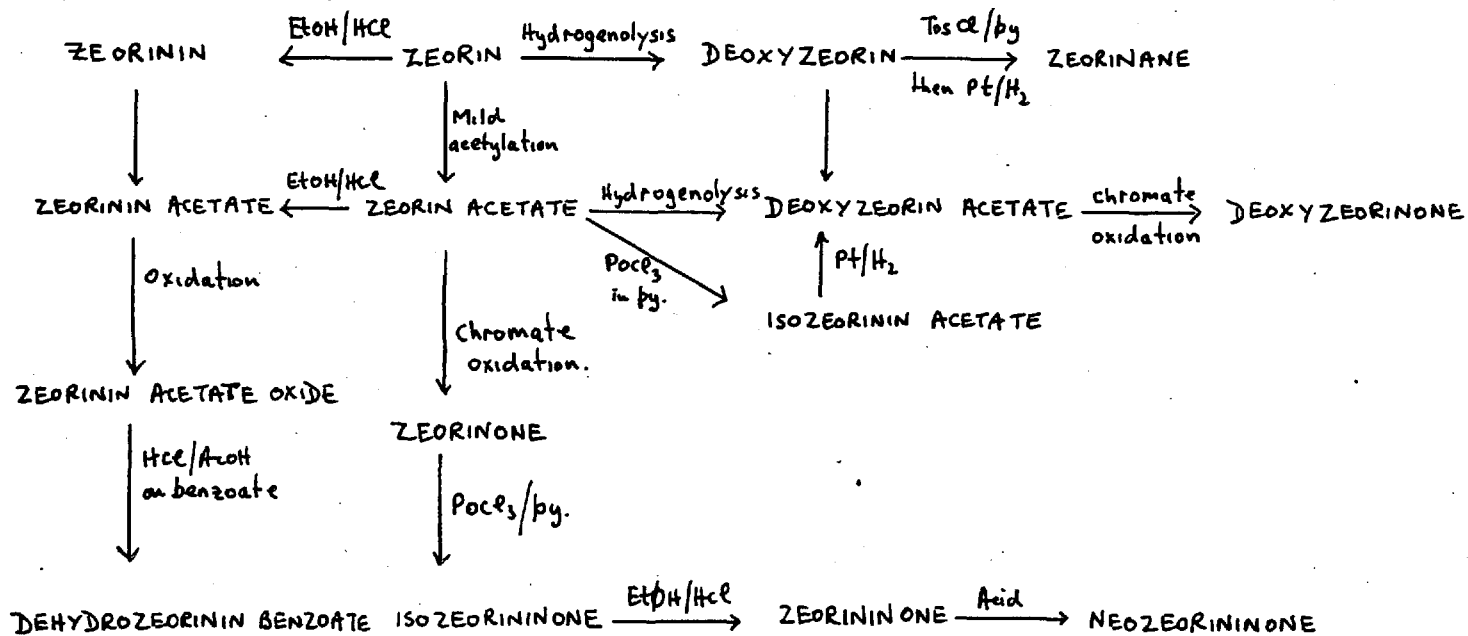


Ozonolysis of crude isozeorinin acetate gave a methyl ketone with the loss of one carbon atom, indicating the part-structure (III) in isozeorinin acetate (that the E ring is five-membered



is shown in the following section). The ozonolysis also produced acetone which suggested the presence of the

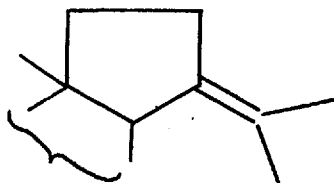
Figure 1. Some reactions of zeorin.



$\text{TosCl} = p\text{-C}_6\text{H}_4\text{Me}\cdot\text{SO}_2\text{Cl}$

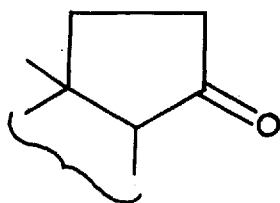
$\text{Py} = \text{pyridine}$ .

isopropylidene isomer (IV) in the crude starting material.



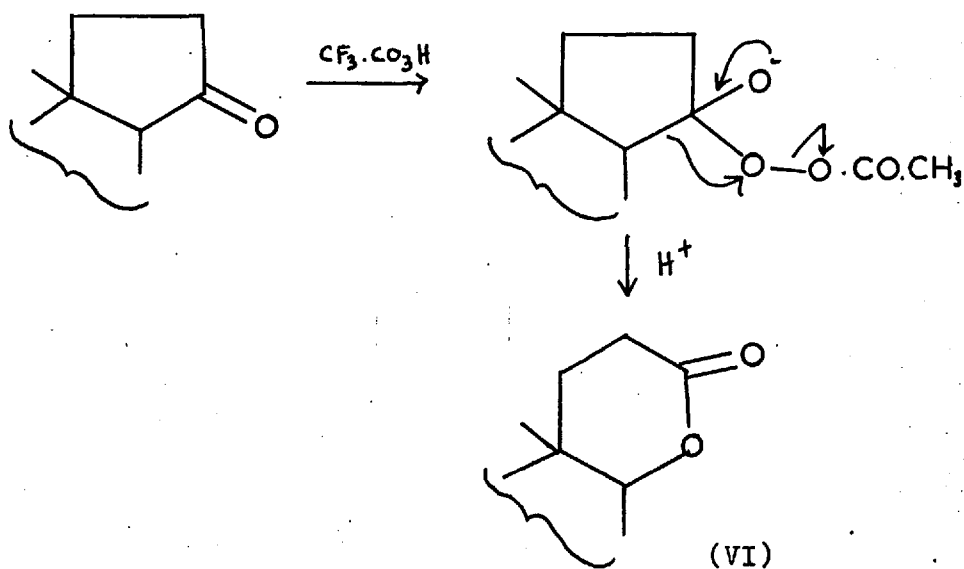
(IV)

Recognition of the ketone (V) was made by further oxidation



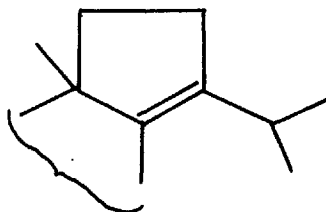
(V)

of the product with trifluoro peracetic acid to give the  $\delta$ -lactone (VI) by the following mechanism.



(VI)

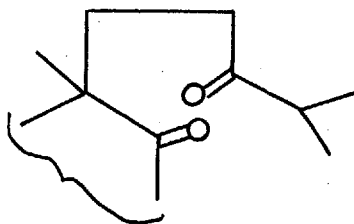
(VI) was recognised as a  $\delta$ -lactone from its infra-red spectrum, and its formation indicated that the E ring must be five-membered. Hence zeorinin was assigned the part-structure (VII)



(VII)

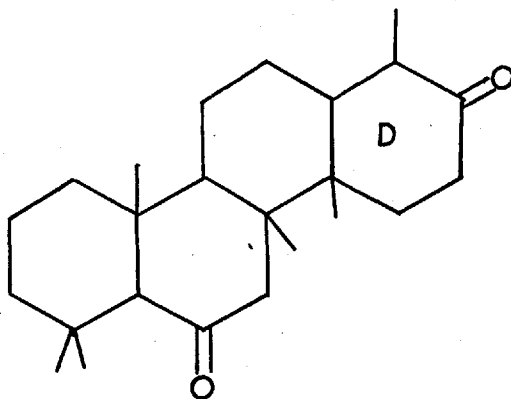
where the double bond of isozeorinin, (III), has migrated into the E ring.

Other oxidative experiments on zeorinin acetate using osmium tetroxide and lead tetra-acetate, resulted in the 1:5 diketone (VIII). Barton et al. predicted that (VIII) should



(VIII)

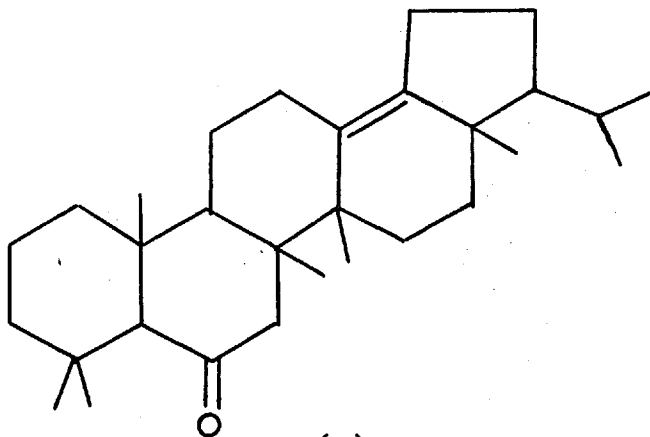
undergo a reverse Michael addition, to give after oxidation, the diketone (IX). The product from the action of alkali in



(IX)

ethylene glycol on (VIII) followed by oxidation showed a single band in the I.R. spectrum at  $1703\text{ cm}^{-1}$ , characteristic of a cyclohexanone structure and confirming that the D ring must be six-membered, as in (IX).

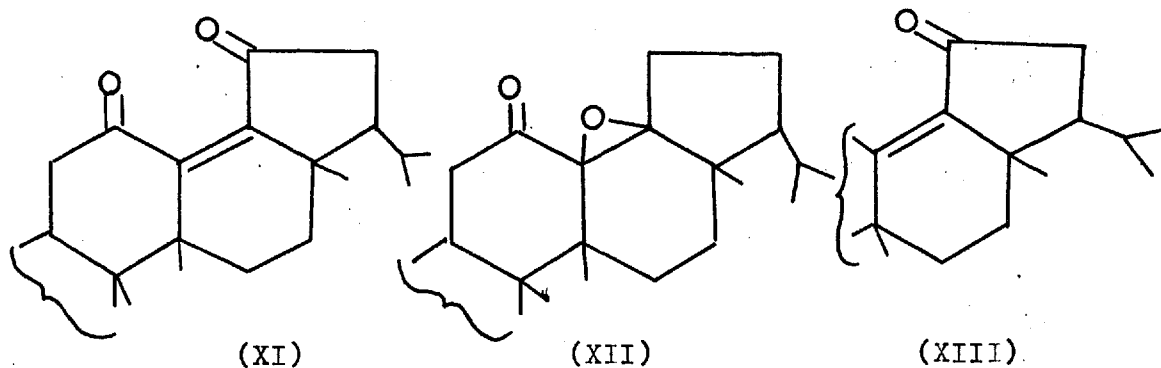
The probable identity of the C ring was determined by studies on neozeorininone, obtained from acid isomerisation of zeorininone. By analogy with other rearrangements in the triterpenoid series, neozeorininone was assigned the structure (X).



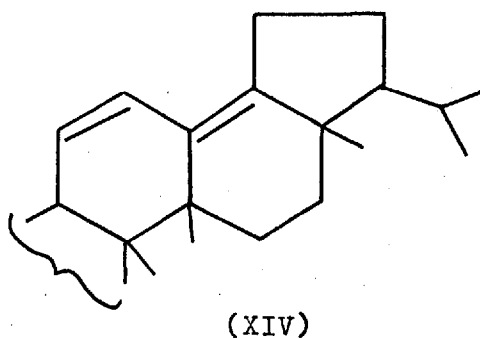
(X)

This was supported by oxidation of neozeorininone with chromic

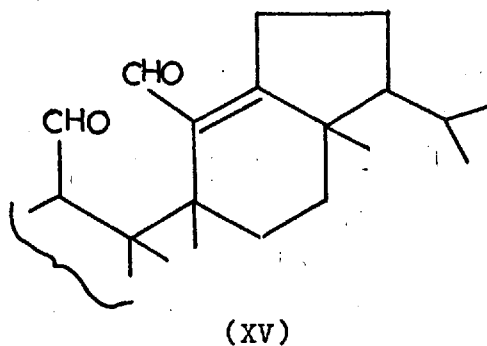
acid to give three products whose spectral properties could be explained in terms of the part-structures (XI), (XII) and (XIII).



Selenium dioxide oxidation of neozeorininone afforded a conjugated, heteroannular diene (XIV), which was converted into an aldol

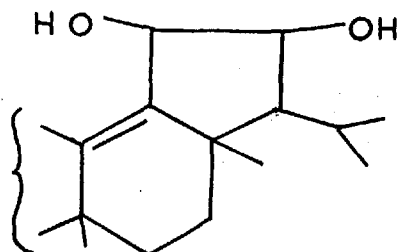


condensation product via the dialdehyde (XV). The formation



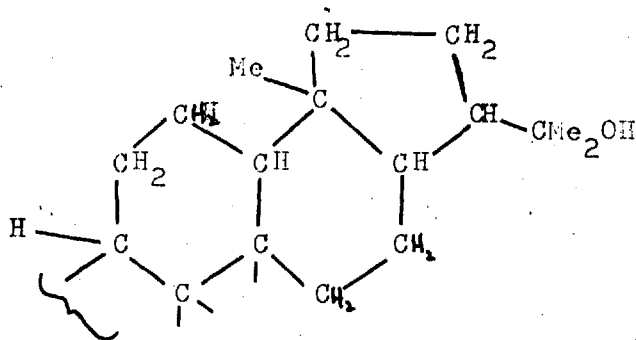


of an aldol condensation product and its probable structure, deduced from spectral properties, excluded the partial structure (XVI) for the parent diol, and together with the reactions so



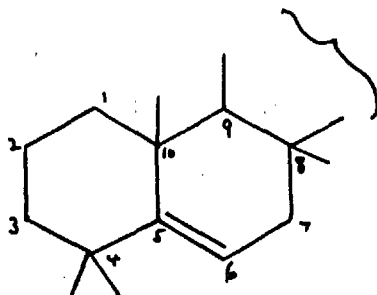
(XVI)

far, suggested the part-structure (XVII) for the C, D and E rings in zeorin.



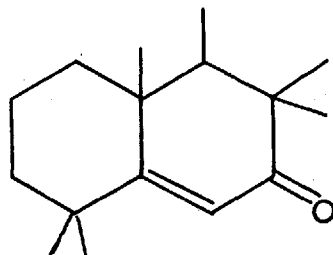
(XVII)

The secondary - OH group is located at the C6 position in the B ring. This was demonstrated by dehydration of deoxyzeorin (obtained by hydrogenolysis of zeorin) to give, as main product, a compound represented by the part-structure (XVIII).



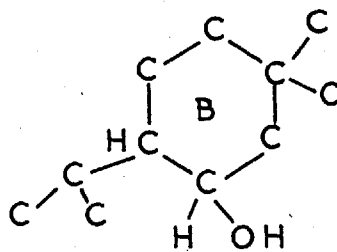
(XVIII)

Chromic acid oxidation of this unsaturated hydrocarbon gave an  $\alpha\beta$ -unsaturated ketone (XIX), which was stable to the action



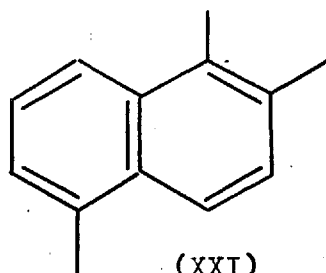
(XIX)

of bromine and selenium dioxide, in agreement with the absence in (XIX) of a replaceable  $\alpha$ -hydrogen atom, and suggesting that the B ring possesses the part-structure (XX).



(XX)

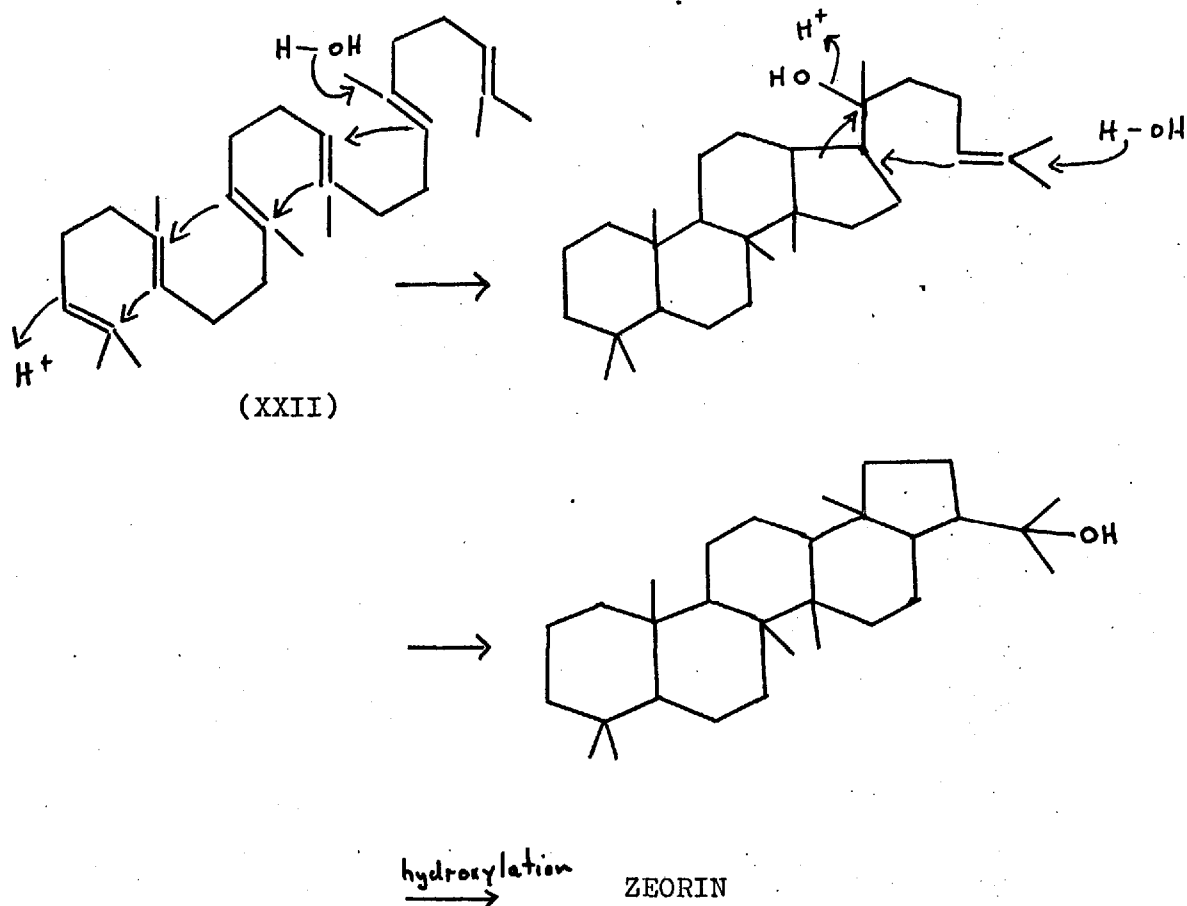
The structure of the A and B rings was further supported by the fact that Asahina and Yosioka obtained 1 : 2 : 5 trimethyl naphthalene (XXI) from zeorin. It is not likely that the C



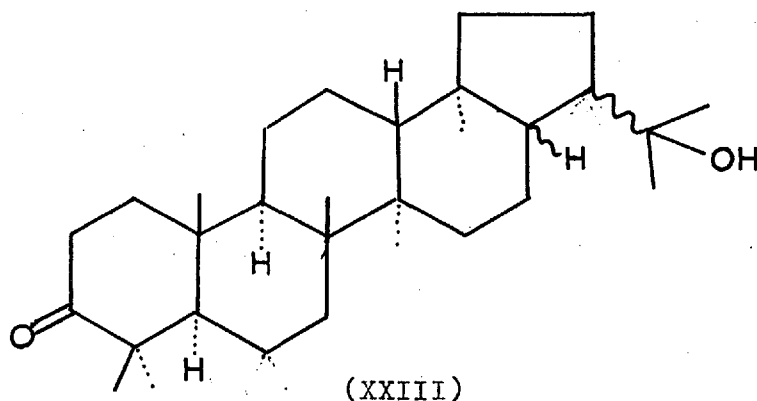
(XXI)

and D rings would have given this product.

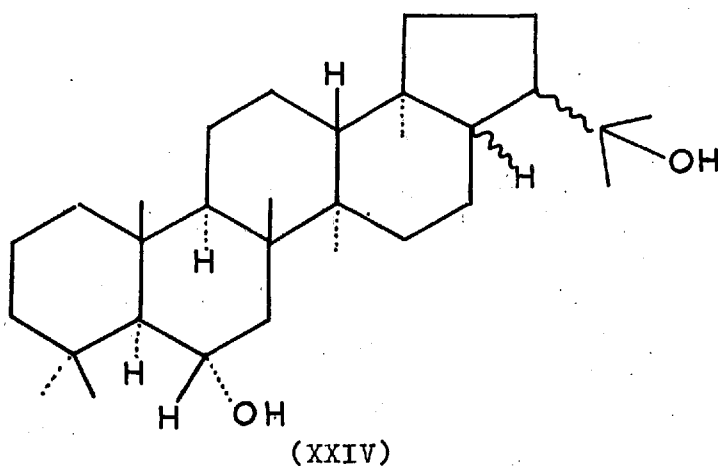
Barton, de Mayo and Orr (1958) then suggest that it is 'attractive' to place the part-structure (XVI) and the A and B rings together as implied in structure (II) so that the bio-genesis of zeorin, with squalene as precursor, (XXII), can be represented by the cyclisation of squalene followed by re-arrangement and hydroxylation, as follows :



Structure (II) has also received support from the elucidation of the structure of hydroxyhopanone (XXIII), a



triterpenoid obtained from dammar resin. This compound, studied by Dunstan et al. (1957), Schaffner et al. (1957) and Fazakerley, Halsall and Jones (1959) forms a series of compounds analogous to zeorinone. By consideration of the molecular rotation changes between the derivatives, it is suggested that seven of the nine asymmetric centres in zeorin can be assigned as in hydroxyhopanone, only the stereochemistry at C17 and C21 being ambiguous. Thus zeorin can be written as in (XXIV), the



- OH at C6 being  $\alpha$ -equatorial, as suggested by the ease of acetylation. Similarities between the zeorin and hydroxyhopane series have also been pointed out by Huneck (1961). Wolff - Kishner reduction of zeorinone produced 6-deoxyzeorin, which was shown by physical methods to be probably identical to hydroxyhopane. Huneck (1963) used nuclear magnetic resonance spectroscopy on zeorin acetate to deduce that the proton at C6 is  $\beta$ -axial, and that the protons at C17 and C21 are both  $\beta$ -axial.

Thus, the chemical work that has been described establishes the structure of zeorin fairly well, but it was felt that a confirmation of the structural details was desirable. Two crystalline derivatives of zeorin were initially supplied by Professor D.H.R.Barton of this department, with a view to determining the crystal structure by the Heavy-Atom method. However, both zeorin iodoacetate and zeorin-m-iodobenzoate deteriorated very rapidly when exposed to X-rays.

Crystals of zeorin acetate, again supplied by Professor Barton, did not deteriorate noticeably when exposed to X-rays for long periods. Although lack of a heavy atom in the crystal would cause substantial crystallographic problems, it was felt that the postulated structure and stereochemistry of the molecule would provide a useful starting point in an X-ray

analysis by Patterson searching techniques. It was considered that if the method had proved successful, it might have been applicable to similar compounds in the triterpene series and in the steroids.

Another possible means of determining the crystal structure of zeorin acetate was by one of the 'Direct Methods' of phase determination (e.g. Harker and Kasper (1947), Sayre (1952), Hauptman and Karle (1953)) but these methods are difficult to apply to non-centrosymmetric crystals. Zeorin acetate is in fact noncentrosymmetric (spacegroup  $P2_1^2_1^2_1$ ) and of the two possible centrosymmetric projections, down a (8.78 Å) and b (11.59 Å) preliminary investigations (Chapter 8) indicated that the former was an inconvenient 'edge-on' view of the molecule and a considerable degree of overlap would occur in the latter.

CHAPTER 7Interpretation of the Patterson  
for Complex Structures

In recent years there have been basically two different approaches towards interpreting the Patterson of molecules containing a large number of similarly weighted atoms. All the methods are dependent upon the use of a high-speed digital computer.

If no reasonable assumptions concerning the structure of the molecule can be made, it may be possible to achieve a solution by the use of an image-seeking function to compare for each point in the unit cell (x, y, z), values of the Patterson corresponding to all vectors between x, y, z and its symmetry-related points. Mighell and Jacobson (1963) have used this method which they call Vector Verification; if all the vectors have corresponding peaks in the Patterson, then the point may define an approximate atomic location. The validity of all suggested positions can then be tested by computing vectors between them and searching the Patterson for the corresponding peaks.

Simpson et al. (1963) made use of the Symmetry Minimum Function (SMF) in the solution of the structure of iso - B<sub>18</sub>H<sub>22</sub>:

The method is essentially the same as that of Vector Verification and was used first to locate trial atomic positions, and then, in conjunction with normal image-seeking procedures to locate the rest of the molecule. Methods along similar lines have been developed by other authors (Alden et al. (1964), Hamilton (1965)).

The second approach to the problem of Patterson interpretation is to presuppose that the molecule contains a fragment of approximately known internal geometry. Such a method has been described by Nordman and Nakatsu (1963), Nordman and Kumra (1965) and more recently by Nordman (1966).

The orientation of the molecular fragment in the unit cell can be expressed in terms of three Eulerian angles  $\phi, \theta, \psi$  with respect to a Cartesian system, fixed in relation to the crystallographic axes. The position  $(x_0, y_0, z_0)$  of one atom of the fragment is then required to define uniquely the location of the entire group in the unit cell. The vector set of the molecular fragment is computed over ranges of  $\phi, \theta, \psi$ , and at each angular combination the Patterson values at the ends of the vectors can be examined by an image-seeking function. Nordman and Nakatsu chose the minimum function

$$M_p(\phi, \theta, \psi) = \text{Min.}(P_1, P_2, \dots, P_p)$$

where  $p$  is the number of vectors in the vector set and  $P_p$  is



the value of the Patterson at the end of the p'th. vector. The values of  $\phi, \theta, \psi$  in this 'orientation search' that give peaks in the three-dimensional minimum function may then define possible orientations of the molecular fragment in the unit cell.

To find possible values of the positional parameter  $(x_0, y_0, z_0)$ , a second search (location search) of the Patterson is carried out, but this time computing vectors between atoms in the suitably orientated fragment and their symmetry-related positions. Vectors within a particular fragment are excluded as they have already been considered in the orientation search, so the vector set used will comprise Harker and general vectors. Selecting any arbitrary values as starting point (unless there is evidence of a limited range) the search ranges are successive values of  $x, y, z$  along the three-Cartesian axes. The search is less than three-dimensional whenever the origin of the unit cell is arbitrary in one or two dimensions. If tentative values of  $x_0, y_0, z_0$  can be found, the rest of the molecule can be identified by normal image-seeking techniques or by Fourier methods. Nordman (1966) has described improvements to the method that include the assignment of vector weights, and a vector refinement procedure to maximise and differentiate between different 'fits' that may be obtained in practice.

A similar method which presupposes a known molecular

fragment has been developed by Hoppe (1957) and is termed the Convolution Molecule Method. It is possible to calculate the 'partial Pattersons' corresponding to both vectors within a molecular fragment and those between symmetry-related fragments. The resulting 'convolution molecules' are termed 'even-indexed' and 'mixed-indexed' respectively as they are calculated by Fourier summations using as coefficients  $F_i F_i^*$  and  $F_i F_j^*$  where  $F_i$ ,  $F_j$  are 'molecular structure factors'.

The even-indexed convolution molecule may then be used in an orientation search and the mixed-indexed function in a translational search as described for the previous method. In theory, the degree of fit at each orientation and translation could be judged by subtracting the convolution molecule from the Patterson value (both on the same scale) at all points in Patterson space and then summing separately, the positive and negative differences. A large negative sum is unacceptable but a large positive value merely indicates that additional peaks are present in the Patterson due to vectors not accounted for in the convolution molecule. However, this is impracticable in terms of computing time (automated by Huber (1965)) and so the procedure is limited to the maxima of the convolution molecules. The weight of each vector is naturally taken into account by virtue of using the peak heights in this way.

### The Computer Programs Used

In view of the structure proposed for zeorin as a result of chemical evidence (Chapter 6), it seemed reasonable to attempt an interpretation of the Patterson of zeorin acetate by an approach in which this information could be utilized. The A, B, C, D, and E rings most probably form a rather rigid system, parts of which would be suitable to define a molecular fragment. The automated version of the Convolution Molecule method was not available but Dr. Nordman of the University of Michigan kindly supplied the listings of computer programs similar to those used by Nordman and Nakatsu (1963). Slight modifications have been made and the programs are now available for use on the I.B.M. 7090 at Imperial College. The three distinct programs are written mainly in MAP (Macro Assembly Programming Language) with several FORTRAN IV subroutines for input and output.

### Orientation Search

A flow diagram is shown in Figure 1.

1. The relative coordinates of the atoms in the molecular fragment are input to the program as unweighted Cartesian vector components (A), together with three Eulerian-angle search ranges (for convenience the angles  $\phi, \theta, \psi$  will be written

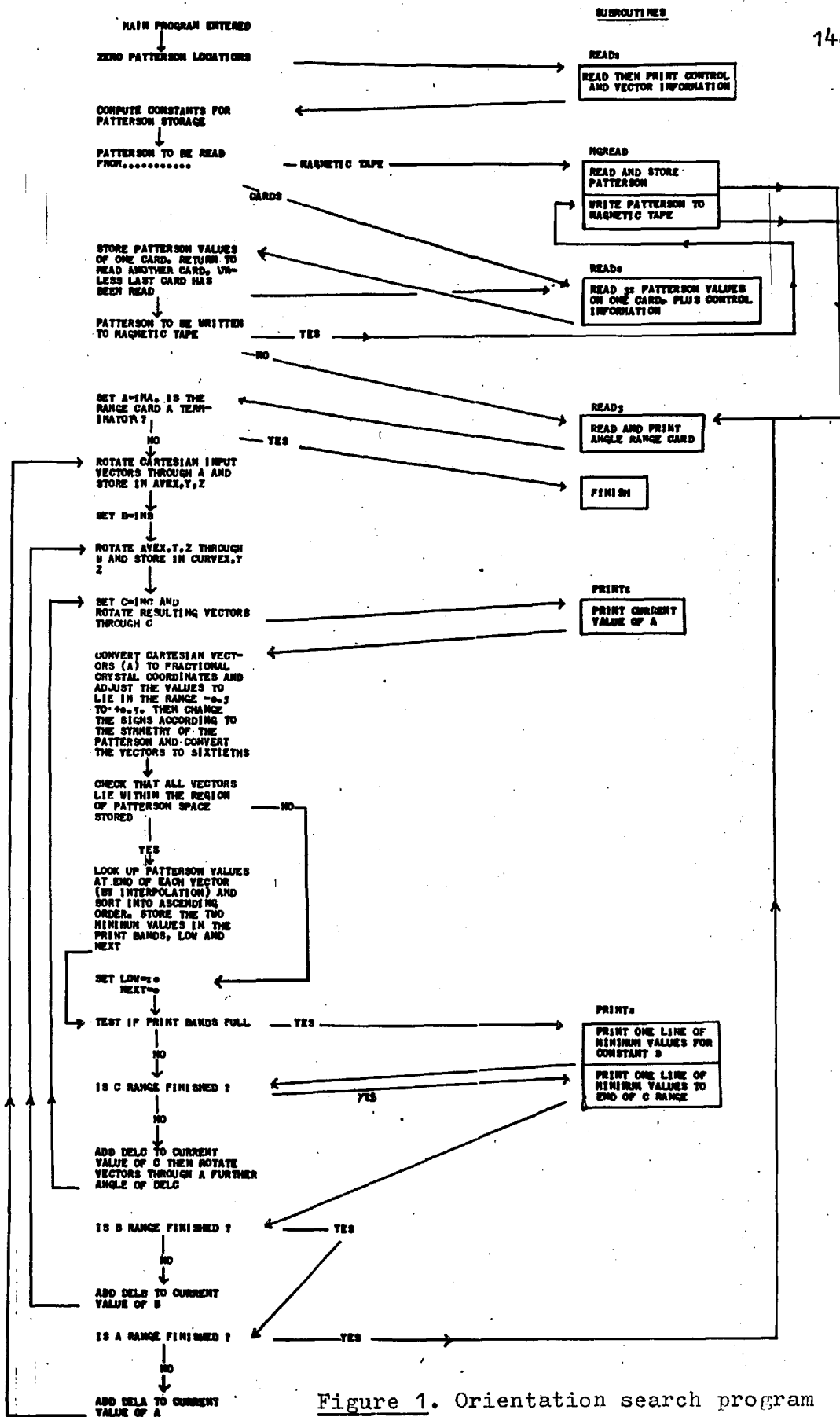


Figure 1. Orientation search program

as A, B, C) and the precomputed Patterson (section 5, page 151), which is stored in the computer in a packed format.

2. The search ranges are input as nine angles :-

(i) The values through which the vectors are initially rotated to the starting point of the search (INA, INB, INC).

(ii) The values by which A, B, and C are to be successively incremented (DELA, DELB, DELC)

(iii) The final values of the three angles (FINA, FINB, FINC).  
The system is shown in Figure 2, where X, Y and Z are the Cartesian axes of Patterson space. The input vectors are first rotated about the X axis through INA. This rotation also moves the Y and Z axes to Y' and Z' in the YZ plane, making angles of INA with the original axes. Then follows a rotation of INB about Y', which also rotates the X axis through INB to give the X'' axis. The third rotation of INC is about X'' to give the vectors their starting orientation for the search.

3. Further rotations are best described by the three nested loops shown below, which also include the starting orientation.

Rotate about the X axis, by INA(DELA)FINA to give a Y' axis

```

..... Y'..... INB(DELB)FINB..... X''.....
..... X''..... INC(DELC)FINC.....

```

Calculation

REPEAT

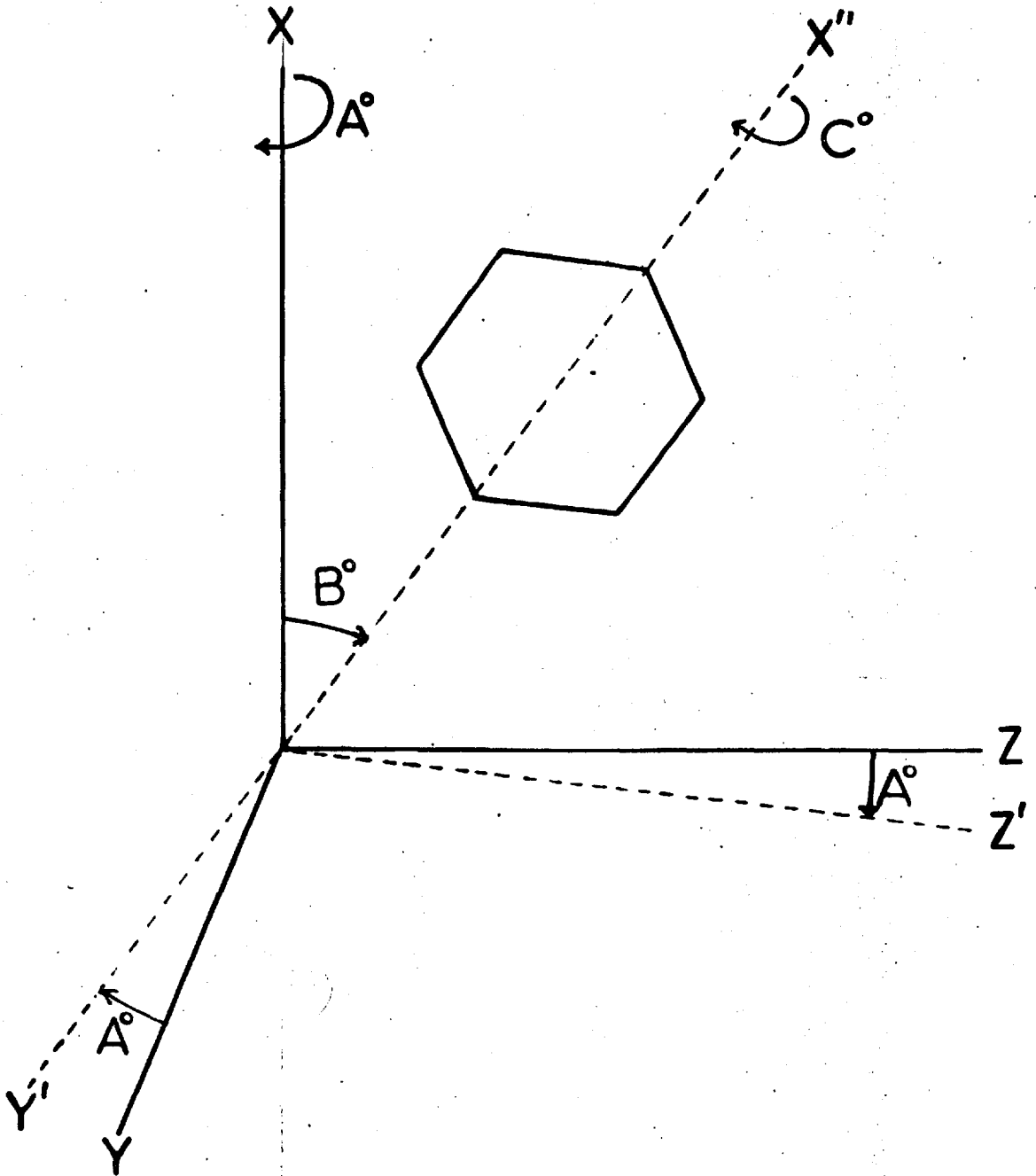
Reset C = INC

REPEAT

Reset B = INB

REPEAT

Figure 2. The Eulerian angles.



4. At each orientation, the appropriately transformed Cartesian vector components are converted to fractional crystal coordinates, which are adjusted to lie in the range  $-\frac{1}{2}$  to  $+\frac{1}{2}$  by successive addition or subtraction of unity, and then their signs are changed according to the Patterson symmetry, i.e.  $2/m$  for monoclinic and  $mmm$  for orthorhombic spacegroups. The vectors are then expressed in sixtieths, as this, at the moment, is the only permissible grid interval. The Patterson values at the ends of the vectors are then evaluated by linear interpolation between four neighbouring grid points, and the two minimum values are stored in the print bands LOW and NEXT, which are subsequently printed out to give the rotational minimum function.

5. The routines for reading and packing the Patterson function in core storage require that the Patterson be initially input on punched cards in a strict format. This is rather unsatisfactory in that it limits each Patterson value to two digits (otherwise the number of cards becomes excessive). A better approach would have been to revise the input routines to accept off I.B.M. magnetic tape, a Patterson with a larger range of values. Unfortunately, no satisfactory Fourier program was available and so it was found expedient to calculate and store the Patterson on I.C.T. magnetic tape using BOSS, and then punch the required cards by a simple Atlas program, 'Patterson Search Punch' (PSP).

### Location Search

A flow diagram is shown in Figure 3.

1. A set of Cartesian coordinates (A) of the molecular fragment are input to the program together with one or more possible sets of Eulerian angles A, B and C, obtained from the orientation search. Up to three symmetry-element matrices are input for the generation of the equivalent positions of the fragment, and also three search ranges as follows :-

(i) The initial values in fractional coordinates to be added to the input positions (INX, INY, INZ).

(ii) The values by which the positions are to be incremented along the crystallographic axes (DELX, DELY, DELZ).

(iii) The final values (FINX, FINY, FINZ).

After input of the Patterson and rotation of the fragment through the Eulerian angles, the Cartesian coordinates are converted to fractional values and the fragment then moved to some arbitrary starting point by addition of INX, INY, INZ to its atomic positions.

2. One or more symmetry-related fragments are then generated and the unique vectors between them and the original fragment are computed. The vectors are adjusted and vector-end Patterson values interpolated and printed as in the orientation search.

3. The fragment is then moved in the crystallographic



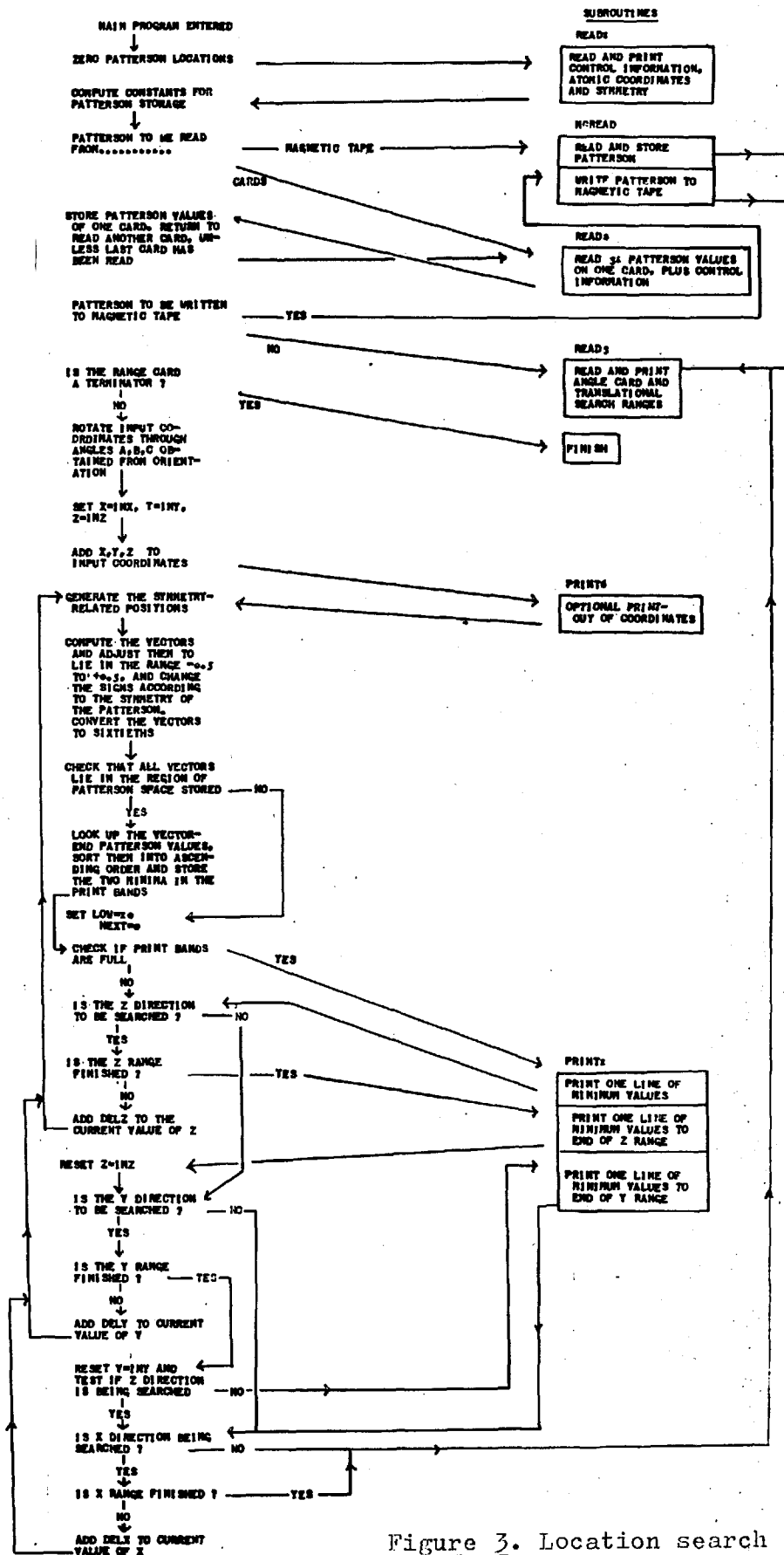


Figure 3. Location search program.

directions through the specified search ranges and (2) is repeated at every stage. The process can be described by three nested loops as follows :-

```

INX(DELX)FINX
INX(DELY)FINX
INX(DELZ)FINX
Calculation
REPEAT
Reset Z = INZ
REPEAT
Reset Y = INY
REPEAT

```

### Superposition

A flow diagram is shown in Figure 4.

1. The positions of the known molecular fragment (plus the symmetry-related positions if required) are input as fractional coordinates together with the search ranges INX, Y, Z; DELX, Y, Z; FINX, Y, Z and the Patterson function.
2. Vectors from input positions to the point INX, INY, INZ are computed, then adjusted and the Patterson values interpolated and printed as in the previous two programs.
3. The process is repeated by computing vectors from the input positions to all the points generated by the search ranges

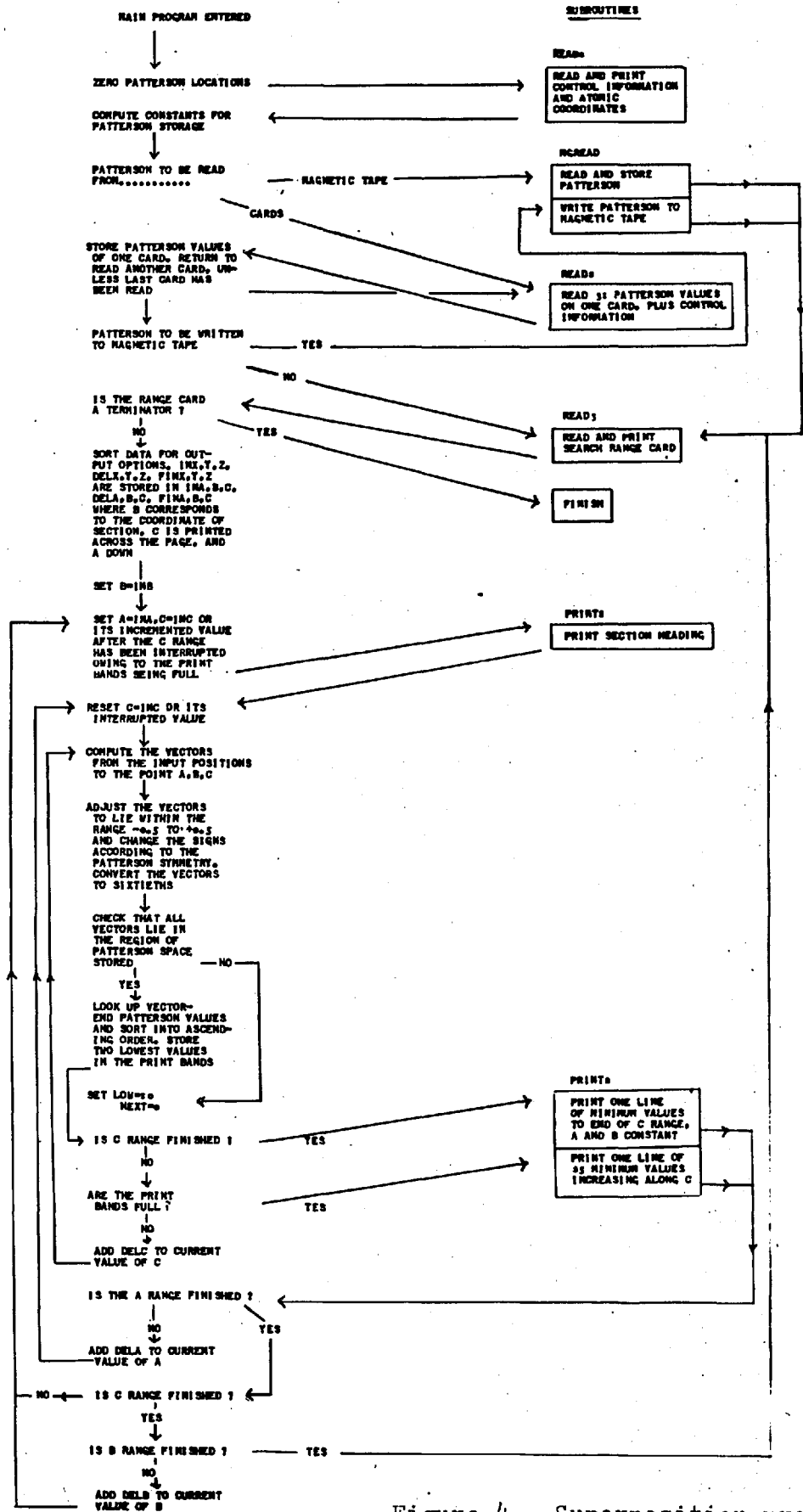


Figure 4. Superposition program.

as follows :-

```

    INX(DELX)FINX
    INY(DELY)FINY
    INZ(DELZ)FINZ
    Calculation
    REPEAT
    Reset Z = INZ
    REPEAT
    Reset Y = INY
    REPEAT
  
```

4. The minimum function is printed as parallel sections up an optional crystallographic axis, in a form suitable for contouring.

Further details of the programs are described in "Patterson Search Programs" by Hunt (1966). Many difficulties were initially experienced in attempting to generalise and make the programs available for any I.B.M. 7090/7094 installation. It soon became evident that the programs had been written mainly for one spacegroup, P2/m, and consequently many routines were, in the author's opinion, illogical and unnecessary when applied to other symmetries. Changes have been made in a way to make most use of what was already given, and the result (as the flow diagrams indicate), is a rather inefficient sequence of operations. Nevertheless, the computing times on the I.B.M. 7090 are quite realistic, for example an orientation

search with 66 vectors (i.e. all the vectors within a molecular fragment of 12 atoms) over 7000 angular combinations took approximately 25 minutes, though increasing the number of vectors above this value leads to excessive computing times. The location search and the superposition programs are both approximately as fast as in the example given.

CHAPTER 8

An X-Ray Investigation of the  
Crystal Structure of Zeorin Acetate.

Preliminary Data

The crystals were colourless orthorhombic laths, elongated along [100] with (001) prominent. The dimensions of the crystal selected for data collection were approximately 0.40 x 0.15 x 0.12 mm. The structural formula proposed by Barton, de Mayo and Orr (1958) is shown in Figure 1.

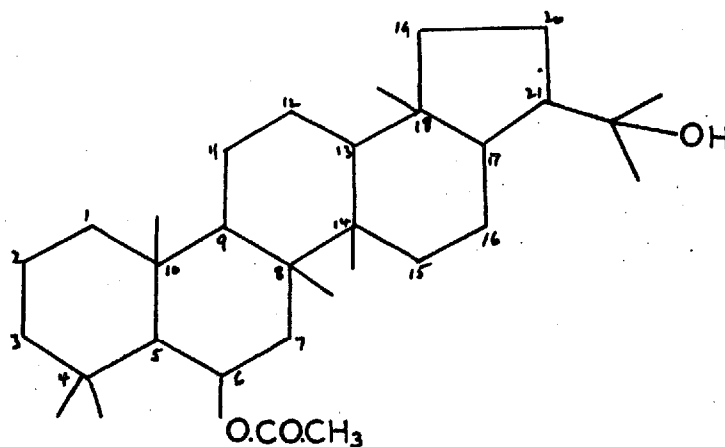


Figure 1. The proposed structure of zeorin acetate.

Formula  $C_{32}H_{54}O_3$       Molecular Weight (formula) = 486

Unitcell Dimensions :     $a = 8.78 (0.02) \overset{\circ}{\text{A}}$ ,     $b = 11.59 (0.02) \overset{\circ}{\text{A}}$ ,  
 $c = 29.15 (0.04) \overset{\circ}{\text{A}}$ .     $V = 2967 \overset{\circ}{\text{A}}^3$ ,     $Z = 4$ ,  $F(000) = 1080 \text{ e.}$

Mass absorption coefficient for  $\text{CuK}\alpha, \mu = 5.2 \text{ cm}^{-1}$

$$D_{\text{obs}} \text{ (flotation)} = 1.09 \text{ g.cm}^{-3} \quad D_{\text{calc}} = 1.09 \text{ g.cm}^{-3}$$

Absent spectra only among

$$h00 \text{ for } h = 2n + 1$$

$$0k0 \text{ for } k = 2n + 1$$

$$00l \text{ for } l = 2n + 1$$

so that the spacegroup is uniquely determined as  $P2_12_12_1$ .

Intensity data for the layers  $0kl$  to  $7kl$  were estimated visually using three graduated wedges to take account of spot-shape changes on the higher layers. In view of the dimensions of the crystal used and the low value of the absorption coefficient, corrections for absorption were considered unnecessary. The data were correlated by comparison with reflexions common to  $h0l$ , giving a total of 2490 independent reflexions.

The Wilson plot based on three-dimensional data is shown in Figure 2. The data were divided into 25 shells each containing 110 - 140 reflexions, and unobserved reflexions were included as zero. The abnormality in the curve is not surprising in view of the structure proposed for zeorin acetate. It is evident from the Patterson (Figure 3) that many inter-atomic vectors accidentally coincide so that at certain  $\sin^2 \theta$  values the intensity averages will be abnormally high. The least-squares method gave  $B = 3.2$ ,  $K = 23.7$  and

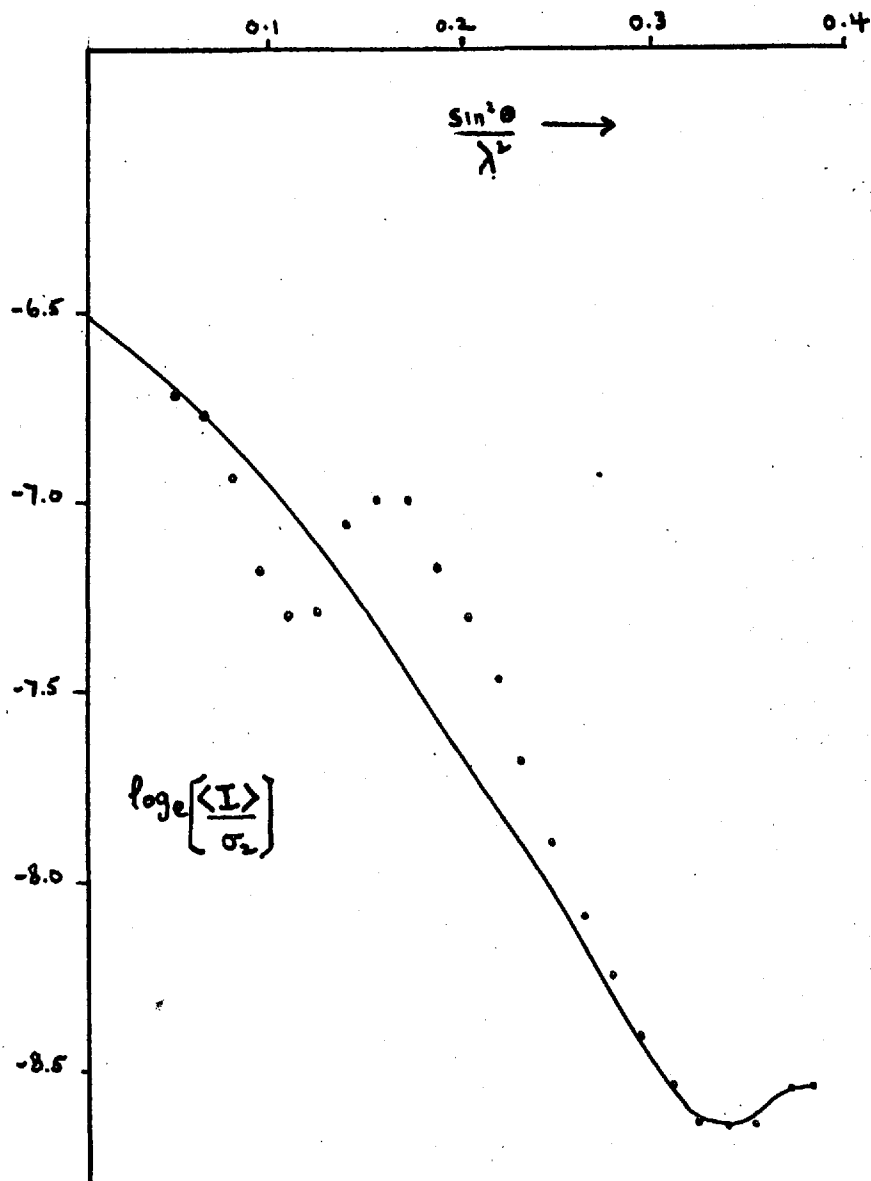


Figure 2. Zeorin acetate Wilson plot based on three-dimensional data.



the graph  $B = 3.8$ ,  $K = 25.8$ .

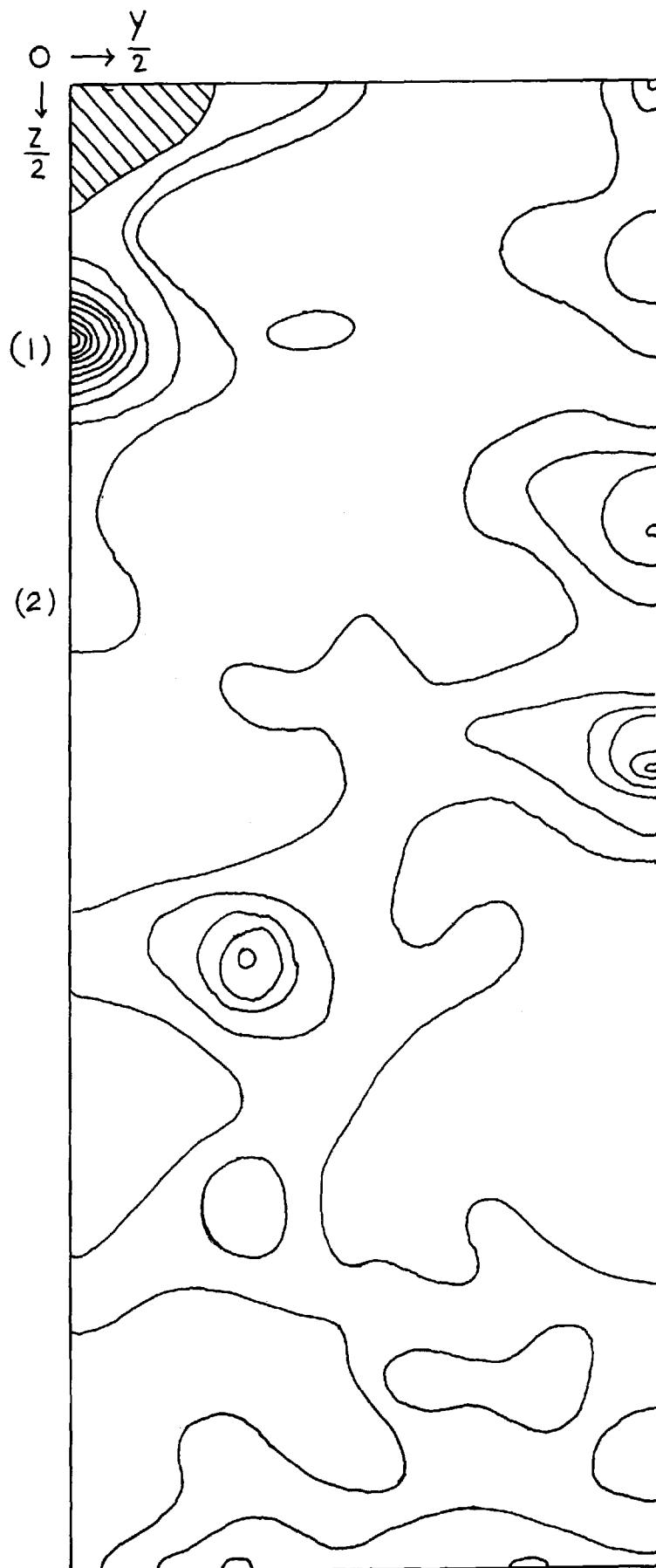
The approximate length of the triterpenoid nucleus (i.e. the A, B, C, D and E rings) is 12 Å and the lengths of the a and b axes (8.78 Å and 11.59 Å) are too short to accommodate this dimension including the side chain. This strongly suggests that the length of the molecule lies in the c direction. A brief examination of the crystals with a polarizing microscope and quartz wedge showed  $n_c > n_a > n_b$ , (where n is the refractive index along the axial direction denoted by the suffix) but the birefringencies were not large. This confirmed that the molecules have their longest dimension parallel to c and suggested that their planes are roughly parallel to (010). The latter conclusion was corroborated by the observation that the two strongest reflexions are from (020) and (021).

#### Visual Examination of the Patterson

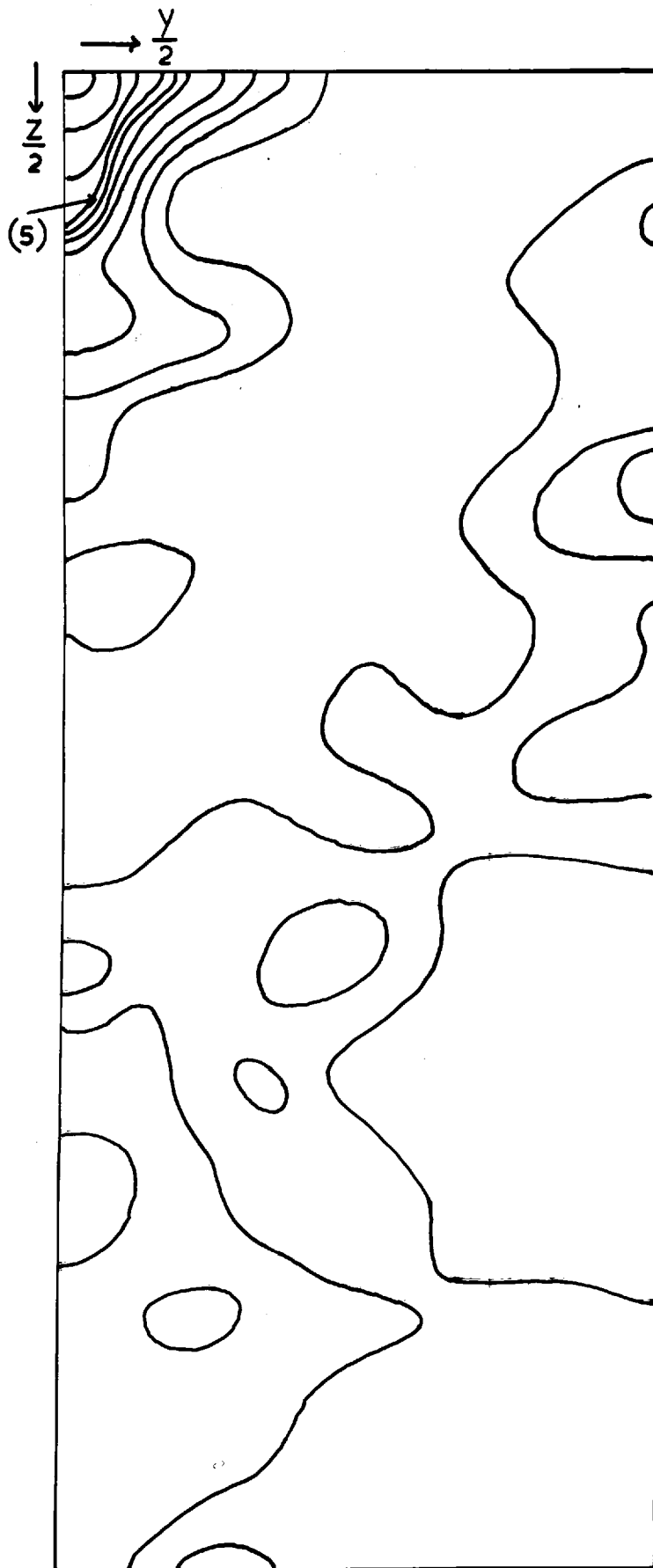
The unsharpened, three-dimensional Patterson function is shown in Figure 3 on pages 162 to 170, computed as sections normal to the a axis (the axes have been labelled x, y and z). The function is on an arbitrary scale and contoured at levels of 50 starting at 0. The computation did not include the term  $F(000)^2$  and the negative parts of the Patterson have not been contoured, though to avoid ambiguity the areas within the

Figure 3.

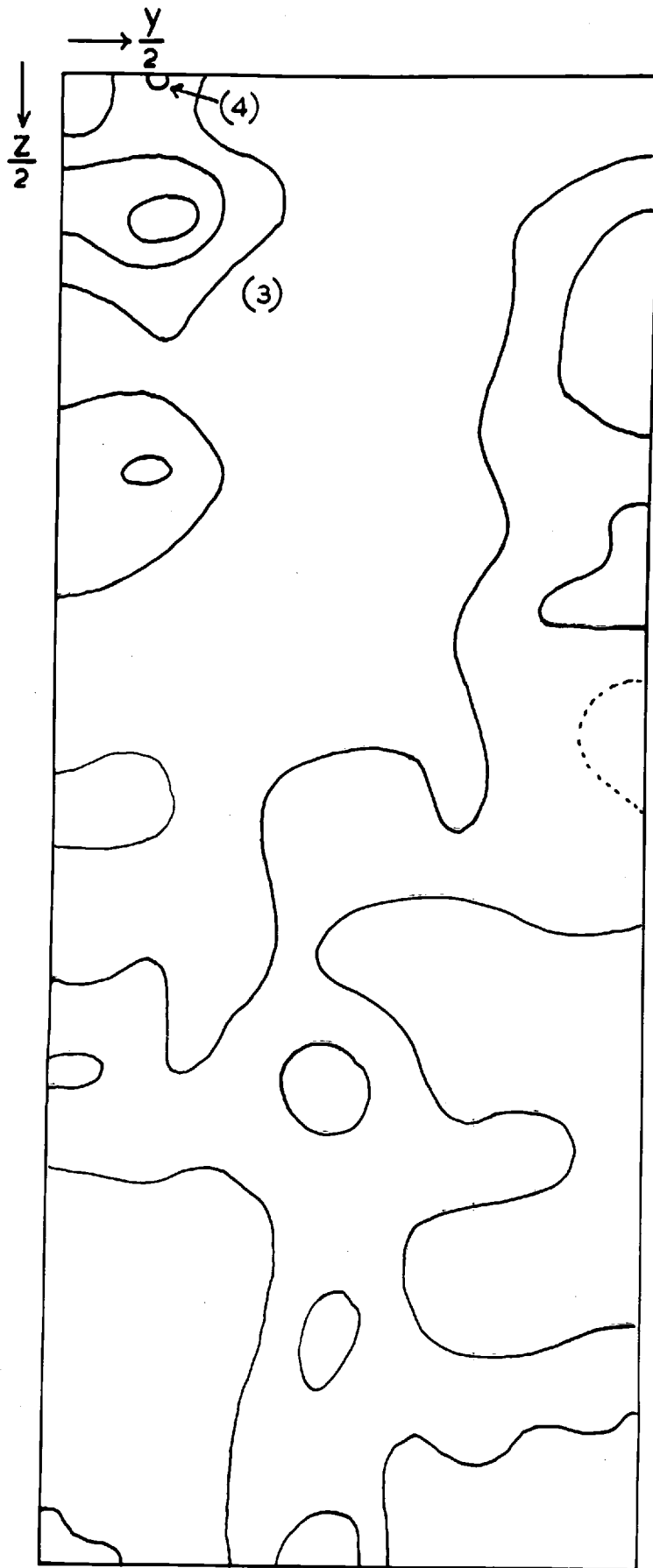
Zeorin acetate  
unsharpened Patterson.



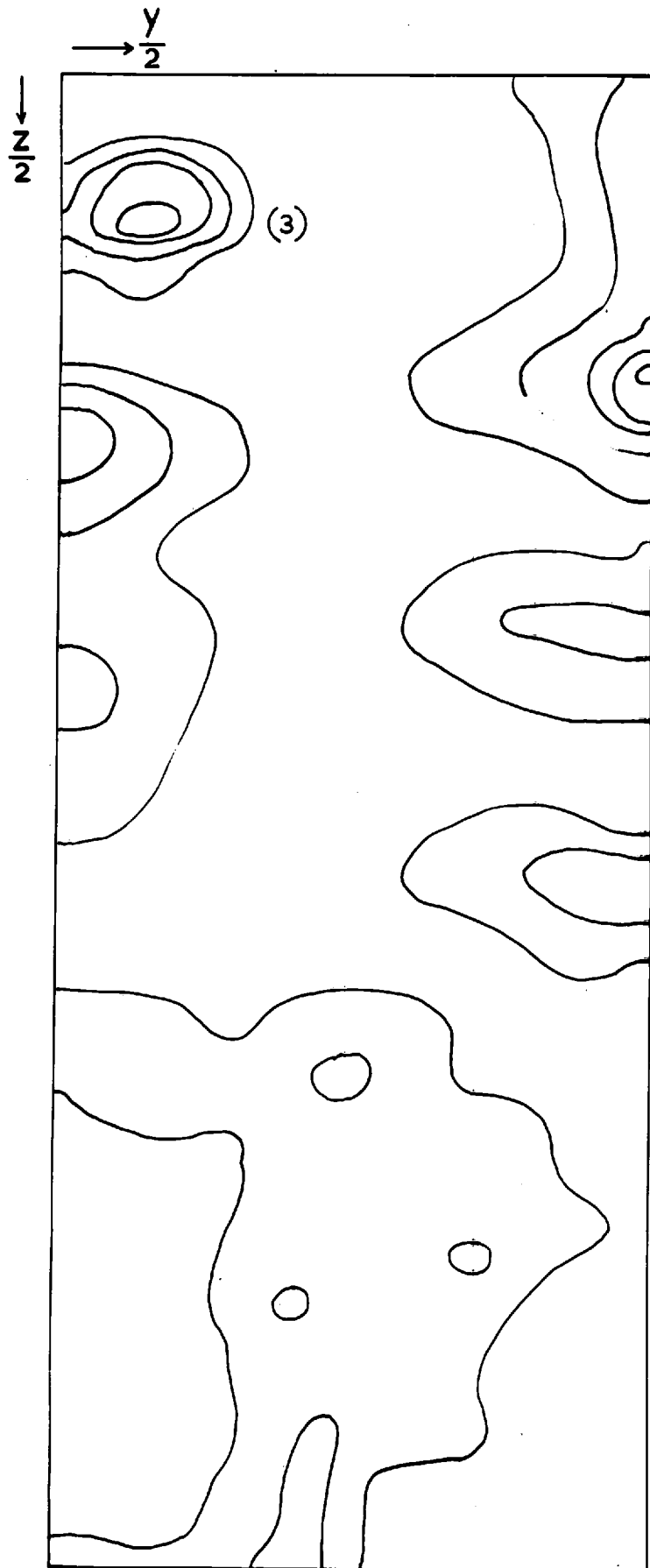
$$x = \frac{0}{12}$$



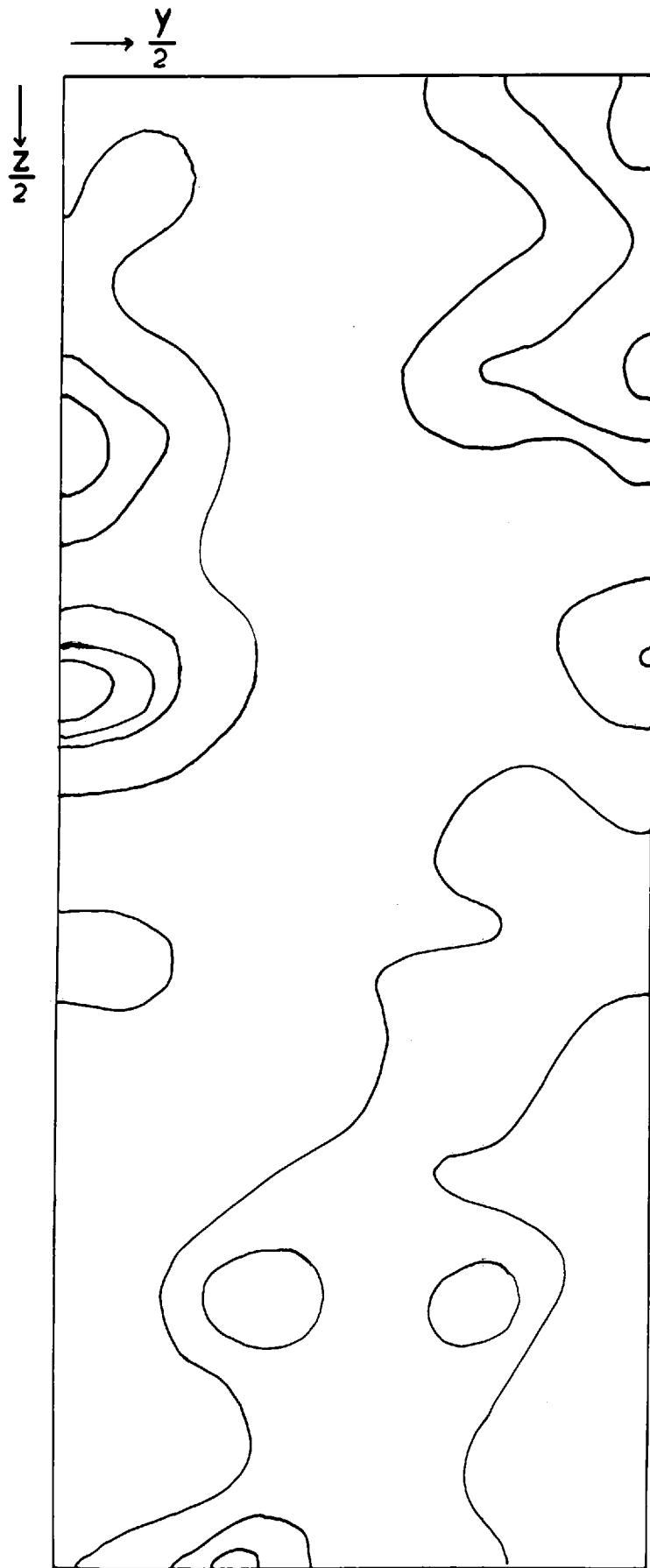
$$x = \frac{1}{12}$$



$$x = \frac{2}{12}$$



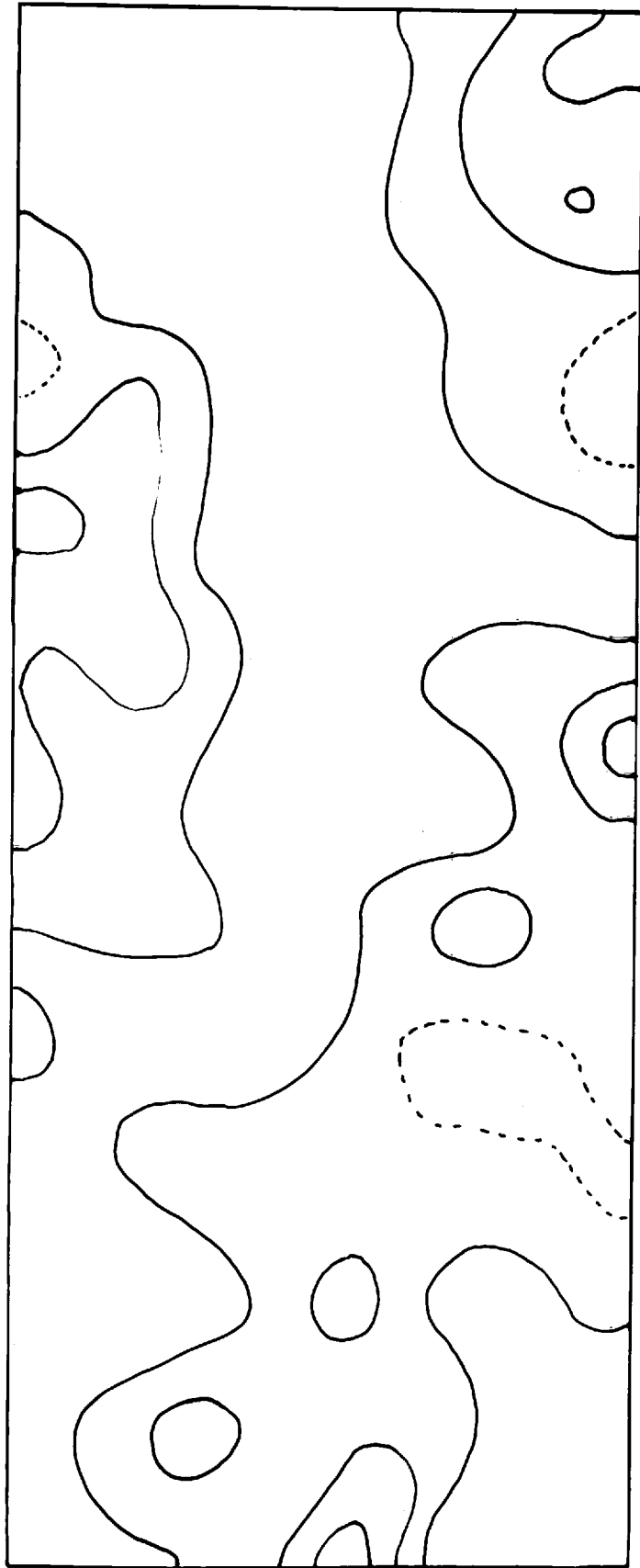
$$x = \frac{3}{12}$$



$$x = \frac{4}{12}$$

$$\frac{y}{2}$$

$$\frac{z}{2}$$



$$x = \frac{5}{12}$$



→  $\frac{y}{2}$

↓  $\frac{z}{2}$



$x = \frac{6}{12}$



broken contours are negative,

The height of the origin peak on an arbitrary scale is 2000 and this is proportional to  $\sum_{i=1}^n f_i^2 = 5592$ . Thus, the peak heights corresponding to single inter-atomic vectors should be approximately :-

Vector	Peak Height
C - C	14
C - O	17
O - O	24

These peaks will be indistinguishable in the negative areas of the Patterson, and are dwarfed by multiple peaks.

The set of points corresponding approximately to the postulated structure of the A, B, C and D rings is shown in Figure 4a. The system is puckered and the points marked (●) are regarded as above the plane of the paper. Figure 4b is the vector set of the points in Figure 4a; it forms three parallel 'sheets' and in broadside view the points make up an equilateral triangular mesh. These in the central sheet are 'strongest' and form the larger mesh of side  $\approx 2.4 \text{ \AA}$ . The points in the other two sheets are mirror images, offset by roughly  $0.5 \text{ \AA}$  and approximately  $1.5 \text{ \AA}$  apart. Peaks in the Patterson corresponding to the outer sheets will probably not be as easily distinguished as those in the central layer.

The Patterson does, in fact, exhibit a broad, flattish region of high density around the origin. It is fairly well

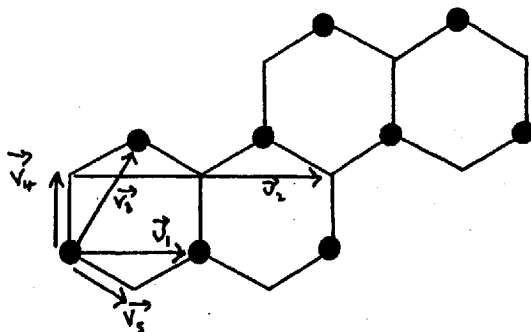


Figure 4a. The postulated structure of the A, B, C and D rings.

The system is puckered, atoms marked ( ● ) are regarded as being above the plane of the paper.

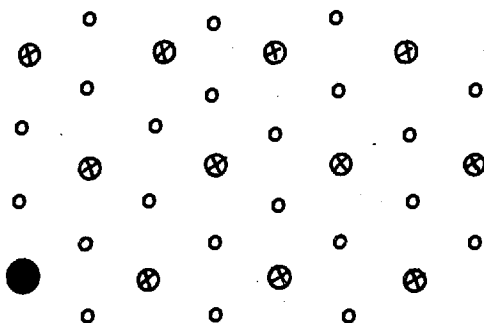


Figure 4b. Part of the vector set of the points in Figure 4a.

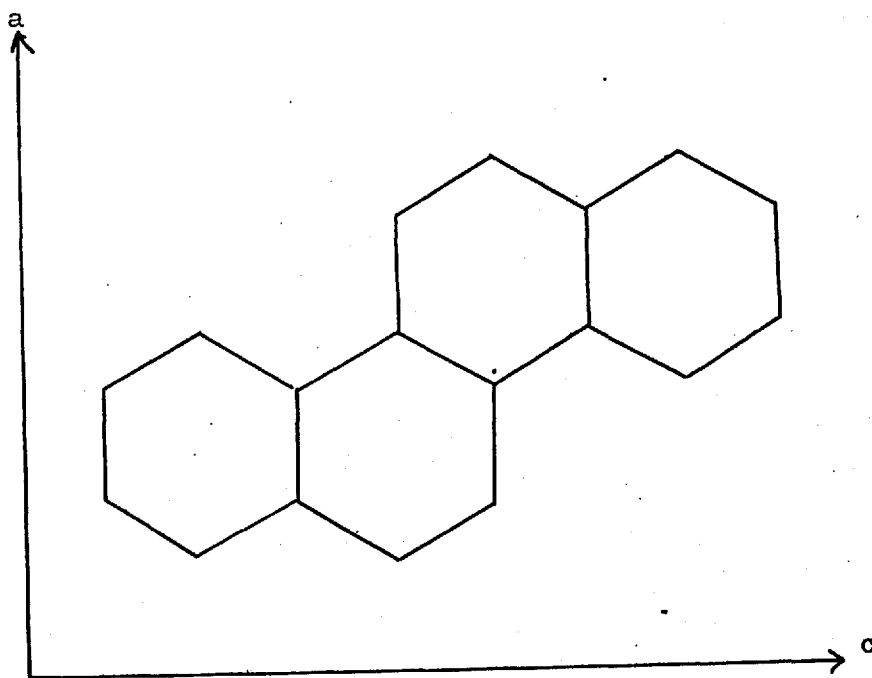
Points marked ( ⊗ ) lie in the central sheet

Points marked ( o ) represent superimposed points  
athwart the central sheet.

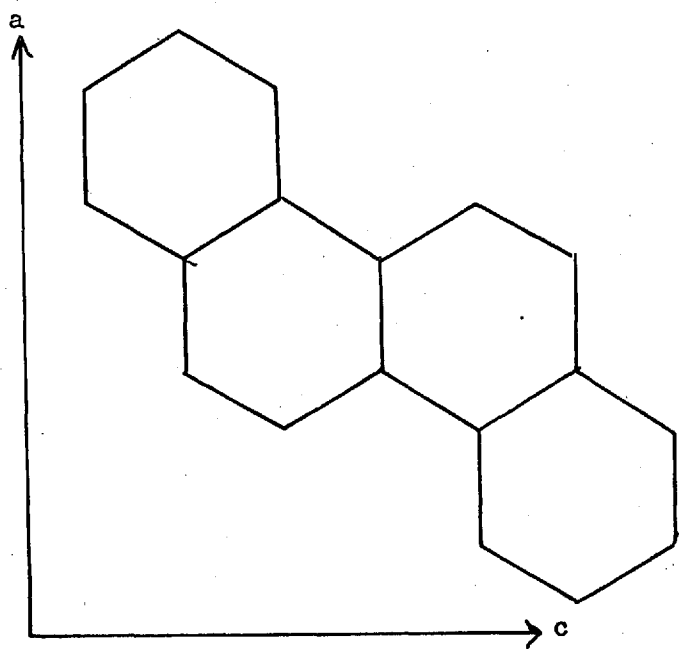
confined to the  $(u, \theta, w)$  plane, so all the molecules in the cell must be roughly normal to  $\underline{b}$ . The peak clusters around  $(u, \frac{1}{2}, w)$  and  $(\frac{1}{2}, v, w)$ , presumably between the  $\underline{b}$  and  $\underline{a}$  screw-related molecules also confirm the general alignment.

In the  $u = 0$  section of the Patterson (page 163), the strong peak labelled (1) was attributed to the accumulation of vectors of the type  $\vec{v}_1$  in Figure 4a and peak (2) to those of type  $\vec{v}_2$ . The length of the vectors from the origin to these peaks (2.4 Å and 4.9 Å respectively) agrees with the calculated distances across the cyclohexane rings. The strong peak (3) (pages 165 and 166) was attributed to vectors of the type  $\vec{v}_3$  in Figure 4a, its distance from the origin being 2.5 Å. Thus, the origin peak and peaks (1) and (3) form the equilateral triangular mesh associated with the points in the central layer in Figure 4b. Their positions suggest two possible orientations for a zeorin acetate molecule as shown in Figures 5a and 5b.

The projection of the vector from the origin to peak (3) on to (001) makes an angle with (010) of approximately,  $\alpha = 30^\circ$ . With the aid of Dreiding models it was apparent that this peak could arise from two possible orientations of the molecule seen 'end-on' as in Figures 6a and 6b (the vectors marked are as in Figure 4a). If the orientation is similar to that shown in Figure 6b, then there should be a peak in the Patterson

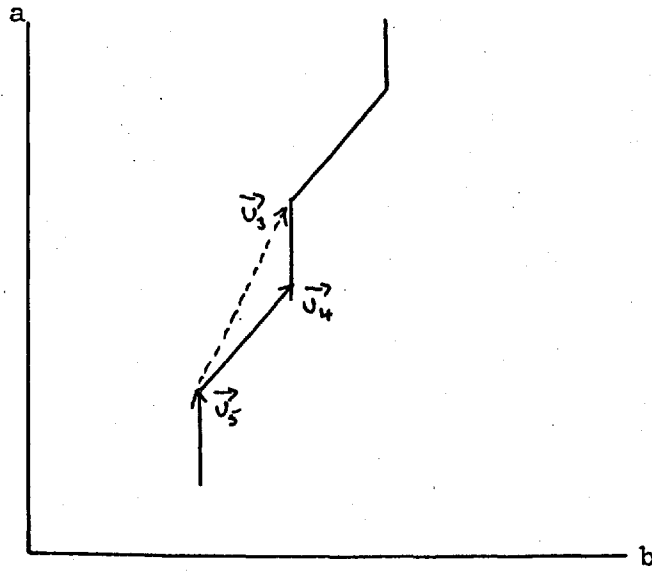


(a)

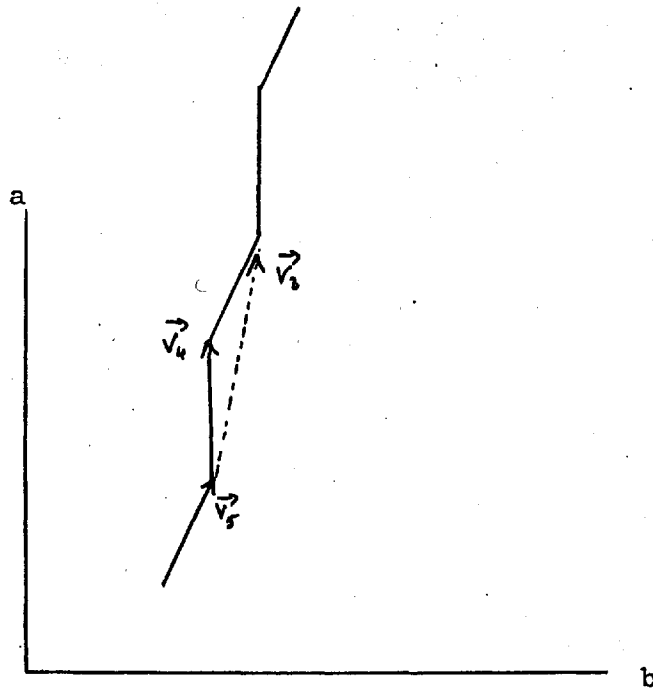


(b)

Figure 5. Two suggested orientations for zeorin acetate  
in 'broadside' view.



(a)



(b)

Figure 6. Idealized 'end-on' view of the A, B, C and D rings.

approximately 1.5 Å from the origin, on or close to the a axis and corresponding to  $\vec{v}_4$ . No such peak was discernible. However, assuming an orientation similar to that in Figure 6a, it was possible to locate Patterson peaks corresponding to the vectors  $\vec{v}_4$  and  $\vec{v}_5$ . These peaks, (4) and (5) are shown in Figure 3 on pages 165 and 164, their distances from the origin being approximately 1.6 Å and 1.5 Å respectively.

### The Use of Patterson-Searching Techniques

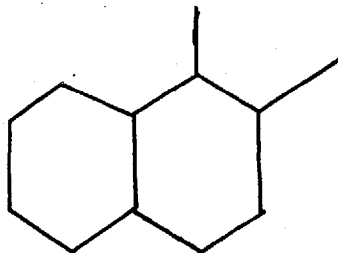
The method and computer programs used have been described in Chapter 7.

As shown in Figures 4a and 4b, the vector set of a single molecule (postulated) consists of three parallel sheets (considering the ring system only). The peaks in the Patterson corresponding to the inmost sheet are the strongest and there should be several less than 3.4 Å (i.e. they will be clear of inter-molecular vectors). Although the longer vectors are more sensitive to angular changes, they may run into the region of inter-molecular vectors and be difficult to disentangle. It therefore seemed advisable at first to deal only with the shorter and medium-length vectors.

Considering only the rings A, B, C and D, they form



an approximately centrosymmetric group with vectors too numerous and too long to use in initial searches. Computing time becomes excessive with more than about 78 vectors (i.e. all the vectors between 13 atoms). A cyclohexane ring is too small a unit and occurs too often either as complete or incomplete rings. A decalin ring is possibly acceptable but it was decided to use the group



as the computing times would still be reasonable and it would possibly be more selective than the ten-atom group; it can occur four times in the molecule and possibly more considering the five-membered ring and other substituent groups.

As the unit cell contains four symmetry-related molecules, the region round the origin in the Patterson contains sets of peaks corresponding to four overlapping sets of intra-molecular vectors. However, this is implicit in the *mmm* symmetry of the Patterson so that only one quadrant of space need be searched. Any multiple fits are then due to repetition of the search group within one molecule.

The structure of methyl melaleucate iodoacetate (Figure 7)

determined by Hall and Maslen (1965), was used to define the

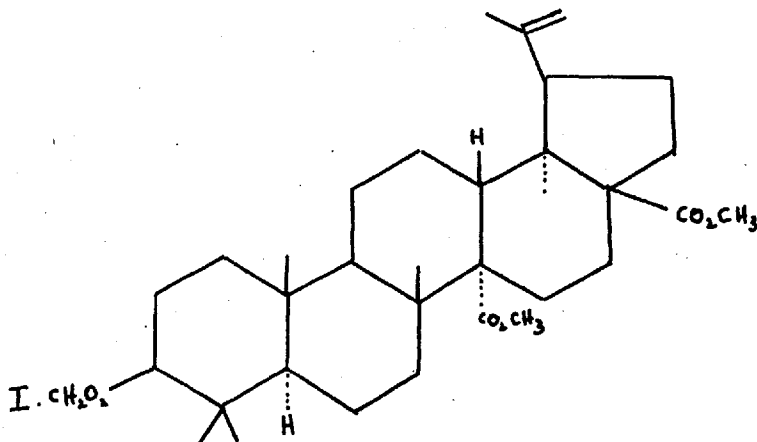
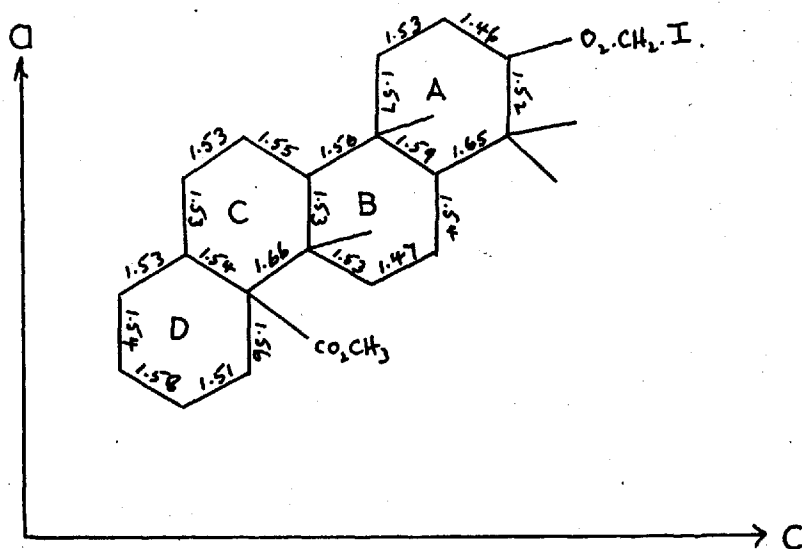
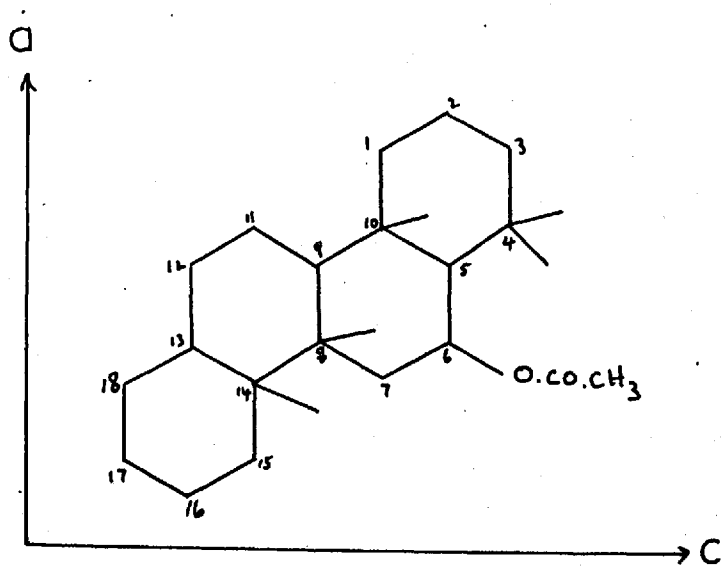


Figure 7. Structural formula of methyl melaleucate iodoacetate.

geometry of a molecular fragment. The bond distances of the A, B, C and D rings are shown in Figure 8a, which also gives the approximate orientation of the molecule projected down  $[010]$ . The naming of the axes in Figure 8a is not the same as that given by Hall and Maslen. The a and c axes have been interchanged so that the orientation is similar to one postulated for zeorin acetate. Hall and Maslen noted that the degree of substitution at carbon atoms bears a direct relationship to the lengthening of the C - C bonds. Long range steric effects may also account for some of the abnormal bond lengths and angles. As the substitution in zeorin acetate (Figure 8b) is probably very similar to that in methyl melaleucate iodoacetate, except at  $C_3$ , it is reasonable to assume that the geometry of the A, B, C and D rings of the two compounds will not differ to a great extent.



(a)



(b)

Figure 8. (a) Bond lengths in methyl melaleucate iodoacetate.  
 (b) The A, B, C and D rings in the postulated structure of zeorin acetate.

## Work with the Unsharpened Patterson

### Orientation Search

As the unsharpened Patterson had given an approximate orientation of the molecule, it was decided to proceed with the unsharpened function for the search. This was computed on a 31 x 31 x 31 grid and punched on cards with PSP. As mentioned in Chapter 7, input format requires not more than two digits for each Patterson grid point. Consequently, the Patterson as shown in Figure 3 was scaled down so that most values fell within the range -48 to +48. Each value was then adjusted by addition of 48 to give the range 0 to 96. Any negatives were punched as 0 and those above 99 (mainly in the origin peak) as 99. The origin peak was not removed, which would reduce the power of the search in that the Patterson values at the ends of the vectors between adjacent atoms would be obscured by the origin peak in some orientations. In Figure 3, only peak (5) (of those visible) was affected in this way and it was considered that this would have little effect on the position of the minimum, especially as it is the coordinates of the longer vectors that are more susceptible to angular changes and hence define the position of the minimum more accurately.

The 66 vectors between the atoms C1 - C11, C14 of methyl melaleucate iodoacetate (Figure 3a) were input to the orient-

ation search program (although they form rather a deformed group, especially about C3 and C5). Increments of  $10^\circ$  were initially employed to make computing time practical.

The highest peak in the rotational minimum function had  $LOW = 41$ , (0 in Figure 3 corresponds to 48 in the Patterson used for the search),  $NEXT = 43$  with  $A = 0^\circ$ ,  $B = 60^\circ$  and  $C = -10^\circ$ , and corresponds approximately to a clockwise rotation, by  $60^\circ$  about the b axis, of the A and B rings (as shown in Figure 8a), to give the orientation shown in Figure 9. This

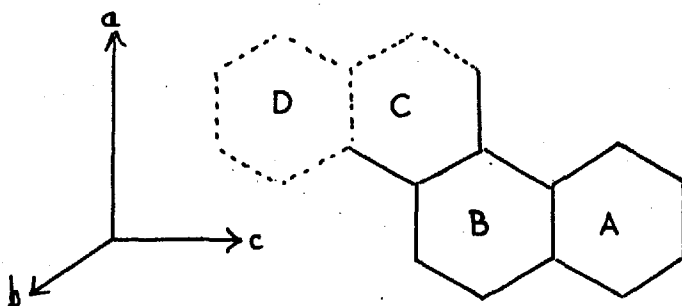


Figure 9.

corresponds quite closely with a possible position suggested by the preliminary investigations of the Patterson. Other peaks in the minimum function with  $LOW \approx 36$  occurred in the Euler-angle ranges

$$A = -30^\circ \text{ to } +20^\circ \left\{ \begin{array}{ll} B = -70^\circ \text{ to } -60^\circ & C = 10^\circ \\ B = -30^\circ \text{ to } -20^\circ & C = 20^\circ \\ B = 85^\circ \text{ to } 95^\circ & C = 30^\circ \end{array} \right.$$

The first peak may be accounted for by a fit with the B/C rings

as shown in Figure 9.

The increment was reduced to  $5^\circ$  and the Patterson searched over ranges that included all four peaks. The minimum values for the latter three still remained at approximately 36, but for the first peak were LOW = 42, NEXT = 43. Decreasing the increment to  $1^\circ$  showed that this peak was in fact triplet with

$A^\circ$	$B^\circ$	$C^\circ$	LOW/NEXT
0	58	-14	43/43
-1	61	-13	43/43
-1	52	-14	41/41

Two of these peaks could be accounted for as representing the fit of the molecular fragment with the A/B and C/D rings respectively, suggesting that the C and D rings are as shown in Figure 9. The third peak which is fractionally weaker may represent the partial fit with a single ring and its appendages. However, the boundaries between the three peaks are ill-defined and the differences between the assumed and actual geometry must be a factor that contributes to this effect.

The orientation of the molecular fragment with  $A = 0^\circ$ ,  $B = 58^\circ$  and  $C = -14^\circ$  is shown projected down the b axis in Figure 10a, and down the c axis in Figure 10b.

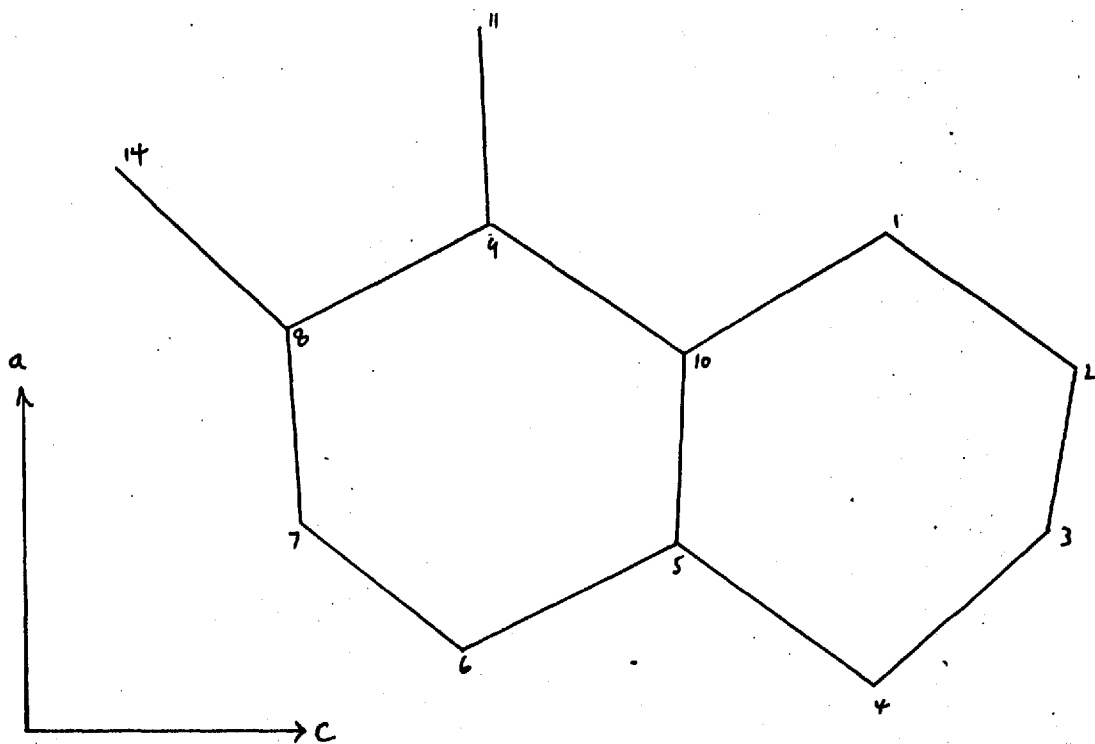


Figure 10a. The molecular fragment  
projected down b

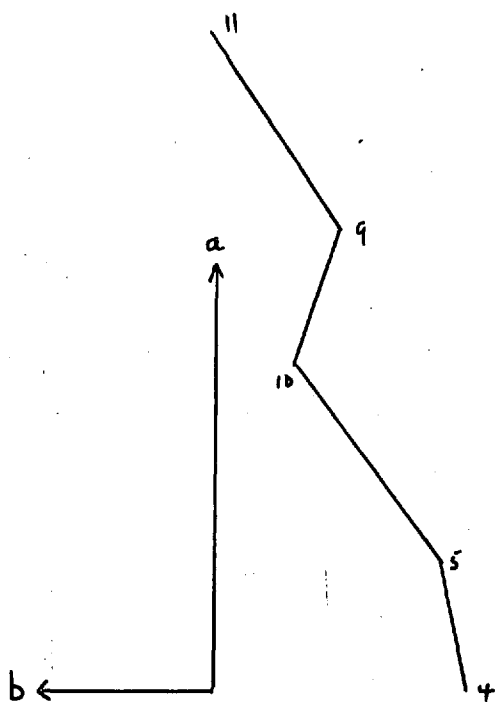


Figure 10b. The atoms  $C_4$ ,  $C_5$ ,  $C_{10}$ ,  
 $C_9$  and  $C_{11}$  projected down c

## Location Search

For the spacegroup  $P2_12_12_1$ , this process can be carried out by two separate two-dimensional searches. With the molecular fragment in the orientation  $A = 0^\circ$ ,  $B = 58^\circ$  and  $C = -14^\circ$ , the Patterson function was searched along the  $X$  and  $Y$  directions, computing vectors between the fragments related by the  $c$  screw. The appropriate ranges were :-

$$\text{INX, Y} = 0.0 \quad \text{DELX, Y} = 0.01 \quad \text{FINX, Y} = 0.50$$

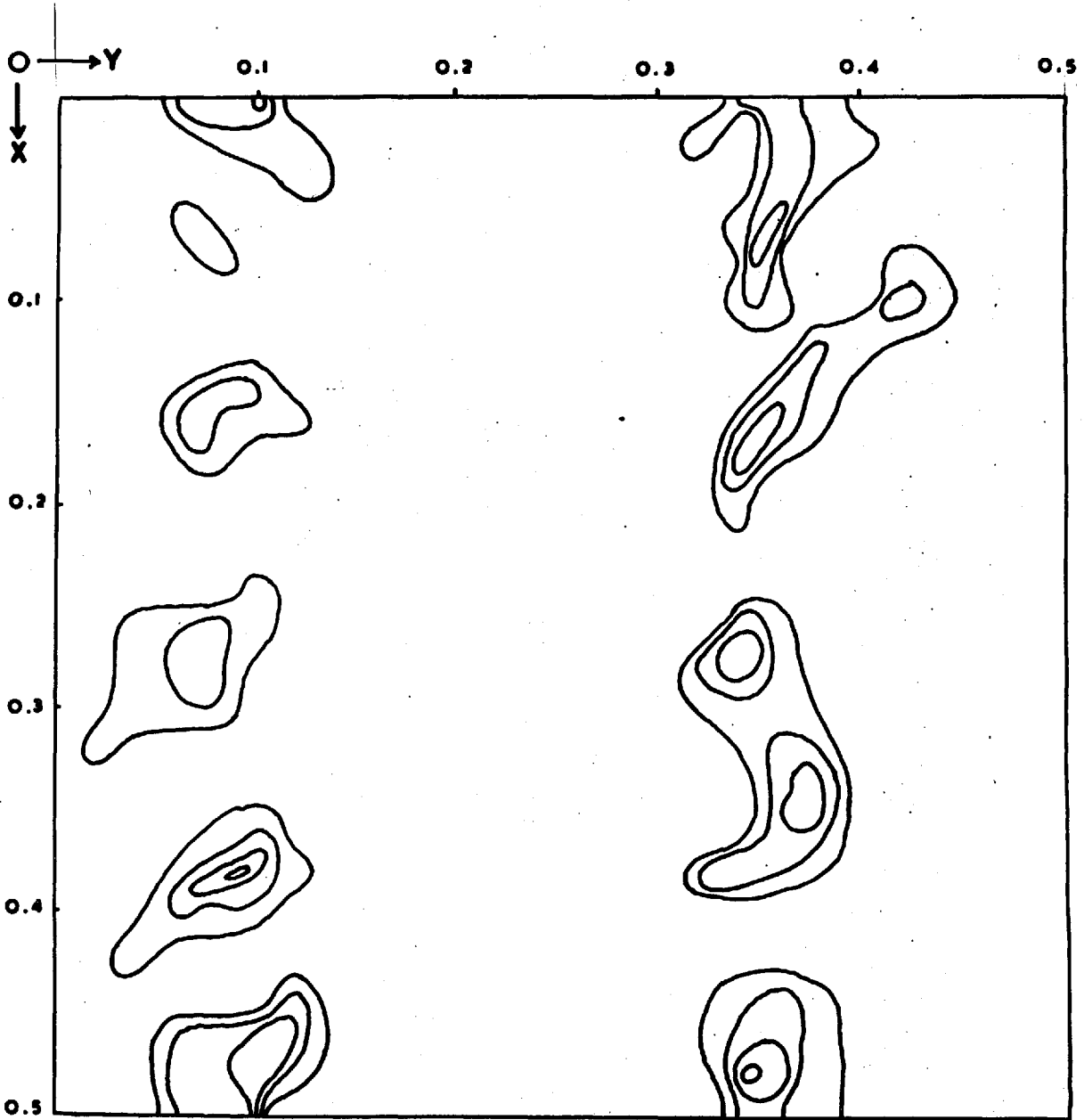
The increments are approximately 0.1 Å and the searching was carried out in the unique part of the unit cell.

The translational minimum function is shown in Figure 11. Only the values of LOW are contoured at the levels 38, 40, 42 and 44. The background level was generally between 25 and 32. The peak heights agree quite well with those of rotational minimum function but as can be seen, the function is poorly resolved especially in the X direction, although the highest values are confined to two narrow ranges in the Y direction, from 0.34 to 0.37 and 0.07 to 0.10.

The translational search computing vectors across the  $a$  screw tended to confirm the ranges for the Y values shown in Figure 11. Outside these ranges the minimum function was generally of the order 25 to 32 although there were, in places, peaks as high as 39. The function also suggested that



Figure 11. Translational minimum function in the Y and Z directions.



two different Z ranges, 0.40 to 0.44 and 0.36 to 0.38, are associated with the two peaks at  $Y = 0.07$  to  $0.10$  and  $Y = 0.34$  to  $0.37$  respectively. A third search computing vectors across the b screw did little to define the minimum more clearly and gave a minimum function in which the peak heights were generally lower than in the other two searches.

In an attempt to find unambiguously, the translational parameters ( $x_0, y_0, z_0$ ) (page 144), two three-dimensional searches were carried out. Both were over the complete X range (0.0 to 0.5) but with different Y and Z ranges corresponding to those suggested by the two-dimensional minimum functions. The resulting peak heights (background level = 30 to 34) were generally lower than those in the two-dimensional maps. The four highest peaks are shown in Table 1.

Table 1. The highest peaks in the three-dimensional, translational minimum function.

Peak	X	Y	Z	LOW/NEXT
A	0.14	0.34	0.37	39/39
B	0.14	0.07	0.43	39/40
C	0.08	0.33	0.39	39/39
D	0.23	0.08	0.43	38/39

Table 1 shows that the differences between the heights of the four peaks are very small and thus from the results so far it was felt that the original Patterson was not sharp

enough to define, unambiguously, the translational parameters  $x_0$ ,  $y_0$ ,  $z_0$ . However, two three-dimensional Fourier maps were computed using the coordinates of the two highest peaks in Table 1 (A and B) as values of  $x_0$ ,  $y_0$ ,  $z_0$  for the structure factor calculations. The agreement between the observed and calculated structure factors (scale of 20.0 applied to  $F_0$ ) was 0.55 in each case. It was difficult to interpret the Fourier map derived from the coordinates of peak A in a way consistent with the expected geometry of the zeorin acetate molecule. The Fourier derived from peak B was a little more encouraging and gave tentative positions for 18 atoms as shown schematically in Figure 12. The peaks corresponding to the atoms marked 12 and 16 in Figure 12 were extremely weak. An attempt was

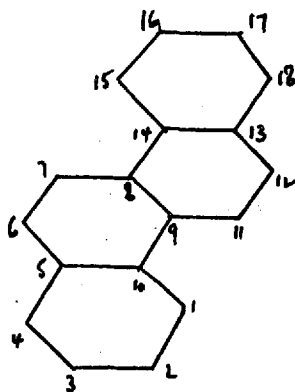


Figure 12.

made to refine these coordinates by the Fourier Refinement program of the X-Ray '63 System. This program, written by J.R.Holden calculates the 27-point block Fourier around each

atomic positions, estimates the coordinates of the point of maximum electron density within the block and then repeats the process with these peak positions as new atomic coordinates. The method, when applied to the 18 positions in Figure 12, reduced the R value to only 0.52 and some of the inter-atomic bond lengths attained unacceptable values. The shifts of the atomic positions were unsystematic and did not indicate that the group as a whole ought to be moved in any particular direction. A difference Fourier derived from the original positions was similarly uninformative.

## 2. Work with the Sharpened Patterson

In view of the ambiguity in the determination of the translational parameters,  $x_0$ ,  $y_0$ ,  $z_0$  that has been described, the method was repeated using the Patterson function sharpened to point atoms at rest by the modification

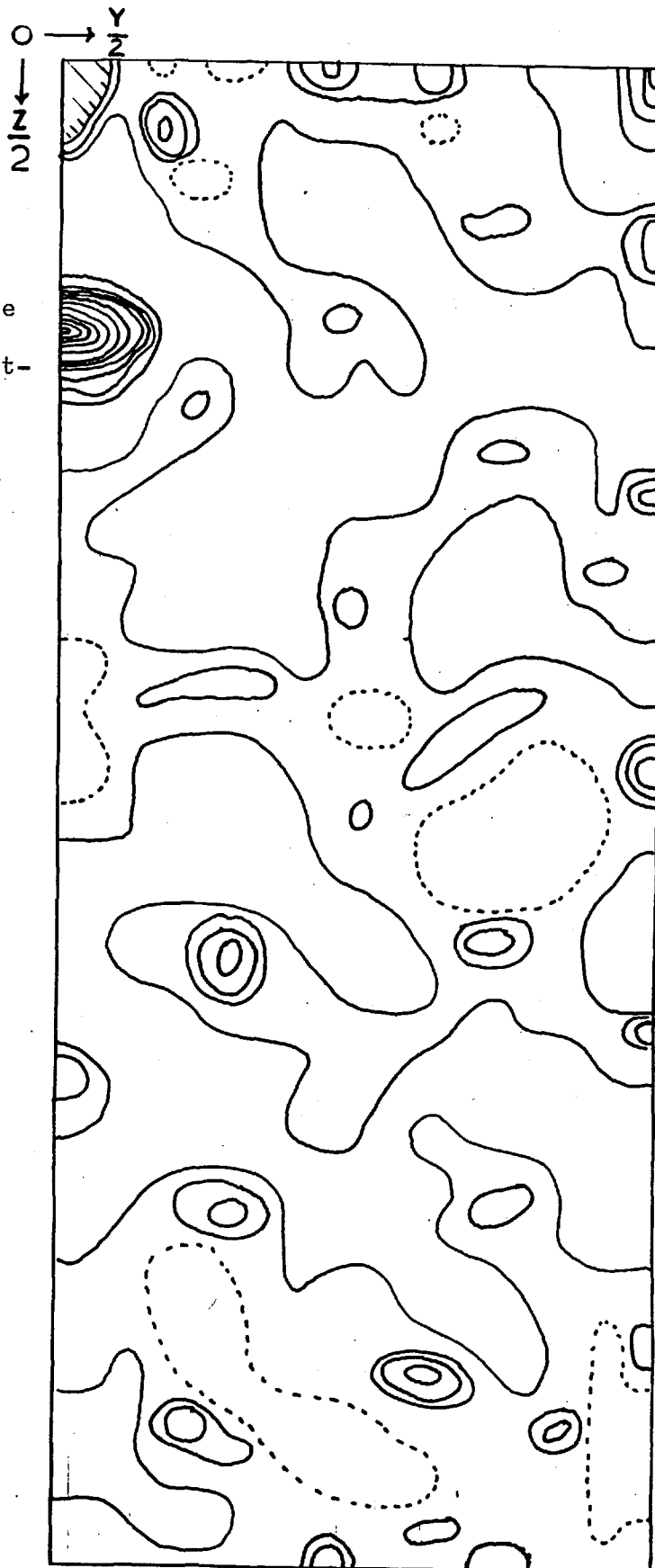
$$1/f^2 \cdot \exp(6 \sin^2 \theta / \lambda^2)$$

where  $f$  is the formfactor for carbon. The resulting Patterson did not exhibit any serious diffraction ripple except in the neighbourhood of the origin peak and the zeroth section is shown in Figure 13 which can be compared with the corresponding section of the unsharpened Patterson on page 163. A sharpening

Figure 13.

Zeorin acetate  
sharpened Patt-  
erson.

Section  $x = 0$



function of the type

$$\exp ( 6 \sin^2 \theta / \lambda^2 )$$

similar to that used by Nordman and Nakatsu (1963), did not produced any marked differences between the sharpened and unsharpened Pattersons.

#### Orientation Search

During the course of the work with the unsharpened Patterson, there were indications that the distortion of the molecular fragment may have contributed to the poor resolution of the minimum functions. Consequently, the ten atoms comprising the B and C rings of Hall and Maslens's (1965) determination of methyl melaleucate iodoacetate were selected as molecular fragment. In the orientation search, vectors between adjacent atoms were excluded to avoid the effects of the ripple near the origin peak. The approximate orientation of the molecule had been fairly well defined, as described in the preceding sections and so the ranges of the rotational search were limited to  $A = -30^\circ$  to  $+30^\circ$ ,  $B = -90^\circ$  to  $+90^\circ$  and  $C = -50^\circ$  to  $+50^\circ$ .

The minimum function showed four strong peaks for which LOW and NEXT were approximately 36 and 37 respectively compared with the background level of 10 - 25 (0 in Figure 13 was adjusted

to 36 for the search). After decreasing the angular increments the values shown in Table 2 were obtained for the four peaks,

Table 2. Rotational parameters of the four highest peaks in the minimum function.

Peak	A°	B°	C°	LOW/NEXT
1	-5	-70	10	36/37
2	+7	-59	23	37/39
3	-2	47	-35	39/40
4	1	57	-19	37/38

although the angles could not be fixed within  $\pm 2^\circ$ . The orientation of the molecular fragment defined by the parameters of peak 2 in Table 2 is shown projected down the b axis in Figure 14a and down the c axis in Figure 14b and roughly agrees with the positions deduced in the earlier work. The values of the angles  $\alpha_1 = 39^\circ$  and  $\alpha_2 = 28^\circ$  can be compared with the corresponding angle of  $30^\circ$  obtained from peak (3) in the unsharpened Patterson.

Table 2 shows that the peaks occur in two pairs 1,2 and 3,4 related to each other by a rotation of approximately  $120^\circ$  about the b axis. The differences between peaks 1 and 2 can be explained by the fits of the molecular fragment with the A/B and C/D rings respectively, similar to the situation described for the unsharpened search (there were also three peaks with LOW  $\approx$  32 in the ranges A =  $-5^\circ$  to  $+5^\circ$ , B =  $-10^\circ$  to

+10°, C = -10° to +25° which may have been due to fits with the B/C rings and the A and D rings plus appendages, but they were not investigated further). However, the differences between peaks 1 and 2 are in this case quite marked and strongly suggest that the molecule is situated in the unit cell as shown in Figure 15. This is different from that suggested by the Fourier

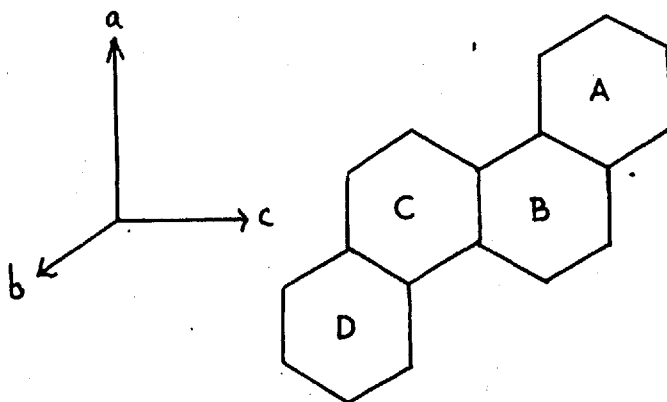


Figure 15.

maps derived from the unsharpened Patterson.

Using Dreiding models it was seen that with the molecular fragment in the orientation corresponding to peak 2 (Figures 14a and 14b), the position of peak 4 is equivalent to an approximate rotation of the group through 180° about the c axis. The relationship between peaks 2 and 4 occurs because the ten atoms of the molecular fragment approximately form a centrosymmetric set. Rotating the vectors through 180° about a



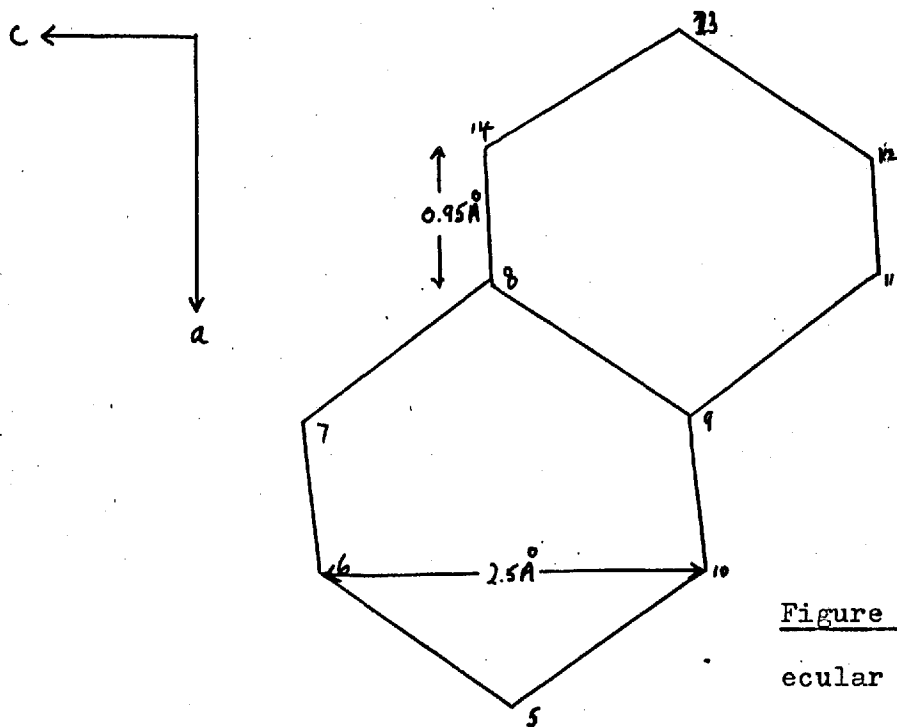


Figure 14a. The molecular fragment projected down the  $b$  axis.

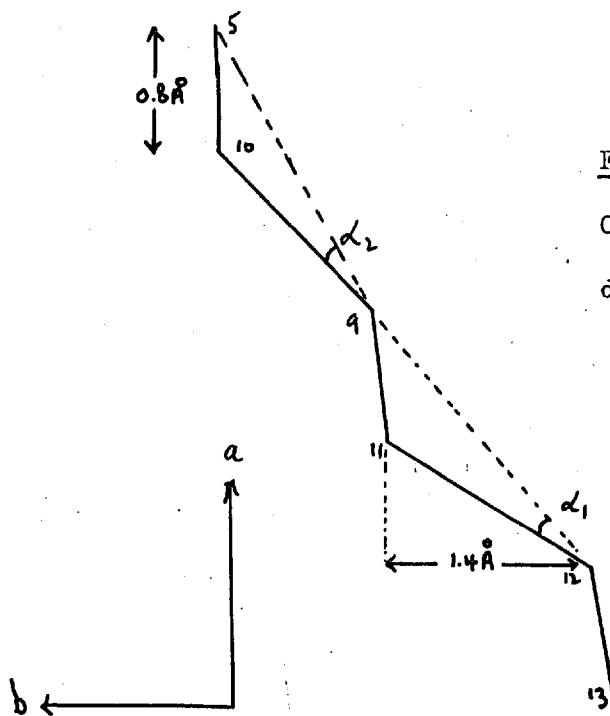


Figure 14b. Atoms  $C_5$ ,  $C_9$ ,  $C_{10}$ ,  $C_{11}$ ,  $C_{12}$  and  $C_{13}$  projected down  $c$ .

crystallographic axis and making all their signs positive to deal with the symmetry of the spacegroup, will give a set of vectors nearly, but not quite, equivalent to the original set. Peak 1 must be related to peak 3 in the same manner.

#### Location Search

The translational minimum function derived from the search along the Y and Z directions with the molecular fragment in the orientation  $A = 7^\circ$ ,  $B = -59^\circ$  and  $C = 23^\circ$  contained a large number of peaks with  $LOW = 32$  to  $39$  compared with the background level of  $15 - 25$ . However, the number of peaks was far too large to enable any unambiguous assignment of values to the translational parameters  $y_0$ ,  $z_0$ . It was noticed that the peaks occurred at very regular intervals,  $0.7 \text{ \AA}$  in Y and  $1.2 \text{ \AA}$  in Z. The search along X and Z showed a similar phenomenon the intervals being  $0.4 \text{ \AA}$  in X and  $1.2 \text{ \AA}$  in Z. These repeat distances are approximately one half of the projected interatomic distances in the molecular fragment shown in Figures 14a and 14b. In order to try and reduce this effect, the positions were calculated for a molecular fragment comprising two trans decalin rings both in the orientation  $A = 7^\circ$ ,  $B = 59^\circ$  and  $C = 23^\circ$ , and joined at C8 - C9 as in Figure 15. In the resulting translational minimum functions the 'periodicity' was not reduced to any marked extent.

Attempts were made to interpret these results by postulating partial fits between the molecule fragment and the postulated structure of zeorin acetate, as the former was translated along the crystallographic directions in the orientation shown in Figures 14a and 14b, and taking into account packing considerations. These methods proved abortive and as it was becoming almost as difficult to interpret the translational minimum function as it would be to visually interpret the Patterson, the method was abandoned.

### Conclusion

In retrospect, there are several factors that may have contributed to the failure of this Patterson search technique as a method for the determination of the crystal structure of zeorin acetate.

Certainly for structures that have been solved by this method, the geometry of the molecular fragment has been well defined. The two alkaloid structures analysed by Nordman and Nakatsu (1963) and Nordman and Kumra (1965) contained planar oxindole and indole groups respectively and the solution of a pyrethosin derivative by Nordman and Gabe (1965) was attained using an isoxazolone group and three other atoms as molecular

fragment. In both the sharpened and unsharpened work on zeorin acetate the rotational parameters A, B and C were not well defined, which must have resulted in part from the differences between the geometry of the trans decalin rings in methyl melaleucate iodoacetate and zeorin acetate. The vector refinement program described by Nordman (1966) would probably be useful in this respect but was not available for this work.

The 'periodicity' that was noted in the translational minimum function during the work on the sharpened Patterson suggests that more serious difficulties are present. Although it was not recognised at the time, this effect was also present in the unsharpened work, but to a less marked extent. It was felt that the effect was due to the fact that the molecular fragment must consist of at least a trans decalin ring system, as this is the most well-defined feature of the molecule. The structure postulated from the chemical evidence contains three such systems of the A/B, B/C and C/D rings and a similar system in the part structure defined by the D/E rings. It was conceivable that the 'periodicity' could be reduced by using a molecular fragment comprising a larger number of atoms, though the results in this respect were disappointing. In the previous structure determinations to which this method has been applied, the compounds have all possessed only one, unique part structure that was used as molecular fragment and their unit cells con-

tained only two molecules (i.e. spacegroup  $P2_1$  in each case).

The Convolution Molecule method that has been developed by Hoppe (1957) and described briefly on page 145 offers an alternative approach to the determination of the structure of zeorin acetate that would possibly not involve some of the difficulties encountered here. Attention is, in fact, now being turned towards this method.

It does seem that this method is not seriously dependent upon an accurate knowledge of the geometry of a molecular fragment. Huber and Hoppe (1965) have described the structure determination of the steroid, ecdysone, in which a ring junction initially assumed to be trans fused was later shown to be cis. However, it is not clear whether the 'periodicity' effect would be a problem. The Convolution Molecule method would also overcome a defect in the Patterson search technique used here, that of applying vector weights. However, it should be a simple modification to incorporate a scheme similar to that described by Nordman (1966) into the Patterson search programs.

References

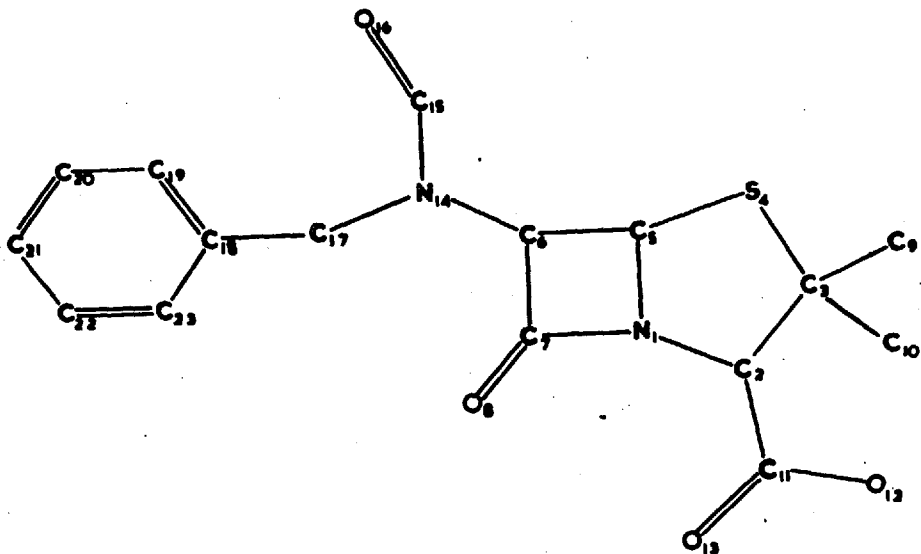
- Abraham and Newton (1955), *Biochem.J.*, 79, 377
- Abrahamsson, Crowfoot Hodgkin and Maslen (1963), *Biochem.J.*, 86, 514
- Alden, Stout, Kraut and High (1964), *Acta Cryst.*, 17, 109.
- Asahina and Akagi (1938), *Ber.*, 71, 980.
- Asahina and Yosioka (1940), *Ber.*, 73, 742.
- Barton and Bruun (1952), *J.Chem.Soc.*, 1683.
- Barton, de Mayo and Orr (1958), *J.Chem.Soc.*, 2239.
- Beevers and Robertson (1950), *Acta Cryst.*, 3, 164.
- Booth (1948), 'Fourier Technique in X-Ray Organic Analysis',  
Cambridge, University Press, page 62.
- Bragg (1929), *Proc.Roy.Soc.*, 123A, 537.
- Buerger (1959), 'Vector Space', Wiley, New York.
- Cahn, Ingold and Prelog (1966), *Angew.Chem.Internat.*, 5, 385.
- Clastre and Gay (1950), *Compt.rend.*, 230, 1876.
- Cocker, Cowley, Cox, Eardley, Gregory, Lazenby, Long, Sly and  
Somerfield (1965), *J.Chem.Soc.*, 5015.
- Collins and Richmond (1962), *Nature*, 195, 142.
- Crowfoot, Bunn, Rogers-Low and Turner-Jones (1949), 'The  
Chemistry of Penicillin', Princeton, University  
Press, page 310.
- Crowfoot Hodgkin and Maslen (1961), *Biochem.J.*, 79, 393.
- Cruickshank (1959), 'International Tables for X-Ray Crystallo-  
graphy', Vol.2, Kynoch Press, Birmingham.

- Cruickshank (1961), 'Computing Methods and the Phase Problem in X-Ray Crystal Analysis', Pergamon Press, Oxford, Paper 6.
- Diamand (1963), D.Phil. Thesis, University of Oxford.
- Donohue (1950), J.Amer.Chem.Soc., 72, 949.
- Drew (1966), Ph.D. Thesis, University of London.
- Dunstan, Fazakerly, Halsall and Jones (1957), Croat.Chem. Acta, 29, 173.
- Fazakerly, Halsall and Jones (1959), J.Chem.Soc., 1877.
- Fazakerly, Gilbert, Gregory, Lazenby and Long (1965), Paper submitted to the Autumn Meeting of the Chemical Society at Nottingham.
- Fleming (1929), Brit.J.Exptl.Pathol., 10, 226.
- Garrido (1950), Compt.rend., 230, 1878.
- Hale, Newton and Abraham(1961), Biochem.J., 79, 403.
- Hall and Maslen (1965), Acta Cryst., 18, 265.
- Hamilton, Rollett and Sparks (1965), Acta Cryst, 18, 129.
- Hamilton (1965), Acta Cryst., 18, 866.
- Harker (1936), J.Chem.Phys., 4, 381.
- Harker and Kasper (1947), J.Chem.Phys., 15, 882.
- Hauptman and Karle (1950), Acta Cryst., 3, 181.
- Hesse (1906), J.pr.Chem., 73, 113.
- Hoppe (1957), Acta Cryst., 10, 750; Z.Electrochem., 61, 1076.
- Housely and Spooner (1964), Private communication.

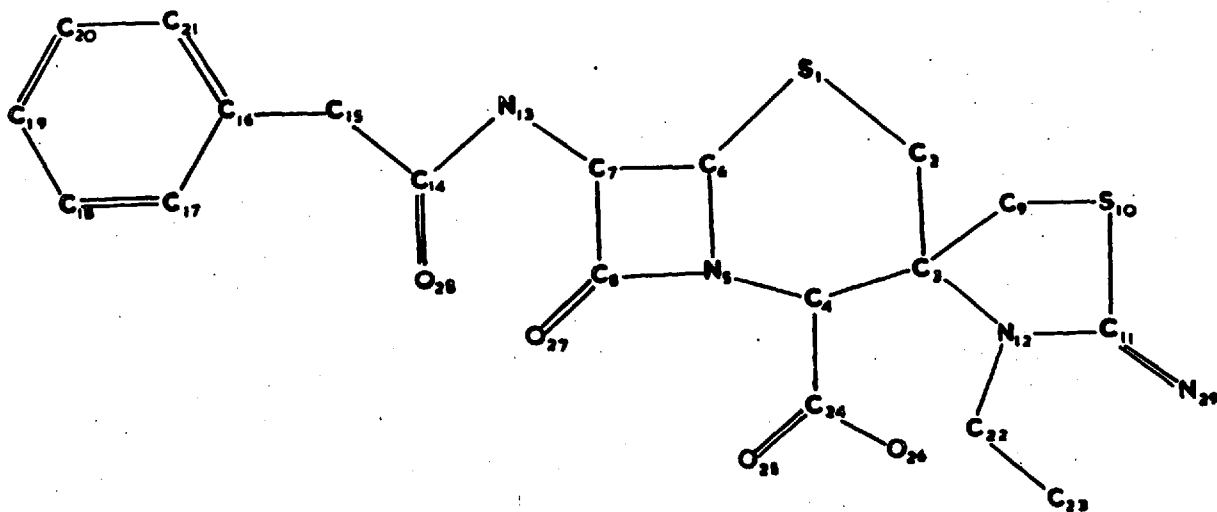
- Huber (1965), Acta Cryst., 19, 353.
- Huber and Hoppe (1965), Ber., 98, 2403.
- Huneck (1961), Ber., 94, 614.
- Huneck and Lehn (1963), Bull.Soc.Chim.France, 1702.
- Hunt and Rogers (1964), Biochem.J., 93, 35c.
- Hunt (1966), Technical Report, X-Ray Lab., Chem.Dept., Imperial College.
- Klug and Alexander (1954), 'X-Ray Diffraction Procedures', Wiley, New York, page 467.
- Lipson and Cochran (1953), 'The Crystalline State', Vol. 3, Bell, London, page 206.
- Loader, Newton and Abraham (1961), Biochem.J., 79, 408.
- Long (1966), Private communication.
- McClachlan (1951), Proc.Nat.Acad.Sci. U.S.A., 37, 115.
- Mighell and Jacobson (1963), Acta Cryst., 16, 443.
- Morin, Jackson, Flynn, and Roeske (1962), J.Amer.Chem.Soc., 84, 3400.
- Muggleton, O'Callaghan and Stevens (1964), Brit.Med.J., 2, 1234.
- Newton and Abraham (1955), Nature, 175, 548.
- Newton and Abraham (1956), Biochem.J., 62, 651.
- Nordman (1966), Transactions of the American Crystallographic Association, 2, 29.
- Nordman and Gabe (1965), Private communication.
- Nordman and Kumra (1965), J.Amer.Chem.Soc., 87, 2059.



- Nordman and Nakatsu (1963), J.Amer.Chem.Soc., 85, 353.
- Park (1958), Biochem.J., 70, 2p.
- Park and Strominger (1957), Science, 125, 99.
- Patterson (1935), Z.Krist., 90, 517.
- Pimentel and McClellan (1960), 'The Hydrogen Bond', Freeman,  
San Francisco.
- Rogers (1965), 'Computing Methods in Crystallography', Pergamon  
Press, Oxford, Chapter 16.
- Rollett (1961), 'Computing Methods and The Phase Problem in  
X-Ray Crystal Analysis', Pergamon Press, Oxford, Paper 9.
- Rollett (1965), 'Computing Methods in Crystallography', Pergamon  
Press, Oxford, Chapter 8.
- Rollett and Sparks (1960), Acta Cryst., 13, 273.
- Sayre (1952), Acta Cryst., 5, 697.
- Schaffner, Caglioti, Arigoni, Jeger, Fazakerly, Halsall and  
Jones (1957), Proc.Chem.Soc., 353.
- Shoemaker, Barieau, and Donohue (1953), Acta Cryst., 6, 241.
- Simpson, Falting, Dobrott and Lipscomb (1963), J.Chem.Phys.,  
39, 2339.
- Sutton (1965), 'Interatomic Distances', Supplement, The Chemical  
Society London Special Publication Number 18.
- Tipper and Strominger (1965), Proc.Nat.Acad.Sci. U.S.A., 54, 1133.
- Wilson (1942), Nature, 150, 152.
- Wrinch (1939), Phil.Mag., 27, 98.
- Zopf (1909), Annalen, 364, 273.



Structural formula for 6-NBF-PA.



Structural formula for the 3-spiro-thiazolinium-7-PAC derivative.